Journal of Paleontology, 90(3), 2016, p. 525–554

0022-3360/16/0088-0906
doi: 10.1017/jpa.2015.70

Journal of PALEONTOLOGY
A JOURNAL OF THE PALEONTOLOGICAL SOCIETY

Frasnian Late Devonian conodont biostratigraphy in New York: graphic correlation and taxonomy

Gilbert Klapper[1] and William T. Kirchgasser[2]

[1]Department of Earth and Planetary Sciences, Northwestern University, Evanston, Illinois 60208, USA ⟨g-klapper@northwestern.edu⟩
[2]Department of Geology, State University of New York at Potsdam, Potsdam, New York 13676, USA ⟨kirchgwt@potsdam.edu⟩

Abstract.—Two regional composite sections in the Frasnian, Upper Devonian, of New York State result from graphic correlation of conodont species. The first extends from Frasnian conodont zones 3 to 7, the second from Frasnian zones 11 to 13c (we prefer this terminology to "Montagne Noire" or "MN" zonation as the zone-defining species occur throughout the Devonian tropics). Key beds, widely traceable bases of prominent black shales, have been used with only a few exceptions to position the lines of correlation (LOC) in the graphs. Other key beds, not used for positioning, fall exactly on the LOC supporting the hypothesis of their synchrony. Fifty-five conodont species in the New York regional composites are compared with their ranges in the global Frasnian Composite Standard proving no major discrepancies. The taxonomy of *Ancyrodella nodosa* Ulrich and Bassler, widely misidentified in the past, has been clarified through restudy of the type specimens, resulting in its distinction from *A. hamata* Ulrich and Bassler (= *A. buckeyensis* Stauffer). A new species of *Polygnathellus* Bassler, which is restricted to Frasnian Zone 4, is kept in open nomenclature because the rarity of specimens is insufficient to determine the extent of intraspecifc variation and whether one or two species are represented in our New York and Western Australian collections.

Introduction

This report on the taxonomy, zonal and graphic correlation of Frasnian (lower Upper Devonian) conodonts from New York State contributes to a long collaborative effort to refine the sequence initially compiled by John Huddle (*in* Klapper et al., 1971, fig. 3). Huddle's monograph on Genesee Group conodonts added considerable detail, particularly in the lower part of the sequence (Huddle, 1981). These early studies used conventional biostratigraphy to correlate with the European conodont zonation (Ziegler, 1971) based mainly on species of the genus *Palmatolepis* and *Mesotaxis* that eventually became the Standard Frasnian Zonation (Ziegler and Sandberg, 1990). With the faunas then at hand, correlation between the New York sequence and the European zonation proved difficult, especially in the absence or apparent absence of key *Palmatolepis* species, particularly in the lower Frasnian (Huddle *in* Klapper et al., 1971; Huddle, 1981). Fortunately the European conodont zones were aligned with the long established European ammonoid (goniatite) cephalopod zones (Ziegler, 1971, chart 4). Following the discovery by House (1962) that all the major Upper Devonian European ammonoid zones could be recognized in New York, conodont sampling there focused on horizons with zone-defining ammonoids, thus providing the potential for a check on the alignment and international correlation of both groups. As a consequence we follow the stratigraphic terminology, locality and bed-numbering system developed by House and Kirchgasser (1993 and 2008) for their monograph on the New York ammonoid sequence (Figs. 1–6). As noted below, the conodont sequence presented here, incorporates species from several genera and is aligned by graphic correlation with an alternate zonation, the thirteen-fold zonation first developed in the Montagne Noire, southern France (Klapper, 1989; Table 1 herein), but recognized now throughout the Devonian tropics. For this reason, we term it the "Frasnian conodont" zonation rather than the "Montagne Noire" or "MN" zonation as used previously.

The preliminary survey analyzed 20 sections from the Genesee and overlying Sonyea groups (Klapper et al., 1995). The ranges of 28 conodont species and the stratigraphic positions of 23 key beds (mostly the bases of traceable black shales) were compiled by graphic correlation (see below), into a New York Regional Composite. The New York composite was in turn correlated with a global Frasnian Composite Standard with data from 27 sections and scaled to the thirteen-fold "Montagne Noire" zonation (Kirchgasser and Klapper, 1992; Klapper and Kirchgasser, 1992; Klapper et al., 1995). In this final report we expand our analysis, adding 17 sections from the West Falls Group (or Java Group for the Pipe Creek and Hanover shales) such that the New York Regional Composite currently incorporates the ranges of 55 conodont species whose New York ranges are compared with their global ranges in a Frasnian Composite Standard developed through graphic correlation (Table 2). The Frasnian Composite is currently based on data from 42 sections (including the two New York composites; the other 40 are individual sections), in North America, Europe, European Russia and Australia. The results, summarized in correlation charts (Figs. 3, 5), also show alignments with the

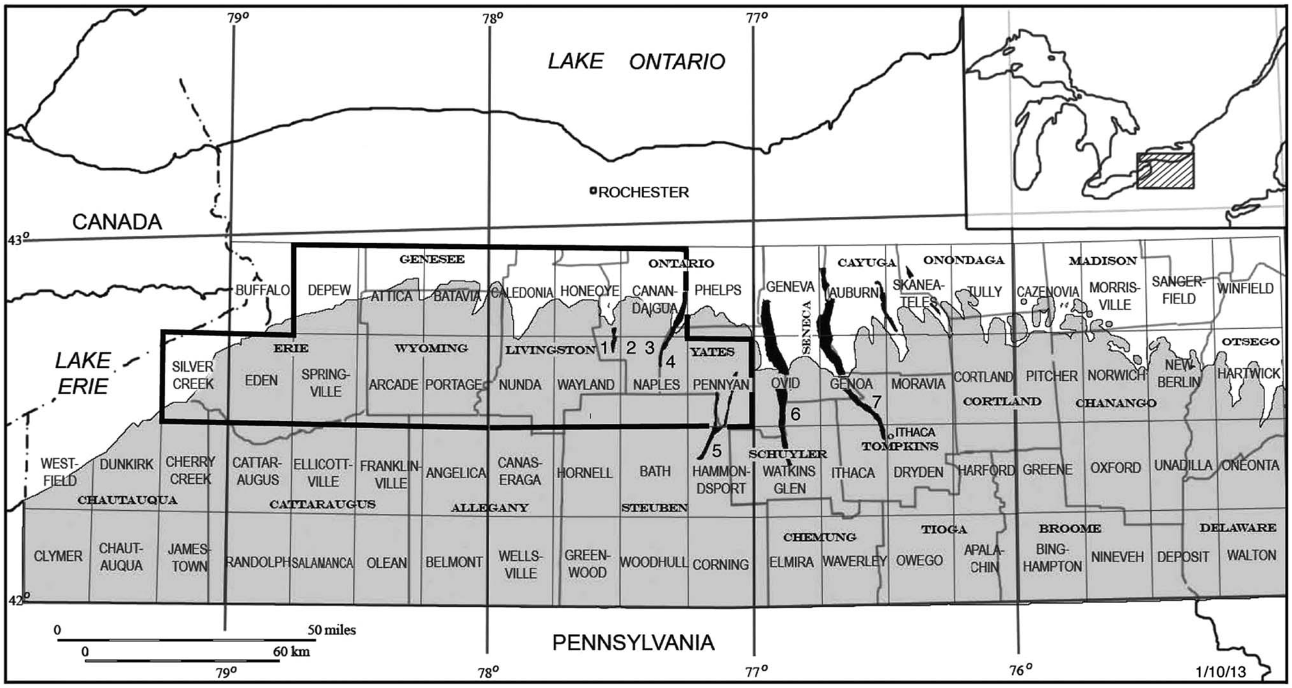

Figure 1. Map of upstate New York showing outcrop area of late Devonian rocks (Tully Limestone Formation and younger [shaded]) and area of 15' Quadrangles (bold outline) and counties of sampled localities (Appendix 1). Finger Lakes illustrated in black (west to east): (**1**) Conesus; (**2, 3**) Hemlock, Honeoye (not shown); (**4**) Canandaigua; (**5**) Keuka; (**6**) Seneca; (**7**) Cayuga.

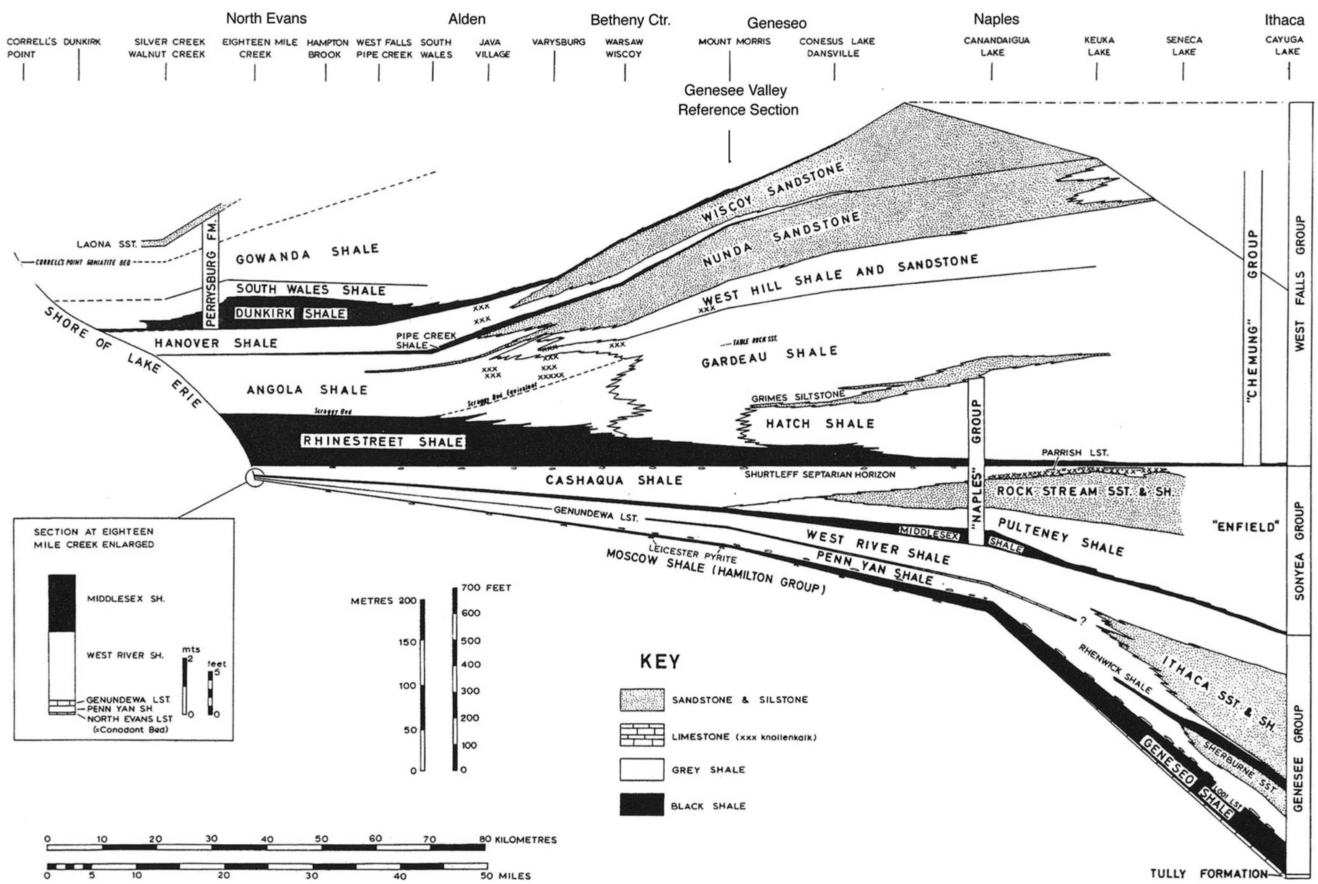

Figure 2. Late Devonian facies in western New York, modified from House and Kirchgasser (2008). Note position of Genesee Valley Reference section. Recent work by Cszonka et al. (2013) on ranges of benthic taxa in the Chemung (sandstone) facies (Nunda-Wiscoy sandstones) indicates that the Frasnian/Famennian boundary may be miscorrelated in the Genesee Valley region. Our conodont samples from the interval in question are from sections to the west where we are confident of the positions of the Pipe Creek Shale, Hanover Shale and Dunkirk Shale, the base of the latter being at or near the base of the conodont-defined Frasnian/Famennian boundary.

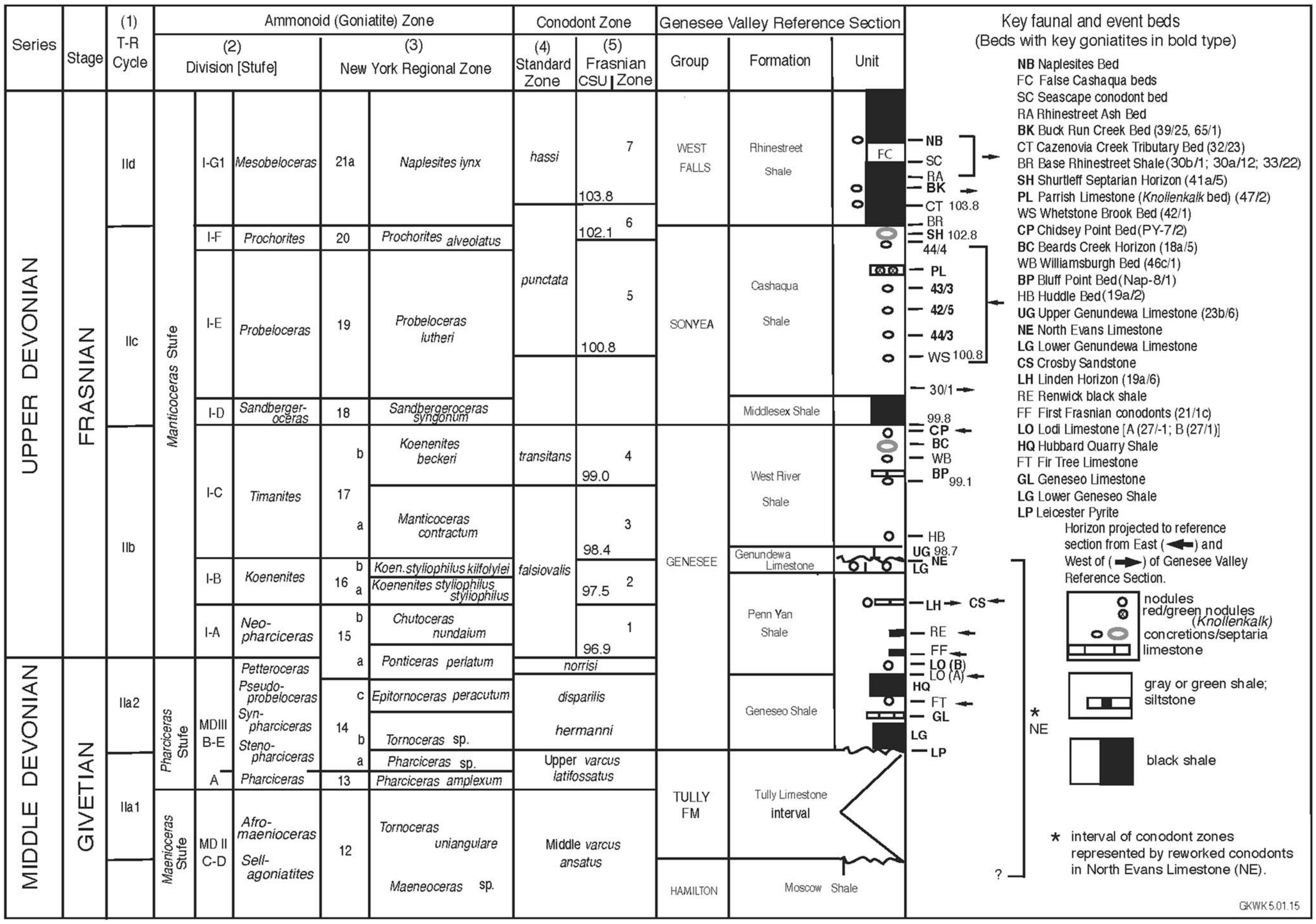

Figure 3. Correlation of major units, Transgression-Regression (T-R) cycles and key faunal and event beds of the Geneseo Shale to lower Rhinestreet Shale in western New York. (**1**) T-R cycles after Johnson et al. (1985). (**2**) Ammonoid (Goniatite) Divisions (Stufen) after Becker and House (2000), House and Kirchgasser (1993, 2008), Aboussalam and Becker (2011). (**3**) New York Regional Zones after House and Kirchgasser (1993, 2008). (**4**) Standard conodont zones of Ziegler and Sandberg (1990) with alignment to numbered Frasnian conodont zones following Klapper and Becker (1999). (**5**) Numbered Frasnian Conodont Zones and Composite Standard Unit (CSU) values for base of each zone by graphic correlation; CSU values also given for selected faunal and event beds.

Standard Frasnian Conodont Zones (Ziegler and Sandberg, 1990) and the global and regional Ammonoid (Goniatite) Zones.

Stratigraphy

The Frasnian (Upper Devonian) rocks in New York State are part of the Catskill Delta, a succession of siliciclastic sediments deposited in the northern Appalachian Foreland Basin during tectophases of the Acadian Orogeny (Woodrow and Sevon, 1985; Ettenson, 1985; Ver Straeten et al., 2011). The conodonts reported here from western New York (Fig. 1, Appendix 1) are mostly from calcareous horizons and sedimentary lag accumulations in the shales (mudrocks) of the distal margin of the basin. Above the Hamilton Group and Tully Formation (Givetian, Middle Devonian), is a series of cycles (sequences) of black and gray shale of varying scales of thickness, a record of sea-level change, basin subsidence and episodic influx of clastic sediments from the east and southeast (Fig. 2). The succession is subdivided by the major (thickest) cycles into three stratigraphic groups: (1) Genesee Group (black Geneseo Shale and gray Penn Yan Shale (with the Givetian /Frasnian boundary near its base), Genundewa Limestone and gray West River Shale; (2) Sonyea Group (black Middlesex Shale and gray-green Cashaqua Shale); (3) West Falls Group (black Rhinestreet Shale and gray Angola Shale, black Pipe Creek Shale and gray Hanover Shale. Alternatively, the Pipe Creek and Hanover shales comprise the Java Group (Figs. 3, 5).

The major cycles are thought to track eustatic changes in sea level corresponding to the global-scale transgressive-regressive T-R cycles of Johnson et al. (1985). The black shales (Geneseo, Middlesex, Rhinestreet and Dunkirk, the base of which is slightly above the base of the Famennian Stage) record the transgressive (deepening) events with bottom anoxia and the succeeding gray shales, the regressive (shallowing) events with bottom dysoxia. The depositional cycles also record changes in basin configuration, notably the westward migration of the basin axis (thickest sections of Geneseo, Middlesex, Rhinestreet and Dunkirk black shales) and the westward shift of clastic wedges of siltstone and sandstone (Sherburne, Ithaca, Rock Stream, Grimes, West Hill, Nunda, Wiscoy) (Fig. 2). As a result of these shifts in facies (depositional environments), the pelagic conodont and ammonoid faunas are unevenly distributed through the succession, with productive horizons, key faunal and event

Frasnian Zone	3		4				5							6		7			
Genundewa Limestone		West River Shale					Cashaqua Shale								Rhinestreet Shale				
Horizon	**UG**	HB	**BP**	WB	**BC**	**CP**	30/1	**WS**	**44/3**	**42/5**	**43/3**	**PL**	44/4	**SH**	BR	CT	**BK**	SC	**NB**
Icriodus symmetricus	←x	x	x	x	x	x	x	x	x	x	x	x	x	x	x	x	x	x	x
Ancyrodella recta	x	x																	
Ancyrodella triangulata	x	x																	
Polygnathus collieri	←x		x	x		x													
Polygnathus dengleri	←x	x	x	x	x	x													
Polygnathus dubius	←x	x	x	x	x	x	x	x	x	x	x	x	x	x	x	x	x	x	x
Polygnathus pennatus	←x	x	x	x	x	x													
Ancyrodella alata		x	x	x	x	x													
Mesotaxis asymmetrica			x	x	x	x	x	x						x	aff.			aff.	
Ancyrodella rugosa *	x		x	x	x	x													
Mesotaxis ovalis			x	x	x	x													
Palmatolepis transitans *			x		x	x	?x	x											
Polygnathus dengleri n.f.			x	x															
Polygnathellus n. sp.						x													
Ancyrodella africana					x														
Ancyrodella r. rotundiloba					x														
Ancyrodella r. pristina					x														
Ancyrodella nodosa							x	x	x	x	x	x	x	x	x			x	
Palmatolepis punctata *							?x	x	x	x	x	x	x	x	x	x	x	x	x
Mesotaxis johnsoni								x											
Ancyrognathus ancyrognathoideus																x	x		
Ancyrognathus primus *														x		x			
Palmatolepis spinata														x					
Ozarkodina bidentatiformis															x				
Ozarkodina nonaginta *																x			
Ancyrodella curvata e. f.																	x		
Ancyrognathus n. sp. L ?																		x	GKWK 09.09.14

Figure 4. Ranges of key conodonts from sampled horizons in the Upper Genundewa Limestone, West River Shale, Cashaqua Shale and lower Rhinestreet Shale with correlations to Frasnian Conodont Zones. Abbreviations of key horizons and locality/bed-numbers refer to Figure 3 and Appendix 1; horizons with key goniatites in bold type. Asterisk indicates zone-defining conodont species. (Note: The horizon taken as the Williamsburgh Bed [WB] at Chidsey Point, Keuka Lake [PY-7/2] by House and Kirchgasser [2008] correlates by graphic correlation to a position above the Beards Creek Horizon [BC] at Beards Creek [18a/5] and is here designated the Chidsey Point Bed [CP] and is our topmost faunal horizon of the West River Shale.) The Shurtleff Septarian Horizon (SH) at North McMillan Creek (Appendix 1, SH) lacks *Ancyrognathus ancyrognathoideus* but the species is present at this level in the type locality, Shurtleff's Gully (House and Kirchgasser, 2008, p. 40, loc.41). *Ancyrodella recta* occurs in the North Evans Limestone just below the Upper Genundewa Limestone (UG).

beds sensu Brett et al. (2003; Figs. 3, 5 and Appendix 1, see below) typically separated by monotonous shale intervals with poor faunas or devoid of fossils.

Conodont facies: key faunal and event beds

Black shales.—In many parts of the succession, but particularly in the Genesee Group, conodonts are concentrated with pyrite and fish-bone debris in detrital lag deposits along discontinuities at the bases of black shales (Baird et al., 1989). At the very base of the Genesee Group, the Leicester Pyrite (LP), is the classic example of a highly condensed, time-rich, black shale-roofed lag of insoluble debris that accumulated in the deep-water, basinal environment under bottom conditions of near-anoxia, black-mud deposition, pyritization, complete to nearly complete carbonate dissolution and extremely slow sedimentation (that is, sediment starvation associated with high sea-levels). These unusual deposits are the residuals of original carbonate beds, the result of a complex mechanism of internal-wave (pycnocline) shoaling and erosion against the basin-margin slope prior to deepening and burial by black muds (Baird et al., 2006, p. 359 and references therein). The Leicester Pyrite is a placer-like residuum of pyrite, fish debris and conodonts along the Taghanic disconformity, which tracked the westward onlap (transgression) of the black Geneseo Shale on the eroded upper Hamilton Group shales through an interval spanning possibly five conodont zones (Upper Givetian *hermanni* Zone to Frasnian Zone 2).

Similar pyrite-bone-conodont lags occur at discontinuities higher in the succession, sometimes at or near the tops of black shales. However these top-black shale disconformities are overlain by shales and siltstones marking the onset of the regressive (swallowing) phase of the cycle and attendant conditions for submarine erosion. An important one of these top-black shale lags marks the Middle-Upper Devonian

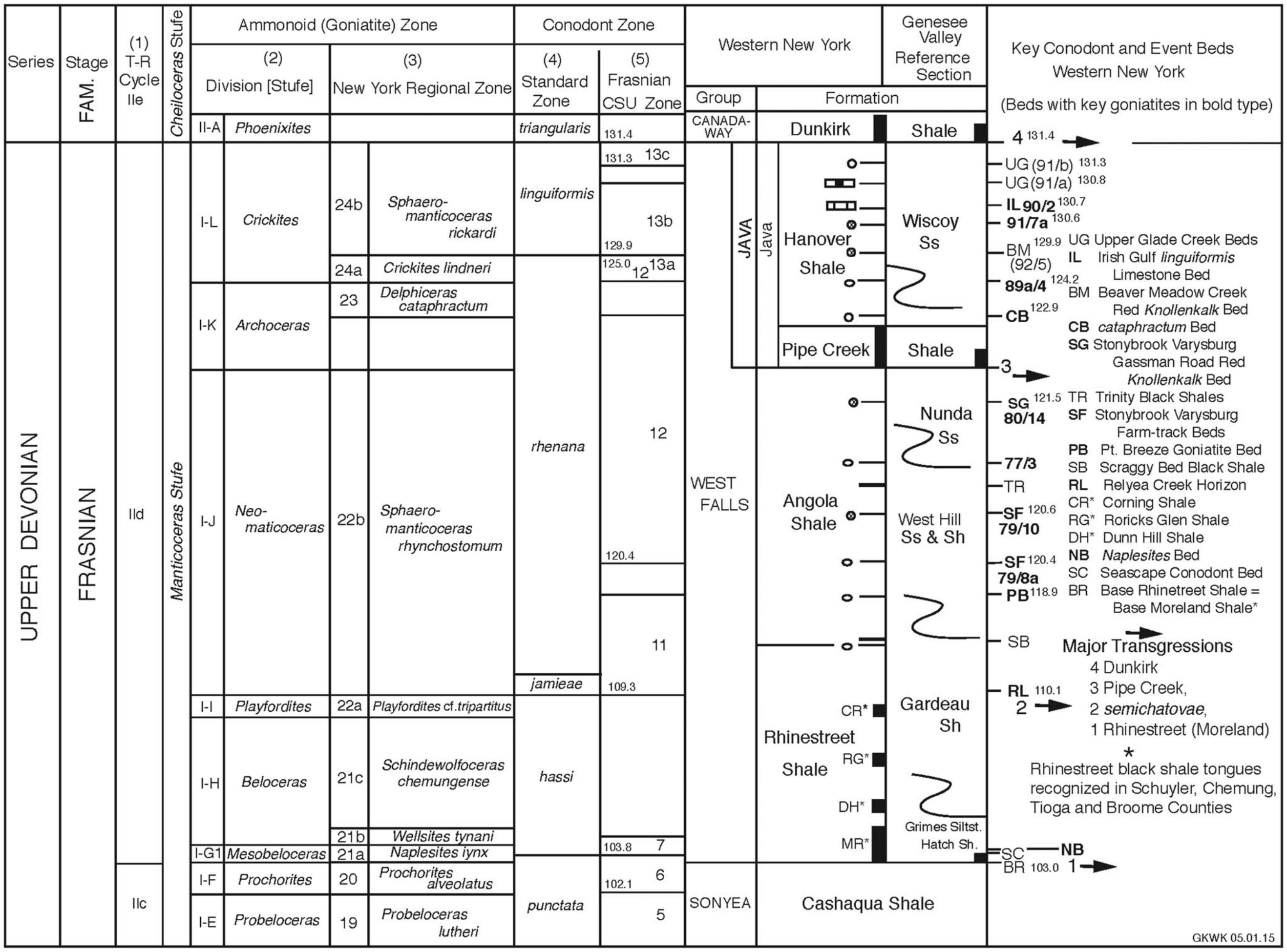

Figure 5. Correlation of major units, Transgression-Regression (T-R cycles) and key faunal and event beds of the Rhinestreet Shale to top of Hanover Shale in western New York. (**1**) T-R cycles after Johnson et al., 1985. (**2**) Ammonoid (Goniatite) Divisions (Stufen) after Becker and House (2000), House and Kirchgasser (1993, 2008). (**3**) New York Regional Zones after House and Kirchgasser (1993, 2008). (**4**) Standard conodont zones after Ziegler and Sandberg (1990) with alignment to numbered conodont zones following Klapper and Becker (1999). (**5**) Numbered Frasnian Conodont Zones and Composite Standard Unit (CSU) values for base of each zone by graphic correlation; CSU values also given for selected faunal and event beds. Note: Position of Frasnian/Famennian boundary may be miscorrelated in the Genesee Valley Reference Section (Cszonka et al., 2013).

(Givetian/Frasnian) boundary in New York with the entry of the first Frasnian conodonts (FF) in the lower Penn Yan Shale of *Ancyrodella rotundiloba pristina* [= *A. rotundiloba* early form] defining Frasnian Conodont Zone 1 (Kirchgasser, 1994; Baird et al., 2006, p. 363; Fig. 3 herein). Recent work by G. Baird (SUNY, Fredonia) has shown that the FF event-bed in the Hemlock-Honeoye area (2–3 of Fig. 1) is a distinctive pyrite-lag that records an interval of submarine erosion that at its maximum cut out the underlying Lodi Limestone (LO) at the base of the Penn Yan Shale and the Hubbard Quarry (HQ) black shale and Fir Tree Limestone (FT) of the upper Geneseo Shale. This new work indicates that the black shale labeled Penn Yan Shale A by Kirchgasser (1994, fig. 3) may in fact be the Hubbard Quarry Member at the top of the Geneseo Shale and the underlying limestone labeled Lodi may be the Fir Tree Limestone. Thus in the Honeoye Valley to Canandaigua Lake region the FF event-bed discontinuity (Givetian-Frasnian boundary) varies in stratigraphic position from at (or near) the top to the base of the Hubbard Quarry Shale (= Black Shale A) at the Geneseo-Penn Yan contact (Fig. 3).

Conodont lags also occur in thin carbonate units on the top surface of black shales, often with fish debris, dacryoconarids (styliolines and annulated forms), and small articulate brachiopods. Like their counterparts at the bases of black shale these deposits are also believed to represent highstand (high sea-level) intervals of sediment starvation and submarine transport and erosion. At Seneca Lake, Lodi Limestone Bed A (LO A of Fig. 3) at the top of the black Geneseo Shale (Hubbard Quarry Member), at the contact with the regressive, gray, Penn Yan Shale (or Sherburne Siltstone) at Mill Creek (Lodi Glen), is an example of this facies (Kirchgasser, 1994, Loc. 17, p. 133). Here the top-Geneseo-basal Lodi level (LO A) yields *norrisi* Zone conodonts of the uppermost Givetian as does the main Lodi Bed (LO B) above (Kirchgasser, 1994). The conodont record shows that the top and bottom surfaces of the Geneseo Shale are regionally diachronous as are many horizons along lesser discontinuities within the Geneseo and in the overlying Penn Yan Shale, Genundewa Limestone and lower West River Shale, specifically the Huddle Bed (HB) (Baird et al., 2006, p. 373, fig. 10).

FRASNIAN Zone	11		12					12/13a	13b				13c
Rhinestreet Shale		Angola Shale					Hanover Shale						
Horizon	**RL**	**PB**	**SF** 79/8a	**SF 79/10**	**77/3**	**SG 80/14**	**CB**	**89a/4**	**BM** 92/5	**91/7a**	**IL 90/2**	**UG** 91/a	**UG** 91/b
Ancyrodella hamata	x		x	x	x	x			x	x	x	x	
Ancyrodella curvata e. f.	←x		x										
Ancyrodella curvata l. f.	x						x	x					
Ancyrognathus sp.	x												
Ancyrognathus iowaensis	x	x	x	x	x	x							
Mehlina sp.	x	x	x										
Palmatolepis hassi s. l.	x												
Palmatolepis amplificata	x	x	x	x		x							
Palmatolepis semichatovae *	x												
Icriodus symmetricus	←x		x										
Polygnathus decorosus	x	x	x	x	x	x	x	x	x	x	x	x	x
Palmatolepis cf. *foliacea*		x											
Palmatolepis winchelli *			x	x				x	x	x	x	x	
Polygnathus aequalis			x	x	x	x							
Ancyrognathus triangularis				x		x							
Ancyrognathus amana						x							
Ancyrognathus? deformis	x					x							
Polygnathus brevis						x				x			
Polygnathus unicornis						x							
Palmatolepis foliacea						x							
Mehlina gradata						x							
Elsonella prima						x							
Polygnathus samueli						x							
Palmatolepis hassi s. s.							x		x				
Ancyrognathus asymmetricus									x				
Ancyrognathus aff. *altus*									x				
Polygnathus webbi									x	x	x	x	x
Palmatolepis linguiformis *											x		
Palmatolepis bogartensis *											x	x	x
Palmatolepis juntianensis												x	
Belodella sp.										GKWK	09.09.14	x	

Figure 6. Ranges of key conodonts from sampled horizons in the Upper Rhinestreet Shale, Angola Shale and Hanover Shale with correlations to Frasnian conodont zones. Abbreviations of key horizons and locality/bed-numbers refer to Figure 5 and Appendix 1; horizons with key goniatites in bold type. Asterisk indicates zone-defining conodont species.

Carbonates.—Most of the conodont faunas reported herein were recovered from calcareous beds with ammonoid cephalopods from the upper part of the regressive, gray-shale phase of the depositional cycles (sequences). The carbonates appear to have accumulated under dysoxic conditions early in the shift to the transgressive phase of the cycle before the return of bottom conditions of anoxia, carbonate dissolution and black shale (mudrock) deposition. The facies include gray-colored nodular and concretionary beds, baritic (white or pink) septarian-concretions, thin styliolinid (dacryoconarid) limestones and thin calcareous siltstones. In detail there are considerable similarities with the discontinuity lags described above, including pyrite mineralization and reworking of biogenic and lithic debris. The Williamsburgh Bed (WB), Beards Creek Horizon (BC), and Chidsey Point Bed (CP) in the upper West River Shale and the Shurtleff Septarian Horizon (SH) in the upper Cashaqua Shale are examples from the major cycles (Genesee and Sonyea groups). The Bluff Point Bed (BP) of the middle West River Shale and the Point Breeze Goniatite Bed (PB) in the lower Angola Shale are representative of the smaller-scale (meter-scale) cycles or microcycles (House and Kirchgasser, 2008). Fossil plants (or fossil logs) often occur in the concretions and are associated with abundant epiplanktonic mollusks, particularly small gastropods, bivalves and ammonoids, sometimes

Table 1. Scale in composite standard units of the 13-fold Frasnian conodont zonation.

Lowest CSU	Base of Zone	Defining Species of Zone
131.4	Lower *triangularis*	*Palmatolepis subperlobata* s.s.
131.0	13c	*P. bogartensis/P. linguiformis* extinct
129.9	13b	*P. linguiformis*
125.0	13a	*P. bogartensis*
120.4	12	*P. winchelli* (= *P. subrecta*)
109.3	11	*P. feisti*
107.9	10	*P. plana*
107.5	9	*P. proversa*
105.2	8	*P. housei*
103.8	7	*Ozarkodina nonaginta*
102.1	6	*Ancyrognathus primus*
100.8	5	*Palmatolepis punctata*
99.0	4	*P. transitans*
98.4	3	*Ancyrodella rugosa*
97.5	2	*A. rotundiloba rotundiloba*
96.9	1	*A. rotundiloba pristina*

CSU, composite standard unit.
The CSU values represent the lowest bases of the zone-defining species of each Frasnian zone. The base of the Famennian Stage coincides with the base of the Lower *triangularis* Zone, defined by the lowest occurrence of *Palmatolepis subperlobata* s.s. and the flood occurrence of *P. ultima,* as recommended by Klapper et al. (2004, p. 375–377) and Klapper (2007b, p. 67–68). *P. triangularis* does not enter at the base of the zone, but somewhat higher. Subzones 13b and 13c are equivalent to the lower and upper *linguiformis* zones, respectively, of Sandberg et al. (2002). *P. linguiformis* is restricted to Subzone 13b and *P. bogartensis* is the main *Palmatolepis* species of Subzone 13c (Girard et al., 2006).

baritized or pyritized, dacryoconarids (styliolines and annulated forms) and lingulid brachiopods.

The Genundewa Limestone (Formation), is a distinctive and widespread mass accumulation of styliolines in the mid-Genesee Group between the Penn Yan Shale and West River Shale. The Genundewa contains a diverse molluscan fauna, including key ammonoids. The Lower Genundewa (LG) is a nodular band with Frasnian Zone 2 conodonts and the Upper Genundewa (UG) a more evenly bedded division with Frasnian Zone 3 conodonts. The North Evans Limestone (NE) (= "Conodont-bed" of Hinde, 1879) occupies a position between the two divisions along a significant disconformity (see below).

Within the lighter-colored shales of the Sonyea Group and West Falls or Java Group (in contrast with the deep-water, dark-colored facies of the Genesee Group) is a particularly distinctive facies of red and green nodular limestones (*Knollenkalk*) often with ammonoids and well-preserved conodonts. The Parrish Limestone (PL) of the Cashaqua Shale (Sonyea Group) is the typical example in New York, and Bed SG of the upper Angola Shale and Bed BM of the upper Hanover Shale are later representatives (Figs. 2, 3, 5). These *Knollenkalk* beds resemble the European *Cephalopodenkalk* or griotte facies and seem to represent relatively shallow-water, well-oxygenated environments associated with submarine rises or shallowing above wedges of siltstone or sandstone (House and Kirchgasser, 2008, p. 67).

Of all the carbonate facies yielding Frasnian conodonts in New York the highest concentrations are from the famous Conodont bed of Hinde 1879 or North Evans Limestone (NE). The North Evans Limestone is a pelmatozoan-rich carbonate unit with reworked fish debris, glauconite grains, concretions and a rich and distinctive mixture of conodonts representing possibly as many as seven conodont zones (Givetian *ansatus* Zone to Frasnian Zone 2). From its type locality at Eighteenmile Creek, at North Evans, Erie County, the North Evans facies and fauna has been traced along a sub-Upper Genundewa Limestone discontinuity eastward to Genesee County and Livingston County (Genesee Valley) where it lies between the Lower and Upper Genundewa divisions, some 100 km distant. Once thought to be a lateral facies equivalent of the Leicester Pyrite along the Taghanic discontinuity at the base of the black Geneseo Shale and Genesee Group, the North Evans lag beneath the Upper Genundewa in fact lies along a significant mid-Genesee discontinuity. The taphonomic and biostratigraphic age of the North Evans lag material is Frasnian Conodont Zone 2 (Baird et al., 2006, p. 372–375). Westward from the

Table 2. Ranges of conodont species in the New York Frasnian sequence.

Conodont species	NY base	CS base	NY top	CS top
Icriodus symmetricus	96.3	97.5	120.4	129.6
Polygnathus dubius	96.3	96.1	103.8	105.3
Polygnathus dengleri	97.7	96.1	99.8	100.3
Polygnathus pennatus	97.7	96.6	99.8	100.1
Ancyrodella rotundiloba pristina	97.8	96.9	99.7	99.7
Polygnathus collieri	97.8	96.6	99.8	99.8
Ancyrodella rotunbiloba rotundiloba	98.3	97.5	99.7	99.7
Ancyrodella recta	98.7	98.2	98.9	99.0
Ancyrodella triangulata	98.7	98.5	98.9	100.0
Ancyrodella rugosa	98.7	98.4	99.8	100.3
Ancyrodella alata	98.9	98.3	99.8	100.4
Mesotaxis asymmetrica	99.1	96.6	102.8	103.6
Mesotaxis ovalis	99.1	99.1	99.8	103.1
Palmatolepis transitans	99.1	99.1	100.8	104.3
Polygnathus dengleri narrow form	99.1	98.1	99.2	102.7
Ancyrodella africana	99.7	99.1	99.7	103.6
Polygnathellus n. sp.	99.8	99.1	99.8	100.0
Ancyrodella nodosa	100.5	100.5	104.8	108.3
Palmatolepis punctata	100.8	100.8	104.8	108.3
Mesotaxis johnsoni	100.8	100.8	100.8	106.8
Ancyrognathus primus	102.8	102.1	103.8	105.4
Palmatolepis spinata	102.8	102.2	102.8	107.8
Ozarkodina bidentatiformis	103.1	102.5	103.1	105.4
Ancyrognathus ancyrognathoideus	103.6	101.6	103.8	104.8
Ozarkodina nonaginta	103.8	103.8	103.8	106.9
Ancyrodella curvata early form	103.9	101.6	120.4	123.8
Ancyrognathus n. sp. L?	104.9	104.9	104.9	104.9
Ancyrodella curvata late form	110.1	107.9	124.2	131.0
Ancyrodella hamata	110.1	107.6	130.8	131.3
Ancyrognathus sp.	110.1	110.1	110.1	110.1
Ancyrognathus iowaensis	110.1	107.5	121.5	123.0
Mehlina sp.	110.1	99.3	120.4	120.4
Palmatolepis amplificata	110.1	108.8	121.5	123.9
Palmatolepis hassi s.l.	110.1	110.1	110.1	110.1
Palmatolepis semichatovae	110.1	110.1	110.1	119.5
Polygnathus decorosus	110.1	108.3	131.3	131.3
Palmatolepis cf. *P. foliacea*	118.9	118.9	118.9	118.9
Palmatolepis winchelli	120.4	120.4	130.8	131.3
Polygnathus aequalis	120.4	101.1	121.5	121.5
Ancyrognathus triangularis	120.6	109.5	121.5	127.5
Ancyrognathus amana	121.5	121.5	121.5	130.6
Ancyrognathus? deformis	110.1	110.1	121.5	121.5
Elsonella prima	121.5	121.5	121.5	121.5
Mehlina gradata	121.5	96.6	121.5	129.5
Palmatolepis foliacea	121.5	118.6	121.5	125.1
Polygnathus brevis	121.5	112.3	130.6	130.6
Polygnathus samueli	121.5	120.5	121.5	123.5
Polygnathus unicornis	121.5	110.1	121.5	129.5
Palmatolepis hassi s.s.	122.9	108.3	129.9	129.9
Ancyrognathus asymmetricus	129.9	124.4	129.9	131.0
Ancyrognathus aff. *A. altus*	129.9	126.5	129.9	129.9
Polygnathus webbi	129.9	96.9	131.3	131.3
Palmatolepis bogartensis	130.7	125.0	131.3	131.4
Palmatolepis linguiformis	130.7	129.9	130.7	131.3
Palmatolepis juntianensis	130.8	126.4	130.8	130.9

Columns 1 and 3 give the lowest bases and highest tops in CSU values of 55 species in New York. Columns 2 and 4 indicate the current CSU value of the lowest bases and highest tops of the same species in the Frasnian Composite Standard.

Genesee Valley to its type area in Erie County the sub-Upper Genundewa or North Evans discontinuity oversteps the lower units (and event beds and discontinuities) of the Genesee Group (Lower Genundewa Limestone, Penn Yan Shale, Geneseo Shale). With the convergence of the North Evans and Taghanic discontinuities around Eighteenmile Creek, where the North Evans lies between Hamilton Group shale and the Upper Genundewa Limestone, the hiatus of the Taghanic Unconformity reaches its maximum, an interval of possibly seven conodont-zones duration as noted above.

It was the occurrence of species and subspecies of the conodont genus *Ancyrodella* (*A. rotundilba pristina* [= *A. rotundiloba* early form]), *A. rotundiloba rotundiloba* [= late form] and *A. recta* in the North Evans Limestone in Erie County that led to the earlier placement of the base of the Upper Devonian (Frasnian) at the base of the overlying Genundewa Limestone (Upper Genundewa) (Huddle in Klapper et al., 1971). As indicated above, the highest stratigraphic position (FF) of the boundary-defining fauna (entry of *A. rotundiloba pristina*) and base of Frasnian Conodont Zone 1, is in the lower Penn Yan Shale.

Frasnian conodont zonation and graphic correlation

The thirteen-fold Frasnian conodont zonation initially developed in the Montagne Noire, southern France (Klapper, 1989) has been widely replicated in many areas of the Devonian tropics, e.g., Timan-Pechora region, Russia, Canning Basin, Western Australia, Alberta Rockies and subsurface of western Canada, Iowa and New York (Johnson and Klapper, 1992; Kirchgasser, 1994; Kralick, 1994; Klapper et al., 1996; McLean and Klapper, 1998; Klapper, 2007a, 2009). It differs in principle from the Frasnian Standard Zonation of Ziegler and Sandberg (1990), which is based exclusively on the ranges of species of the genus *Palmatolepis*. In contrast, the thirteen-fold Frasnian zonation uses all short-ranging species regardless of generic affiliation and numbers for the zones instead of species names. The original Frasnian Zone 13, which spans a significant part of the latest Frasnian, has been subdivided into three subzones (Girard et al., 2006, p. 189–190; Klapper, 2007a, 2009, p. 406). Table 1 indicates the criteria for subdivision. Subzones 13b and 13c coincide with the lower and upper parts respectively of the *linguiformis* Zone as proposed by Sandberg et al. (2002).

For the purpose of testing the validity of species ranges in the Frasnian conodont zonation, we have long been involved in an effort to calibrate the zonation in terms of graphic correlation, the powerful numerical correlation technique first developed by Shaw (1964). A brief history of this research program is given in the introduction to a paper correlating the conodont sequence in the Montagne Noire with two contrasting biofacies sequences in western Canada (Klapper, 1997, p. 113-114), with the bases of the zonally defining species given in terms of their ranges in a Frasnian Composite Standard (Table 1).

Starting in the early 1990s, we constructed two regional composites for the Frasnian of New York State (Fig. 1; Klapper et al., 1995, p. 181) using the technique of supplemented graphic correlation advocated by Edwards (1989). That is we used key beds to position the line of correlation (abbreviated hereafter as LOC), for example, the regionally traceable bases of the Middlesex and Rhinestreet black shales (Fig. 2). These are both at the base of T-R cycle boundaries: IIc and IId (Johnson et al., 1985; Fig. 3 herein). In the lower composite, New York 1, extending from the Geneseo Shale base to the Rhinestreet Shale base, there are 21 measured sections with Beards Creek, Leicester, Livingston County, as the standard reference section (hereafter as SRS, as in Shaw, 1964; locality data are given in Appendix 1). In 17 of the graphs, two key beds were used to position the LOC and in three graphs, three key beds were used. The Middlesex Shale base and Rhinestreet Shale base were used for 19 of the points positioning the LOC. Other regionally traceable key beds were used for 21 positioning points, with one ammonoid (goniatite) and two conodont bases accounting for the three remaining points. In the Eighteenmile Creek graph, the two ends of the LOC were positioned on the Middlesex and Rhinestreet bases, but four traceable black shale beds remarkably lie exactly on the LOC between the two anchors. Such results lend support to the hypothesis of geologic synchrony of the key beds justifying their use in constructing the New York regional composites, the proposed test of our original paper (Klapper et al., 1995, p. 181).

The New York 2 regional composite extends from the base of the Rhinestreet black shale to the base of the Dunkirk black shale. There are eleven measured sections with Cazenovia Creek, Griffins Mills, Erie County, serving as the SRS. Eight of the graphs used two key beds for positioning the LOC, whereas the other two graphs used three key beds. All of the positioning points were key beds with the exception of one conodont base. The graph for Stony Brook, Varysburg, Wyoming County, has two key beds lying exactly on the line anchored by two other key beds.

The two New York regional composites were then graphed against the Frasnian Composite Standard consisting of a total of 42 sections. The resulting ranges of 55 conodont species are given in Table 2 and compared with their maximum bases and tops in the Composite Standard. What this means in terms of the Frasnian conodont zonation can be seen by comparing the Composite Standard Unit (hereafter as CSU) values in Table 2 with the lower boundaries of each of the zones given in Table 1 and partly shown in Figures 3 and 5.

The Upper Genundewa Limestone (Fig. 4) has the lowest occurrences of two species of *Ancyrodella*, *A. rugosa* and *A. triangulata* (for authorship of species and abbreviated synonymy lists, see Appendix 2). This association indicates Frasnian Zone 3, in agreement with the study of Kralick (1994, fig. 2) and in terms of the coincident CSU value of 98.7 for the two species at a position midway in Zone 3 in the Frasnian Composite Standard. *Ancyrodella recta* and *A. triangulata* have tops in the Huddle Bed (HB) at Fall Brook, Geneseo, Livingston County, a position low in the West River Shale but with a CSU value of 98.9 it corresponds to a position very high in Zone 3.

The lower West River Shale above the Huddle Bed (HB) has not been dated by conodonts. However, in about the middle of the formation, *Palmatolepis transitans* (Fig. 8), the defining species for the lower boundary of Frasnian Zone 4, enters in the Bluff Point Bed (BP), in the section at South Middlesex, Yates County, 3 meters below the distinctive, widely traceable Bluff

Point Siltstone. This entry of *P. transitans* in New York is at exactly the same CSU value as the lowest occurrence of this species in the Frasnian Composite Standard at Timanites Hill, Canning Basin, Western Australia (Appendix 1; 98.96; rounded off to 99.0 in Table 2, in which all values are rounded to the first decimal place). Note that this entry, which coincides with the lowest occurrence of *Mesotaxis ovalis* in the Bluff Point Bed, was not used to position the LOC in constructing the New York 1 composite. The close spacing of CSU values for the lower Frasnian zones (Table 1, Zones 1 to 3; all less than 1 CSU) is because the original SRS for the Composite Standard is a highly condensed Montagne Noire section; it is the SRS that determines the scale of the x-axis in graphic correlation and consequently the numerical value of the CSUs.

Higher in Frasnian Zone 4, the rare *Polygnathellus* n. sp. occurs in the Chidsey Point Bed (CP) at 99.8 CSU, a level that projects to less than 0.1 CSU above the Beards Creek Horizon (BC) at the Beards Creek SRS and 0.1 CSU higher than the top of the slightly more abundant occurrence of the same species at Timanites Hill.

The lowest unquestioned New York occurrence of *Palmatolepis punctata*, the defining species for the lower boundary of Frasnian Zone 5, is in the basal 5 cm of the Cashaqua Shale at Eighteenmile Creek, North Evans, Erie County, illustrated by Over et al. (2003, pl. 1, figs. 1, 2). They report a questionable occurrence of *P. punctata* in the underlying Middlesex Shale (op. cit., p. 218–219, fig. 2). Our lowest unquestioned occurrence of *P. punctata* is in the Whetstone Brook Bed (WS) of the lower Cashaqua Shale, 30 cm above the topmost siltstones of the Rock Stream Siltstone that cap the first falls in Whetstone Brook, Honeoye, Ontario County. This graphs at 100.8 CSU and is presently the lowest base for *P. punctata* in the Composite Standard, less than 0.1 CSU lower than the second lowest occurrence in one of the Montagne Noire sections.

Ancyrognathus primus, the defining species for the lower boundary of Frasnian Zone 6, has its lowest occurrence near the top of the Cashaqua Shale in the Shurtleff Septarian Horizon (SH) at North McMillan Creek, Conesus Lake, Livingston County. This horizon graphs at 102.8 CSU and thus represents a midway point in Zone 6. The lowest occurrence of *Ozarkodina nonaginta*, the defining species for the lower boundary of Frasnian Zone 7, is in the Cazenovia Creek Tributary Bed (CT), Spring Brook, Erie County, about 6 m above the base of the Rhinestreet Shale. At CSU 103.8 this occurrence of *O. nonaginta* in New York is less than 0.1 CSU higher than the lowest base of the species in the Composite Standard SRS in the Montagne Noire.

Between the lower Rhinestreet Shale and the upper part of the formation, zonally diagnostic conodont faunas have not yet been found. A large fauna with *Palmatolepis amplificata* as the dominant species of that genus, but accompanied by the key marker species *P. semichatovae*, occurs in the upper Rhinestreet in the Relyea Creek Horizon (RL) at Relyea Creek, South Warsaw, Wyoming County. This horizon graphs at 110.1 only fractionally higher (less than 0.1 CSU) than the lowest occurrence of *P. semichatovae* in the Composite Standard, which is in core 178 in the Voronezh region of the Russian Platform (illustrated in Aristov, 1988). The base of Frasnian Zone 11 is defined by the lowest occurrence of *Palmatolepis feisti* (= *P.* sp. B of Klapper and Foster, 1986 and Klapper and Becker, 1999, see synonymy in Klapper, 2007a, p. 521), which is at 109.3. *Palmatolepis semichatovae* typically enters very low in Zone 11 in sixteen sections in the Composite Standard and its top is also low in Zone 11, except for one anomalous occurrence high in Zone 11 in the Timan-Pechora region of Russia in core 2023 (Klapper et al., 1996, fig. 5).

The sample from the Point Breeze Goniatite Bed (PB; Fig. 6) at Big Sister Creek, Angola, Erie County, in the lower Angola Shale is indeterminate by zonal methods but graphs at 118.9 and thus is in the higher part of Frasnian Zone 11. The entry of *Palmatolepis winchelli* in Bed 79/8a (SF) in the Angola Shale at Stony Brook, Varysburg, Wyoming County, identifies the base of Frasnian Zone 12 and graphs at 120.4, tied with the lowest occurrence in the Composite Standard at La Serre Trench D, Montagne Noire, southern France (Klapper et al., 1995, fig. 1). Note that *P. winchelli* was not used to position the LOC in the Stony Brook graph, because two key beds were used to position the LOC near its ends with two other keys beds lying exactly on the line in between.

A large and diverse fauna occurs high in the Angola Shale in Bed 80/14 (SG) at Stony Brook (Gassman Road), Varysburg, Wyoming County, and graphs at 121.5 relatively low in Frasnian Zone 12. A significant occurrence in this fauna is *Polygnathus samueli*, which occurs in ten sections in the Composite Standard, all but one of which have bases and tops in the lower part of Zone 12. Both the Zone 11 fauna at Relyea Creek and the higher fauna at Stony Brook strongly resemble Sweetland Creek, Iowa faunas (Johnson and Klapper, 1992) in style of preservation.

The low diversity faunas in the lower part of the Hanover Shale (CB and 89a/4, Figs. 5, 6) are indeterminate by zonal methods, but the *cataphractum* bed (CB) with *Palmatolepis hassi* s.s. graphs at 122.9 indicating that this horizon is within Frasnian Zone 12. Bed 89a/4 at Walnut Creek, Silver Creek, Chautauqua County, could fall within Zone 12 or Frasnian Subzone 13a.

The fauna of the Beaver Meadow Creek Bed (BM), Bed 92/5 (Fig. 6) in the upper Hanover Shale at Beaver Meadow Creek, Java, Wyoming County, contains *Ancyrognathus* aff. *A. altus* and *A. asymmetricus* and graphs at 129.9, which coincides with the base of Frasnian Subzone 13b. The lower boundary of Subzone 13b (Girard et al., 2006) is defined on the lowest occurrence of *Palmatolepis linguiformis*, which in the Composite Standard is at Horse Spring in the Canning Basin, Western Australia (Klapper, 2007a). In the New York succession, *P. linguiformis* first occurs together with *P. bogartensis* in the Irish Gulf *linguiformis* Limestone Bed (IL), Bed 90/2 (Fig. 6) high in the Hanover Shale, 4.7 m below the base of the Dunkirk Shale at Irish Gulf, North Boston, Erie County. This horizon graphs at 130.7 CSU within Subzone 13b.

The highest fauna we collected, that of Bed 91/b in the Hanover Shale, 1.1 m below the base of the Dunkirk at upper Glade Creek (UG), Strykersville, Wyoming County, graphs at 131.3 CSU. The only species of *Palmatolepis* in this sample is *P. bogartensis*, indicating a position within Frasnian Subzone 13c according to the CSU value in the Composite Standard. Subzone 13c is defined on several criteria: the extinction of

P. linguiformis, the domination of *P. bogartensis* in an impoverished fauna with few other species of *Palmatolepis*, and the rare appearance of *P. ultima*.

Over (1997, table 2, 3 and figs. 7, 8) reported on a suite of samples across the Frasnian-Famennian boundary at several sections in western New York. At Irish Gulf (op. cit., table 3, fig. 8) Over's sample IG-03b at 2.95 m below the base of the Dunkirk has *Palmatolepis bogartensis* and *P. winchelli*, but also the reported occurrence of *P. triangularis*. The illustrated specimen of the latter from this sample (Over, 1997, fig. 10.1), however, is identified herein as *Palmatolepis ultima* Ziegler, 1958. This is based on a taxonomic distinction published later than Over's paper (Klapper et al., 2004, p. 382-383; Klapper, 2007b, p. 72, 74). *Palmatolepis ultima* has its lowest occurrences in Frasnian Subzone 13c so that its presence in IG-03b together with *P. bogartensis* and *P. winchelli* suggests this highest Frasnian subzone, which is in agreement with the placement of the Frasnian-Famennian boundary at Irish Gulf by Over (1997, fig. 8).

Identification of the lower boundary of the Lower *triangularis* Zone, and consequently the lower boundary of the Famennian, is based on the flood occurrence of *P. ultima* and the lowest occurrence of *P. subperlobata* s.s., as suggested by Klapper et al. (2004, p. 375-377) and accepted by Becker et al. (2012, p. 570).

Systematic paleontology

Abbreviations for the repository of figured specimens are USNM = U. S. National Museum, Washington; SUI = The University of Iowa; GSWA = Geological Survey of Western Australia, Perth.

Genus *Ancyrodella* Ulrich and Bassler, 1926

Ancyrodella rotundiloba rotundiloba (Bryant, 1921)
Figure 7.8, 7.9

Polygnathus rotundilobus Bryant, 1921, p. 26, pl. 12, figs. 1–6, text-fig. 7 [fig. 1 = lectotype, selected by Ziegler, 1958, p. 44].
Ancyrodella rotundiloba rotundiloba; Khalymbadzha and Chernysheva, 1970, p. 91, pl. 1, figs. 9–12; Huddle, 1981, p. B19, pl. 1, figs. 1–3, 6–8, 11–13 [figs. 1, 2 = reillustration of lectotype, not figs. 4, 5, 14, 15 = *A. triangulata* Kralick, 1994, nor figs. 16, 17 = *A.* sp. ?], pl. 3, figs. 20, 21; Bultynck and Jacobs, 1981, p. 17, pl. 10, figs. 1–9; Bultynck, 1982, p. 38, pl. 1, fig. 26 [only], pl. 2, figs. 1, 2 [not fig. 3 = *A. recta* Kralick, 1994].
Ancyrodella rotundiloba; late form of Klapper, 1985, p. 24, pl. 2, figs. 1–4, pl. 3, figs. 1–4, 12, pl. 4, figs. 9–12, pl. 8, figs. 9, 10, pl. 11, figs. 3, 4, text-fig. 3E–3J, M, N; Klapper, 2000, p. 158, pl. 1, figs. 6, 7, 9-14 [figs. 13, 14 = reillustration of lectotype, figs. 10, 11 = reillustration of Klapper, 1985, pl. 4, figs. 11, 12]; Uyeno and Wendte, 2005, p. 163, pl. 1, figs. 4, 5.
Ancyrodella rotundiloba; Sandberg et al., 1989, p. 212, pl. 2, figs. 5, 6 [not figs. 9, 10 = *A. recta* Kralick, 1994], pl. 3, fig. 7 [= reillustration of lectotype; not figs. 1, 2, 5, 6, 8, 9 = *A. recta*, nor figs. 3, 4 = *A.* sp. ?]; Kralick, 1994, p. 1387, figs.3.15–3.24 [figs. 3.21, 3.22 = reillustration of lectotype], figs. 4.7, 4.8, figs. 5.3, 5.4, 5.7–5.11; Gouwy et al., 2007, p. 389, figs. 15E–15G.
Ancyrodella soluta Sandberg et al., 1989, p. 211, pl. 2, figs. 1–4 [only; figs. 1, 2 = holotype]; Liao and Valenzuela-Ríos, 2008, p. 7, figs. 6 K, L.
Ancyrodella rotundiloba; late morphotypes of Kirchgasser, 1994, p. 125, pl. 2, figs. L, M, Q, R.
[not] *Ancyrodella rotundiloba;* Gouwy and Bultynck, 2000, p. 40, pl. 1, figs. 1, 2 [= *A. recta*].
Ancyrodella rotundiloba (Bryant, 1931 [sic]). Miller, 2007, p. 447, figs. 3A–3G, 3K, 3L, 5B, 5C.
Ancyrodella pristina Khalymbadzha and Chernysheva. Miller, 2007, p. 446, figs. 2A–2M, 3H, 3J.

Diagnosis.—Pa element: Platform outline more or less heart-shaped. Denticle or several denticles just posterior of free blade substantially lower than those following to the posterior, or there is a conspicuous gap in denticulation between the blade and carina. Platform covered with numerous coarse nodes. Pit of moderate size. Secondary keels lacking or only weakly developed at right angles to keel.

Remarks.—Based on Montagne Noire material, Klapper (1985) recognized two morphotypes of *Ancyrodella rotundiloba*, an early and a late form. The early form coincides with the types of *A. pristina* Khalymbadzha and Chernysheva (1970) and the late form with the types of *A. rotundiloba*. The morphological differences are not substantial and there are transitional forms between the two indicating that the two taxa should be treated at the most as subspecies.

In an interpreted ontogenetic series from a single sample in the Kozhym River section in the Sub-Polar Urals identified by Miller (2007, fig. 2) as *Ancyrodella pristina*, the smaller specimens (Miller, 2007, figs. 2N–2R) coincide with *A. pristina*, whereas the larger specimens (figs. 2A–2M) coincide with *A. rotundiloba*, especially considering the relative pit size. If this is indeed an ontogenetic series of a single taxon and not a mixture of two taxa, it suggests that the differences between *A. pristina* and *A. rotundiloba* are only at the morphotype level. Nevertheless, a key difference is the conspicuous gap in denticulation between the blade and carina commonly occurring in *A. rotundiloba*¸ although as already noted there is a

Figure 7. In Figures 7–12, abbreviations and locality/bed numbers refer to sampled beds (Figures 4–6; Appendix 1). Zone numbers refer to the Frasnian conodont zonation first developed in the Montagne Noire (Klapper, 1989) but since replicated at many sections in Devonian tropical areas (Klapper, 2007a). Magnifications all ×40; (**1, 4, 7, 9, 10, 11, 14, 16, 17**) are lower views, the rest are upper views of Pa elements. (**1, 2, 6, 7, 11, 12**) *Ancyrodella alata* Glenister and Klapper, (**1, 2**) USNM 608200, CP PY-7/2, Chidsey Point, Keuka Lake, Zone 4; (**6, 7**) USNM 608201, BP Nap-8/1, South Middlesex, Zone 4; (**11, 12**) USNM 608202, HB 19a/2, Fall Brook, Zone 3; (**3, 4**) *A. africana* García-López, USNM 608203, BC, 18a/5, Beards Creek, Zone 4; (**5, 10**) *A. rotundiloba pristina* Khalymbadzha and Chernysheva, USNM 608204, BC 18a/5, Beards Creek, Zone 4; (**8, 9**) *A. rotundiloba rotundiloba* (Bryant), USNM 608205, BC, 18a/5, Beards Creek, Zone 4; (**13, 14, 17, 18**) *A. rugosa* Branson and Mehl; (**13, 14**) USNM 608206, BP Nap-8/1, South Middlesex, Zone 4; (**17, 18**) USNM 608207, CP PY-7/2, Chidsey Point, Keuka Lake, Zone 4; (**15, 16**) *A. recta* Kralick, USNM 608208, HB, 19a/2, Fall Brook, Zone 3.

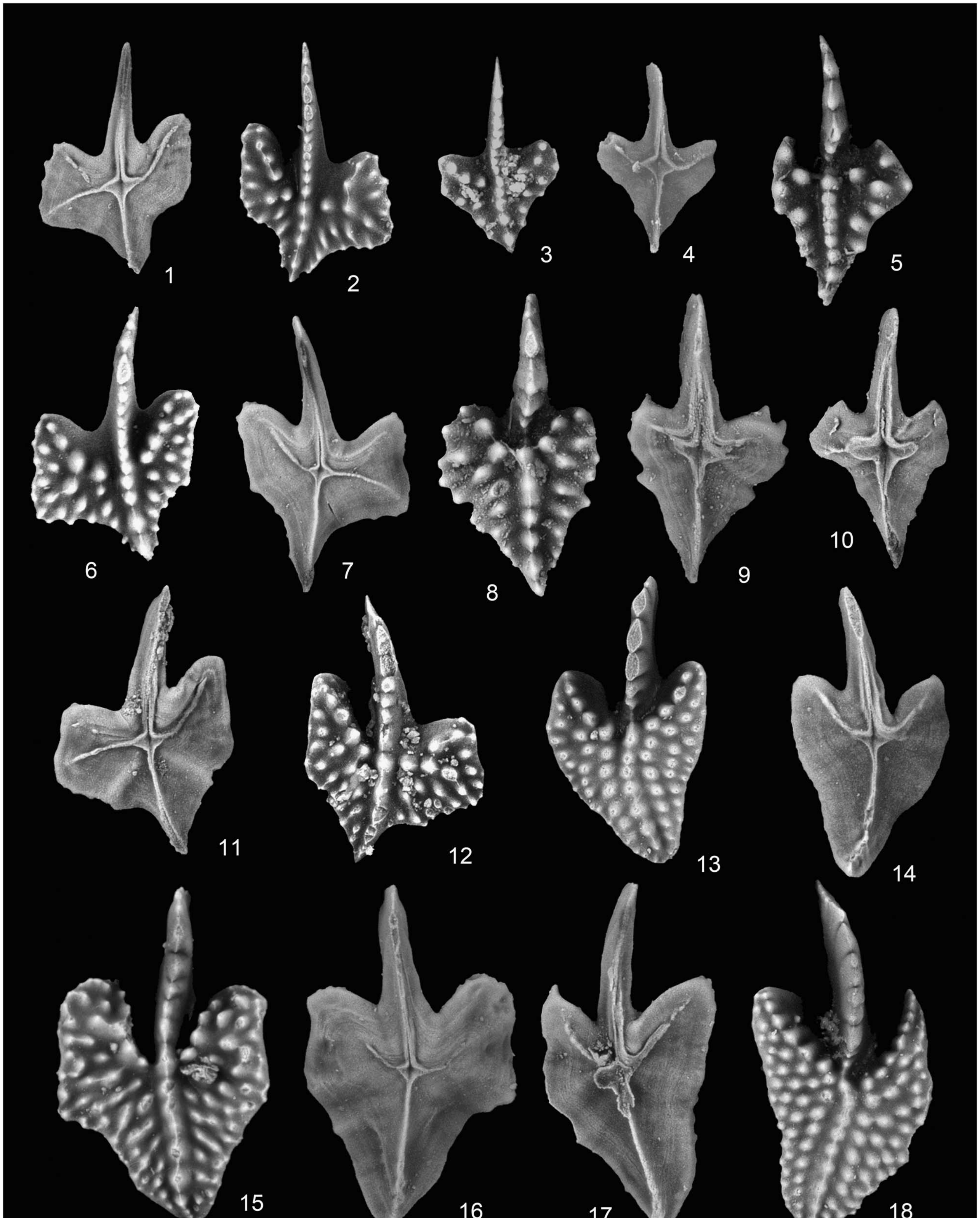

continuous transition between the two taxa. Thus, the two are treated here as subspecies, a possibility suggested by Gouwy et al. (2007, p. 389) and formally used by Aboussalam and Becker (2007).

The holotype of *Ancyrodella soluta* Sandberg et al. (1989, pl. 2, figs. 1, 2) coincides with *A. rotundiloba rotundiloba* as interpreted herein, whereas their other identified and illustrated specimens of *A. soluta* coincide with *A. rotundiloba pristina*

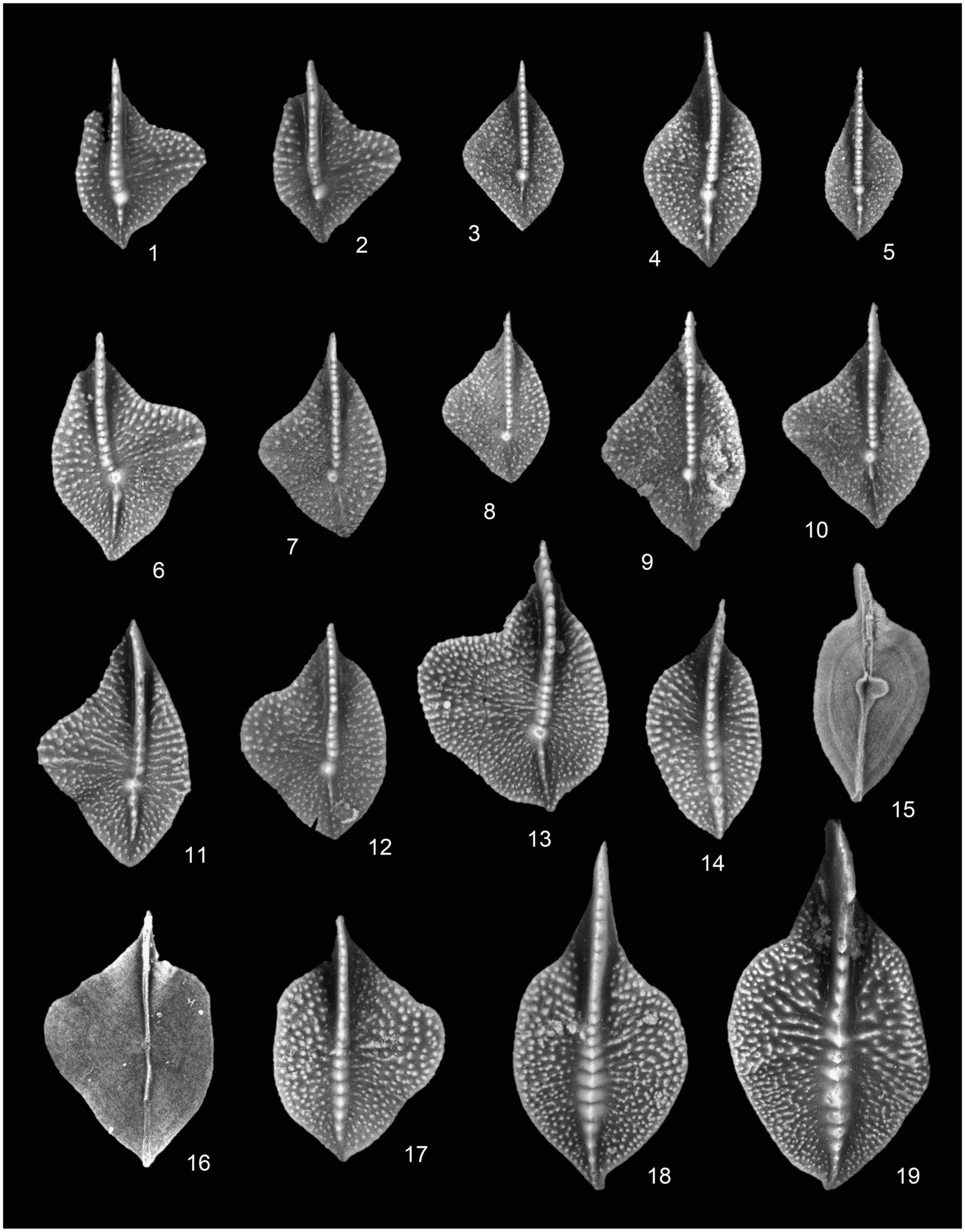

Figure 8. Magnifications all ×40; all are upper views of Pa elements, except *15* and *16* are lower views. (**1, 2**) *Palmatolepis spinata* Ovnatanova and Kuz'min, USNM 608209, 608210, SH 41a/5, North McMillan Creek, Zone 6; (**3–5**) *P. transitans* Müller, USNM 608211-608213, WS 42/1, Whetstone Brook, Zone 5; BC 18a/5, Beards Creek, Zone 4; BP Nap-8/1, South Middlesex, Zone 4; (**6–13**) *P. punctata* (Hinde), USNM 608214-608221; (**6, 11**) SH 41a/5, North McMillan Creek, Zone 6; (**7**) 44/3, Randall Gully, Zone 5; (**8, 9**) WS 42/1, Whetstone Brook, Zone 5; (**10**) PL 47/2, Conklin Gully, Zone 5; (**12, 13**) BK 65/1, Buck Run Creek, Zone 7; (**14, 15**) *Mesotaxis ovalis* (Ziegler and Klapper), USNM 608222, BP Nap-8/1, South Middlesex, Zone 4; (**16, 17**) *M. asymmetrica* (Bischoff and Ziegler) transitional with *Palmatolepis transitans* Müller, USNM 608223, BC 18a/5, Beards Creek, Zone 4; (**18, 19**) *M. asymmetrica*, USNM 608224, 608225, BP Nap-8/1, South Middlesex, Zone 4; CP PY-7/2, Chidsey Point, Zone 4.

(see respective synonymy lists). Earlier but somewhat different interpretations of the lack of validity of *A. soluta* have been given by Kralick (1994, p. 1387), Klapper (2000, p. 154), Gouwy et al. (2007, p. 389), and Miller (2007, p. 450).

Ancyrodella rotundiloba pristina Khalymbadzha and Chernysheva, 1970
Figure 7.5, 7.10

Ancyrodella pristina Khalymbadzha and Chernysheva, 1970, p. 89, pl. 1, figs. 3–8 [figs. 5–7 = holotype]; Sandberg et al., 1989, p. 210, pl. 1, figs. 3, 4, 9, 10, 13, 14; Gouwy et al., 2007, p. 389; Miller, 2007, p. 446, figs. 2N–2T; Liao and Valenzuela-Ríos, 2008, p. 2–3, 7, fig. 6 J [I = ?].
Ancyrodella prima Khalymbadzha and Chernysheva, 1970, p. 88, pl. 1, figs. 1, 2.
Ancyrodella rotundiloba; Kirchgasser, 1970, p. 343, pl. 65, figs. 5, 6, 8, 9.
Ancyrodella binodosa Uyeno, 1967. Bultynck and Jacobs, 1981, p. 16, pl. 8, figs. 1–14, pl. 9, figs. 1, 2, 6 [figs. 3–5, 7, 8 = transitional between *A. binodosa* and *A. rotundiloba pristina*]; Bultynck, 1982, p. 38, pl. 1, figs. 18–24 [not figs. 25, 28–30 = *A. binodosa*].
Ancyrodella rotundiloba rotundiloba; Bultynck, 1982, p. 38, pl. 1, fig. 27 [only];
Ancyrodella rotundiloba; early form of Klapper, 1985, p. 24, pl. 1, figs. 1–20, pl. 2, figs. 5–12, pl. 3, figs. 5–9 [misprinted in original as the late form, but corrected in distributed reprints]; Klapper, 2000, p. 158, pl. 1, figs. 1, 5 [= reillustration of Klapper, 1985, pl. 3, figs. 5, 6]; Uyeno and Wendte, 2005, p. 163, pl. 1, figs. 1, 2.
Ancyrodella soluta Sandberg et al., 1989, p. 211, pl. 1, figs. 5, 6, 11, 12 [only]; Liao and Valenzuela-Ríos, 2008, p. 7, figs. 6 M-P.
Ancyrodella rotundiloba; early morphotype of Kirchgasser, 1994, p. 125, pl. 2, figs. A–K, N–P.
Ancyrodella rotundiloba pristina Khalymbadzha and Chernysheva. Aboussalam and Becker, 2007, p. 364, figs. 9K, 9L, 9O–9R.

Diagnosis.—Pa element: Platform outline more or less triangular. Conspicuous gap in denticulation between the blade and carina generally lacking. Platform covered with numerous coarse nodes in large specimens. Pit of relatively large size. Secondary keels absent or extremely short and at right angles to keel.

Remarks.—Sandberg et al. (1989) indicated that *A. prima* also proposed by Khalymbadzha and Chernysheva (1970) was questionably a junior synonym. Aboussalam and Becker (2007, p. 364) formally treated *A. prima* as the junior synonym, so their action as first revisers must stand regardless of page precedence.

Ancyrodella nodosa Ulrich and Bassler, 1926
Figure 9.1–9.12

Ancyrodella nodosa Ulrich and Bassler, 1926, p. 48, pl. 1, figs. 10–13 [fig. 10 = lectotype, selected by Ziegler, 1958, p. 44]; Ziegler, 1958, p. 44, pl. 11, fig. 1; Glenister and Klapper, 1966, p. 798, pl. 86, figs. 9, 10 [only]; Huddle, 1968, p. 6, pl. 13, figs. 7–10 [only; reillustrations of Ulrich and Bassler, 1926, pl. 1, figs. 10, 11, 13, 12, respectively]; Seddon, 1970b, p. 94, pl. 7, fig. 18; Szulczewski, 1971, p. 14, pl. 2, fig. 4, pl. 5, figs. 2–4 [only]; Druce, 1976, p. 61, pl. 7, figs. 1–3, pl. 8, figs. 2, 3 [only]; Klapper and Lane, 1985, p. 925, figs. 14.6, 14.7, 14.10, 14.11; Baliński, 1979, p. 74, pl. 19, fig. 6; Dzik, 2002, p. 590, fig. 25 F, H [only; D, G = *Ancyrodella* sp. indet. juveniles; E = *Ancyrodella curvata* (Branson and Mehl, 1934) early form of Klapper, 1989; I = Pb, J = M elements of *Ancyrodella* sp. indet.].
Polygnathus spinulosa Youngquist, 1947, p. 110, pl. 24, fig. 9 [= juvenile specimen].
Polygnathus rotundiloba Bryant. Youngquist, 1947, p. 110, pl. 26, fig. 6 [= juvenile specimen].
Ancyrodella sp. Miller and Younguist, 1947, p. 503, pl. 74, fig. 13; Müller, 1956c, p. 1340, pl. 145, figs. 12, 14 [only].
Ancyrodella gigas Youngquist. Seddon, 1970b, p. 94, pl. 7, fig. 7 [only]; Bultynck and Jacobs, 1981, p. 24, pl. 9, figs. 9–11; Klapper, 1985, p. 29, pl. 10, figs. 3–6, 9, 10, 13–16; Gouwy and Bultynck, 2000, p. 40, pl. 1, figs. 9, 10 [only]; Gouwy et al., 2007, p. 389, fig. 15 N [only; fig. 15 M = *A. gigas*].
Ancyrodella gigas Youngquist form 1 of Klapper, 1989, p. 457; Over et al., 2003, pl. 1, fig. 5; Pisarzowska et al., 2006, p. 625, fig. 13D, 13E.

Diagnosis.—Pa element: Platform outline more or less triangular. Upper surface covered with coarse nodes. Secondary carinae well developed, reaching tips of anterior lobes. Nodes of secondary carinae not substantially higher than those of posterior platform. Each secondary carina meets or comes close to a slightly curved row of nodes that parallels the posterior carina and is separated from it by an adcarinal trough. Secondary keels well developed, reaching tips of anterior lobes. Pit relatively small.

Remarks.—The secondary carinae join or come close to a row of nodes on either side of the posterior carina in the Pa element of *A. nodosa* This is well shown by the lectotype and, for example, the Canadian specimens illustrated by Klapper and Lane (1985, figs. 14.6, 14.7, 14.10, 14.11). For the distinction with the morphologically closely related *Ancyrodella hamata*, see under the latter.

An ontogenetic series of specimens from the Montagne Noire (Klapper, 1985, pl. 10, figs. 3–6, 9, 10, 13–16) seems best placed in *Ancyrodella nodosa* although they were originally identified as *A. gigas* Youngquist (1947) and later termed *A. gigas* form 1 (Klapper, 1989, p. 457). They show the characteristic development of the rows of nodes parallel to the posterior carina. Such node rows are not present in the holotype of *A. gigas* (reillustrated in Klapper and Lane, 1985, fig. 14.15). The types of *A. devonica* García-López (1986, p. 448, pl. 3, figs. 1–10) compare closely with the small specimens of the Montagne Noire growth series, as indicated in the synonymy of García-López (1987, p. 60), and thus may also be synonymous with *A. nodosa*.

Ancyrodella hamata Ulrich and Bassler, 1926
Figure 9.13–9.18

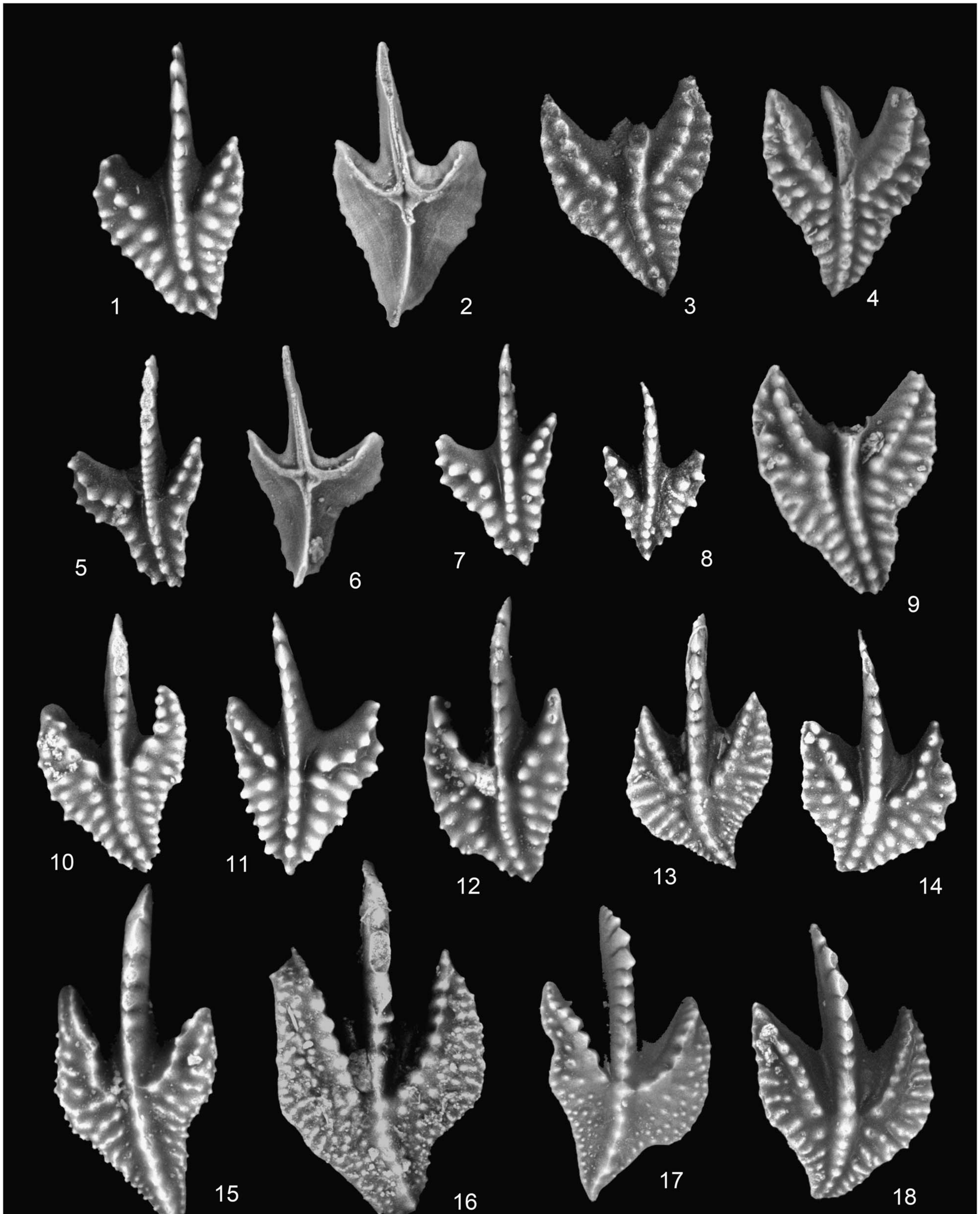

Figure 9. Magnifications all ×40; all are upper views of Pa elements, except *2* and *6* are lower views. (**1–12**) *Ancyrodella nodosa* Ulrich and Bassler; (**1, 2, 7, 8, 11, 12**) USNM 608226-608230, PL 47/2, Conklin Gully, Zone 5; (**3, 4**) paralectotype and lectotype , USNM 145871, 11303, new photographs (see also Huddle [1968, p. 6, pl. 13, figs. 10, 7]), Rhinestreet Shale = BR 30b/1, Acme Shale Co. pit, Weyer of this report, Zone 6; (**5, 6**) USNM 608231, 44/3, Randall Gully, Zone 5; (**9, 10**) USNM 608232-608233, SH 41a/5, North McMillan Creek, Zone 6; (**13–18**) *A. hamata* Ulrich and Bassler; (**13, 16**) SUI 5524c, 5525, new photographs, originally illustrated by Miller and Youngquist, 1947, pl. 74, figs. 12, 14 and identified by them as *A. lobata* and the holotype of *A. magister* (see synonymy), Sweetland Creek, Iowa (Appendix 1); (**14, 18**) USNM 608234-608235, BM 92/5, Beaver Meadow Creek, Zone 13b; (**15, 17**) USNM 608236-608237, RL 60/3, Relyea Creek, Zone 11.

Ancyrodella hamata Ulrich and Bassler, 1926, p. 48, pl. 7, fig. 7 [= holotype, reillustrated in Huddle, 1968, pl. 13, fig. 1]; Müller and Müller, 1957, p. 1091, pl. 136, fig. 4.
Ancyrodella symmetrica Ulrich and Bassler, 1926, p. 49, pl. 8, fig. 1 [reillustrated in Huddle, 1968, pl. 13, figs. 2, 3].
Ancyrodella buckeyensis Stauffer, 1938, p. 418, pl. 52, figs. 17, 18, 23, 24 [figs. 23, 24 = lectotype, selected by Müller and Müller, 1957, p. 1091]; Youngquist, 1945, p. 356, pl. 54, fig. 11; Müller and Müller, 1957, p. 1091, pl. 136, figs. 2, 5 [fig. 5 = reillustration of Müller, 1956c, pl. 145, fig. 13]; Ziegler, 1958, p. 40, pl. 11, fig. 7; Druce, 1976, p. 53, pl. 2, figs. 2, 5 [only]; Over, 1997, p. 172, figs. 11.1–11.9 [fig. 11.7 =reillustration of lectotype; synonymy]; Over and Rhodes, 2000, p. 109, fig. 6.1; Klapper et al., 2004, p. 383, fig. 5.5 [synonymy]; Klapper, 2007a, tables 1–3; Over, 2007, p. 1201, figs. 11.1–11.3; Navas-Parejo et al., 2009, p. 115, figs. 3.1, 3.2.
Ancyrodella plena Stauffer, 1938, p. 418, pl. 52, figs. 21, 22.
Ancyrodella robusta Stauffer, 1938, p. 418, pl. 52, figs. 28, 29.
Ancyrodella lobata Branson and Mehl. Miller and Youngquist, 1947, p. 502, pl. 74, figs. 10–12; Dzik, 2002, p. 590, fig. 27A, 27B [only].
Ancyrodella magister Miller and Youngquist, 1947, p. 503, pl. 74, fig. 14.
Ancyrodella subrotunda Miller and Youngquist, 1947, p. 503, pl. 74, fig. 17; Müller and Müller, 1957, p. 1092, pl. 136, fig. 6.
Ancyrodella nodosa; Youngquist and Miller, 1948, p. 441, pl. 68, figs. 13, 14; Bischoff, 1956, p. 119, pl. 8, figs. 12, 15; Glenister and Klapper, 1966, p. 798, pl. 86, figs. 5–8, 11, 12 [only]; Seddon, 1970a, p. 753, pl. 16, fig. 5; Szulczewski, 1971, p. 14, pl. 2, fig. 5 [only]; Druce, 1976, p. 61, pl. 8, fig. 1 [only]; Orchard, 1978, p. 928, pl. 114, fig. 3; Mouravieff, 1982, p. 113, pl. 2, fig. 8, pl. 3, figs. 8, ?9; Fuchs, 1987, pl. 3, figs. 5, 10 [only]; Uyeno, 1992, p. 72, pl. 16, figs. 1–6.
Ancyrodella sp. Müller, 1956c, p. 1340, pl. 145, fig. 13 [only].
Ancyrodella gigas Youngquist. Müller and Müller, 1957, p. 1091, pl. 141, fig. 8 [not pl. 142, fig. 1 = ? juvenile of *A. gigas*].

Diagnosis.—Pa element: Platform outline more or less triangular. Upper surface covered with coarse to fine nodes. Secondary carinae well developed, reaching tips of anterior lobes. Nodes of secondary carinae substantially higher than those of posterior platform. Secondary carinae meet carina or just short of it at the adcarinal troughs, and are not continued by a row of nodes on each side of posterior carina. Secondary keels well developed, reaching tips of anterior lobes. Pit relatively small.

Remarks.—Over (1997, p. 174, figs. 11.1–11.9) illustrated an ontogenetic series for the species called *Ancyrodella buckeyensis* in much of the Frasnian conodont literature. This evidence demonstrates that the lectotype of *A. buckeyensis* is a juvenile specimen, the mature form of which is represented by *A. hamata* and its many junior synonyms indicated in the above listing.

Ancyrodella hamata (= *A. buckeyensis*) lacks the posterior rows of nodes parallel to the carina that are present in the Pa element of *A. nodosa*. This was noted by Over (1997, p. 174), Over and Rhodes (2000, p. 109), and Klapper et al. (2004, p. 383) as the distinction between *A. buckeyensis* and *A. nodosa*. Furthermore, the secondary carinae are higher than the posterior nodes in *A. hamata*, whereas they are more or less at the same height in *A. nodosa*. The platform outlines of the two species overlap, so this feature cannot be used consistently as a distinction.

Huddle (1968) synonymyzed *Ancyrodella hamata* under *A. nodosa* and Klapper and Lane (1985, p. 925) synonymyzed *A. buckeyensis* under *A. nodosa*. However, the two species can be distinguished as described above. The Pa element of *Ancyrodella gigas* Youngquist (1947) has a longer and narrower platform than in *A. hamata*.

Genus *Polygnathellus* Bassler, 1925

Type species.—*Polygnathellus typicalis* Bassler, 1925 (by subsequent designation, Hass, 1959).

Remarks.—The genus *Polygnathellus* is rare in Frasnian faunas, apparently limited to Zone 4, and consequently poorly understood. Ulrich and Bassler (1926, p. 53, pl. 1, figs. 1–3) described the type species of *Polygnathellus*, illustrating three syntypes of *P. typicalis*. A lectotype for the type species was first designated by Hass (1959, p. 380) who selected the specimen in Ulrich and Bassler (1926, pl. 1, fig. 1). Unaware of Hass' selection, Rhodes (in Rhodes et al., 1966, p. 4) selected the specimen of Ulrich and Bassler (1926, pl. 1, fig. 3) as lectotype, and Huddle (1968, p. 37 and explanation of pl. 4, fig. 10) chose the same specimen as did Hass. As first reviser, Hass' designation of the lectotype must stand. This is a matter of some consequence, as the specimen in Ulrich and Bassler (pl. 1, fig. 3; reillustrated in Huddle, 1968, pl. 4, fig. 3) differs from what has generally been regarded as *Polygnathellus*. Instead it is arguably an element of the form genus *Bryantodus* Bassler (1925), which in turn has been reconstructed as the Pb element of *Ancyrodella* by Klapper and Philip (1972, p. 99). The effect of Rhodes' action (in Rhodes et al., 1966, p. 4) would have made *Polygnathellus* a junior synonym of *Bryantodus*, but his action was invalid as he was not the first to select a lectotype.

Most of the specimens identified herein as *Polygnathellus* n. sp. are interpreted as Pa elements. Admittedly there is a similarity to a Pb element such as *Nothognathella* Branson and Mehl (1934), which is well established as the Pb element of many species of *Palmatolepis*, as well as the Pb element of *Mesotaxis*. Nevertheless, typical Pb elements accompany the Pa elements in one of our Australian collections. This evidence refutes the opinion of Klapper (in Clark et al., 1981, p. W178) in which *Polygnathellus* was treated as a senior synonym of *Nothognathella* and mistakenly regarded as a Pb element.

Polygnathellus n. sp.
Figures 10.15–10.18; 11.1–11.4

Diagnosis.—Pa element: Carinal denticles posterior of cusp extremely low. Inner platform wide with downward flange-like projection at central part of inner margin.

Remarks.—The Pa element of *Polygnathellus* n. sp. is moderately arched anteriorly and more sharply posterior of the cusp. The cusp is commonly distinct and higher than the carinal denticles and the inner platform is wide. The downward flange at the inner margin centrally is either in the shape of a downward

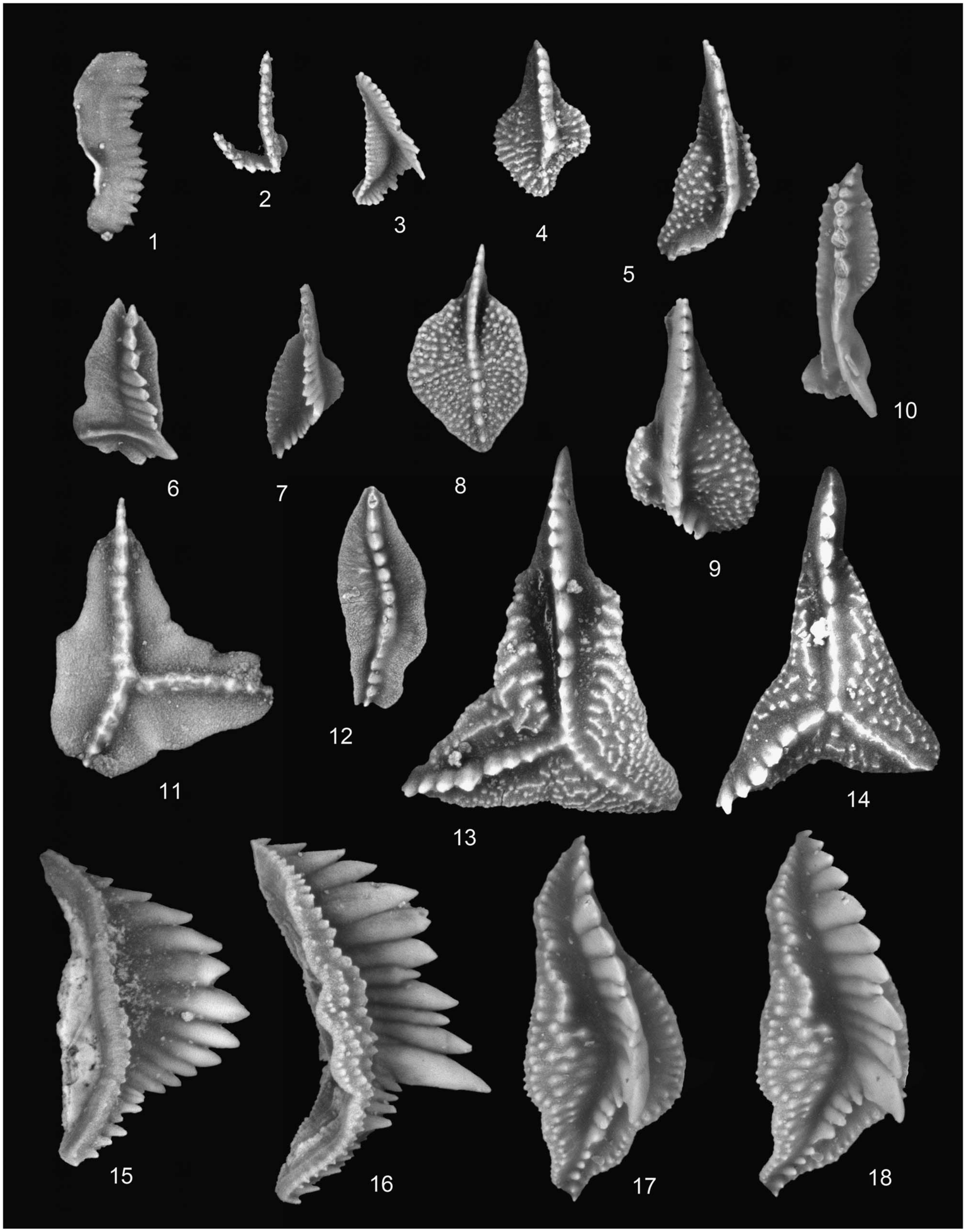

convex curve or it is a double convex curve demarcated by an intermediate sinus. The carina is sinuous and there is a distinct and moderately wide adcarinal trough anteriorly. A strong keel is present anterior and posterior of the evidently small pit that is covered by basal plate material in our Australian material, but is visible and small in the New York specimens.

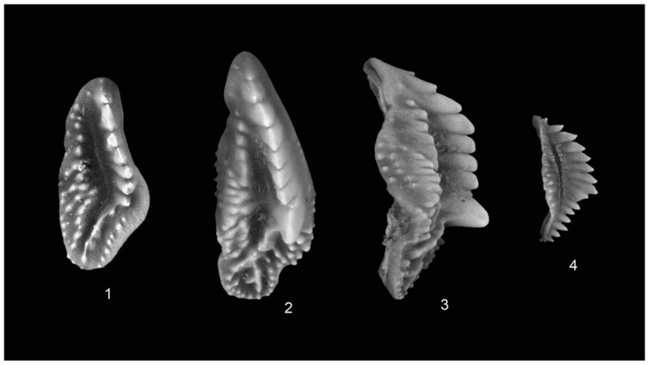

Figure 11. Magnifications all ×20; (**1, 2**) upper views; (**3, 4**) lateral views. All are Pa elements, except (**4**), which is a Pb element. *Polygnathellus* n. sp. (**1**) USNM 608252, CP PY-7/2, Chidsey Point, Zone 4; (**2, 3**) GSWA F52036, Timanites Hill, Canning Basin, sample 370B, Zone 4; (**4**) GSWA F52037, same sample as preceding.

There are three specimens of an accompanying Pb element in one of the Australian collections of the new species (Timanites Hill, 370B). The unit is moderately arched, slightly less than in the Pa element, with some downward arching posteriorly. The carinal denticles are very high anteriorly and extremely low posteriorly as in the Pa element, a unifying characteristic. There is a narrow inner platform in the Pb element.

The carinal denticles posterior of the cusp are strikingly lower in the Pa element of the new species in contrast with those of normal height in *Polygnathellus typicalis* Bassler (reillustrations in Huddle, 1968, pl. 4, figs. 6, 10). Another critical difference is the lack of a downward flange at the inner margin of the platform in the established species.

There are two Pa elements in the New York collections (Chidsey Point, sample 4046). At Timanites Hill in Western Australia, there is one Pa element in sample 370A, five Pa and 3 Pb elements in 370B. There is an obvious difference in the posterior termination of the platform in the Pa element in comparison of the specimens in Figures 11.1 and 11.2 versus that of Figures 10.17, 10.18 (two views of the same specimen). However, there is far too little material to determine the range of intraspecific variation and whether we are dealing with one or two new species, let alone to establish a formally named species. Thus, these specimens are retained in open nomenclature provisionally as one species.

Genus *Palmatolepis* Ulrich and Bassler, 1926
Palmatolepis amplificata Klapper, Kuz'min, and Ovnatanova, 1996
Figure 12.8–12.15

Palmatolepis (Manticolepis) flabelliformis (Stauffer, 1938). Müller and Müller, 1957, p. 1101, pl. 139, figs. 3, 5, 6 [not fig. 4 = *P. rhenana* Bischoff, 1956].
Palmatolepis gigas Miller and Youngquist. Seddon, 1970b, p. 102, pl. 11, fig. 10; Szulczewski, 1971, p. 31-32, pl. 11, figs. 2, 5 [only]; Austin et al., 1985, p. 150, pl. 4.6, figs. 8, 9 [only; re-illustration of Matthews and Riddolls, see below]; Ovnatanova and Kuz'min, 1991, p. 49, pl. 3, fig. 18.
Palmatolepis punctata (Hinde, 1879) transitional to *P. gigas* Miller and Youngquist, Seddon, 1970b, p. 102, pl. 11, fig. 11.
Palmatolepis subrecta Miller and Youngquist. Hass, 1959, pl. 50, fig. 22; Seddon, 1970b, p. 102, pl. 11, fig. 4; Matthews and Riddolls, *in* Selwood et al., 1984, p. 34, pl. 6, figs. 13, 15 [only].
Palmatolepis aff. *P. rhenana* Bischoff, 1956. Klapper and Lane, 1989, p. 474, pl. 1, figs. 11, 13 [not pl. 1, figs. 10, 12 = *P. brevis* Ziegler and Sandberg, 1990].
Palmatolepis kireevae Ovnatanova, 1976. Klapper and Lane, 1989, p. 474, pl. 1, fig. 7.
Palmatolepis amplificata Klapper et al., 1996, p. 140, figs. 7.1, 7.2, 7.4 [fig. 7.2 = holotype; synonymy]; Ovnatanova et al., 1999, p. 356, pl. 2, figs. 7, 10; Ovnatanova and Kononova, 2008, p. 1087, pl. 9, figs. 1–9 [figs. 1–3 = figs. 7.2, 7.1, 7.4 of Klapper et al., 1996].
Palmatolepis manzuri Bardashev, 2009, p. 302, pl. 7, fig. 7.

Diagnosis.—Pa element: Outline of platform roughly triangular. Outer lobe wide, midline of lobe directed laterally, well demarcated by anterior and posterior sinuses. Outer posterior margin convex to weakly convex between first sinus and posterior tip, a second sinus weakly developed in front of tip. Blade much higher than anterior carina, together outwardly curved to almost straight. Posterior carina almost straight to angled inwardly, may reach posterior tip or short of that lying in a shallow groove. Parapet on anterior inner platform consisting of a cluster of nodes, or straight to curved row of nodes. Secondary carina developed in mature specimens.

Remarks.—In a comprehensive synonymy list, Ziegler and Sandberg (1990, p. 54) continued the then long-standing practice of including within the concept of *Palmatolepis gigas* almost any Frasnian named species of *Palmatolepis* based on a Pa element with a widely expanded outer lateral lobe. This concept began after W. Ziegler's study of the holotype in the University of Iowa collections in October 1961, as a result of which he regarded *P. rhenana* Bischoff (1956) as a junior synonym of *P. gigas*, despite the distinctly different platform outlines. His study of the *P. gigas* holotype was too late to affect

Figure 10. Magnifications all ×40; (**1, 15, 16**) lateral views, (**3, 6, 18**) oblique-upper views, the rest are upper views. All are Pa elements, except (**3–5, 7, 9, 15**, which are Pb elements. (**1**) *Ozarkodina bidentatiformis* (Pham), USNM 608238, BR 30a/12, Pike Creek, Zone 6; (**2**) *O. nonaginta* Klapper, Kuz'min, and Ovnatanova, USNM 608239, CT 32/23, Cazenovia Creek Tributary, Zone 7; (**3**) *Palmatolepis spinata* Ovnatanova and Kuz'min, USNM 608240, SH 41a/5, North McMillan Creek, Zone 6; (**4**) *P. punctata* (Hinde), USNM 608241, PL 47/2, Conklin Gully, Zone 5; (**5, 9**) *Mesotaxis asymmetrica* (Bischoff and Ziegler), USNM 608242-608243, BP Nap-8/1, South Middlesex, Zone 4, CP PY-7/2, Chidsey Point, Zone 4; (**6**) *Ancyrognathus primus* Ji, USNM 608244, SH 41a/5, North McMillan Creek, Zone 6; (**7**) *P. punctata?*, USNM 608245, SH 41a/5, North McMillan Creek, Zone 6; (**8**) *M. johnsoni* Klapper, Kuz'min, and Ovnatanova, USNM 608246, WS 42/1, Whetstone Brook, Zone 5; (**10**) *Ancyrognathus? deformis* (Anderson), USNM 608247, SG 80/14 , Stony Brook, Varysburg (Gassman Road), Zone 12; (**11**) *A. primus* Ji, USNM 608248, CT 32/23, Cazenovia Creek Tributary, Zone 7; (**12**) *A. ancyrognathoideus* (Ziegler), USNM 608249, BK 65/1, Buck Run Creek, Zone 7; (**13**) *A. triangularis* Youngquist, USNM 608250, SF 79/10, Stony Brook, Varysburg, Zone 12; (**14**) *A. iowaensis* Youngquist, USNM 608251, RL 60/3, Relyea Creek, Zone 11; (**15–18**) *Polygnathellus* n. sp. (**15**) GSWA F52034, Timanites Hill, Canning Basin, sample 370B, Zone 4; (**16–18**) GSWA F52035, Timanites Hill, sample 370A, Zone 4.

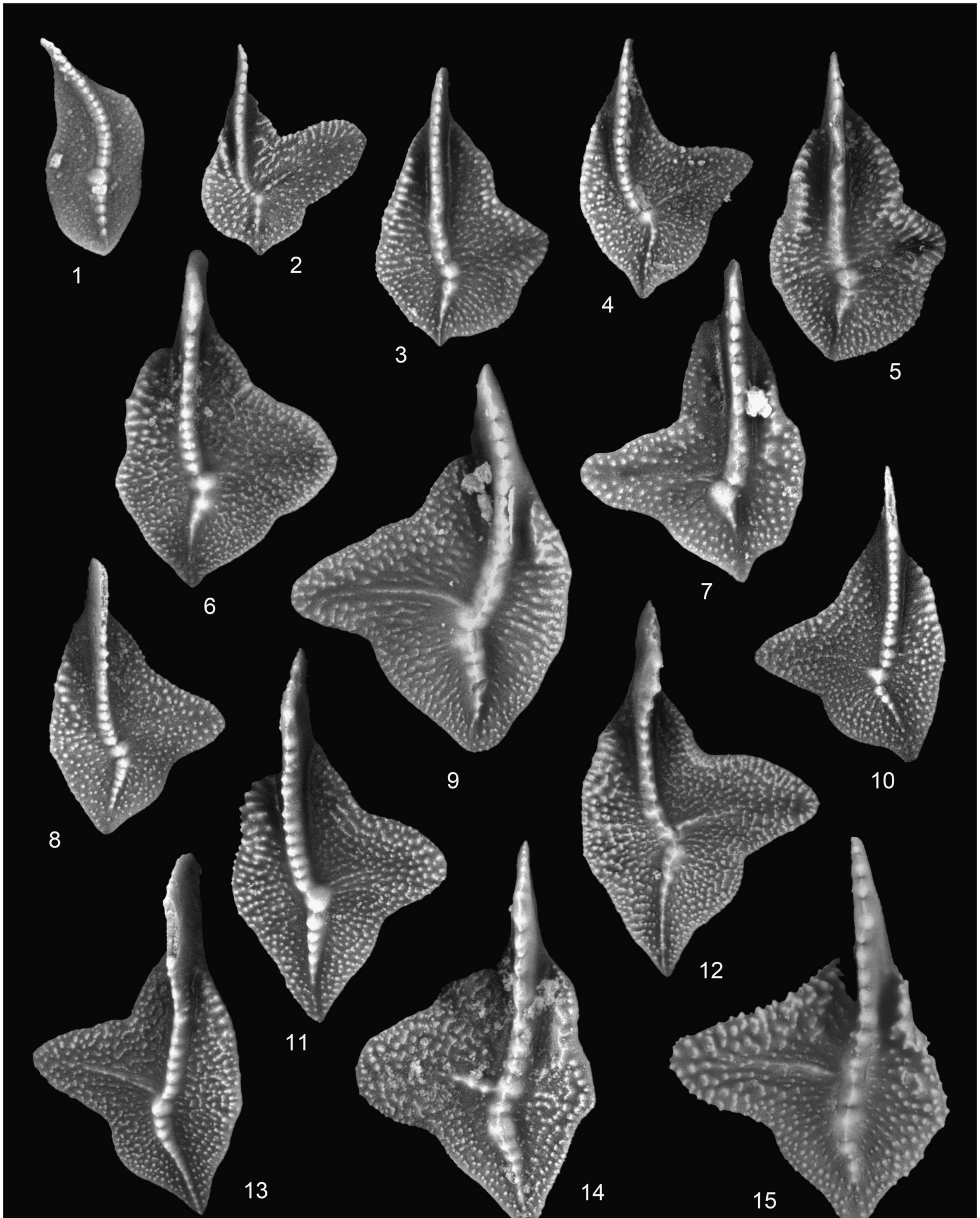

Figure 12. Magnifications all ×40; all are upper views of Pa elements. (**1**) *Palmatolepis linguiformis* Müller, USNM 608253, IL 90/2, Irish Gulf, Zone 13b; (**2**) *P. semichatovae* Ovnatanova, USNM 608254, RL 60/3, Relyea Creek, Zone 11; (**3, 5**) *P. foliacea* Youngquist, USNM 608255-608256, SG 80/14, Stony Brook, Varysburg (Gassman Road), Zone 12; (**4**) *P. hassi* Müller and Müller s.s., USNM 608257, CB 92/2, Beaver Meadow Creek, Zone 12; (**6**) *P. hassi* Müller and Müller s.l., USNM 608258, RL 60/3, Relyea Creek, Zone 11; (**7**) *P. winchelli* (Stauffer), USNM 608259, BM 92/5, Beaver Meadow Creek, Zone13b; (**8–15**) *P. amplificata* Klapper, Kuz'min, and Ovnatanova, USNM 608260-608267; (**8, 14**) SF 79/8a, Stony Brook, Varysburg, Zone 12; (**9, 15**) SG 80/14, Stony Brook, Varysburg (Gassman Road), Zone 12; (**10**) SF 79/10, Stony Brook, Varysburg, Zone 12; (**11–13**) RL 60/3, Relyea Creek, Zone 11.

the nomenclature in Ziegler (1962), the proofs of which he had already returned; the change was noted in Ziegler (1971, p. 267). Ziegler and Sandberg (1990), however, treated the two as separate species due to their different outlines and different lateral profiles of the blade, among other features. But in their synonymy list they considered many specimens and different species such as *P. unicornis* Miller and Youngquist (1947) as falling within the concept of *P. gigas*. The holotype, which is the sole specimen in the Sweetland Creek collection identified by Miller and Youngquist (1947) as *P. gigas*, has not been matched by any subsequently illustrated specimen, especially in terms of the unique platform outline. This uniqueness of the platform outline of the holotype was discussed by Klapper and Foster (1993, p. 31–32) in their shape analysis of potentially related species of *Palmatolepis*. They concluded that "the overall morphology of the *P. gigas* holotype suggests that it can be interpreted as a large, aberrant Pa element of *P. winchelli*." Klapper (2007a, p. 529, 531) formally considered *P. gigas* as a junior synonym of *P. winchelli* (Stauffer, 1938).

Palmatolepis amplificata Klapper et al. (1996) here includes the Iowa Amana beds specimens identified as *P. flabelliformis* Stauffer (1938) by Müller and Müller (1957), though that expands the concept somewhat. However, the New York material of *P. amplificata* (Fig. 12.8–12.15) provides a link between the Timan types and the Iowa specimens. And the Amana specimen of Müller and Müller (1957, pl. 139, fig. 3) with the extremely wide lobe provides a further link to the central Texas specimen illustrated by Seddon (1970b, pl. 11, fig. 10) and the Devon specimen of Matthews and Riddolls (1984, pl. 6, figs. 13, 15). Additional specimens illustrated by Seddon (1970b, pl. 11, figs. 4, 11) agree well with the Timan and New York examples of the species; the specimen identified as *P. subrecta* Miller and Youngquist (Seddon, 1970b, pl. 11, fig. 4) has the following characteristics of the species: strong anterior inner parapet, the posterior carina lying in a narrow trough near the posterior end, and the distal part of the secondary carina curved slightly to the posterior.

The holotype of *Pamatolepis manzuri* Bardashev (2009, pl. 7, fig. 7) is closely comparable if not identical to the center of the range of variation of *P. amplificata*, yet a comparison of the two species was not discussed originally. Other specimens assigned to *P. manzuri* (e.g., Bardashev, 2009, pl. 7, figs. 1, 4, 13, 16) are likely also synonymous with *P. amplificata*.

Acknowledgments

We thank J. Repetski (U.S. Geological Survey, Reston) for loan of conodont slides of the samples collected by J. Huddle in 1974. G. Baird (SUNY Fredonia), C. Brett (Cincinnati University) and D.J. Over (SUNY Geneseo) are thanked for collaborations over many years on the stratigraphy of the Upper Givetian and Frasnian in western New York. C.A. Sandberg (emeritus at the U. S. Geological Survey, Denver) provided much encouragement for the completion of this study and specifically discussed the taxonomic problem surrounding *Polygnathellus* and its relation to the Pb elements of *Palmatolepis* and *Mesotaxis*. We thank Neo McAdams (University of Iowa) for her indispensable help with the Visionary Digital BK Lab System (http://www.visionarydigital.com/IntegratedSystems2.html). This was especially so in her running the software that composites the multiple images taken at different focal planes. We also thank Tiffany Adrain, curator of the conodont and other fossil collections at Iowa, for her expert assistance. Sofie Gouwy (Royal Belgium Institute of Natural Sciences, Brussels) generously provided advice for the running of GraphCor on Windows XP and 7, for which it was not designed. The GraphCor program was designed by Kenneth Hood in the late 1980s and revised until 1995 (version 3.0). We thank Curt Klug who processed and picked the samples G.K. collected with W.K. in 1989 and 1991. Partial funding from NSF grants EAR87-06567 (to G.K.) and EAR89-03475 (to G.K.; supplemented by an NSF ROA to W.T.K., 1990-91) and grants to W.T.K. from SUNY Potsdam. We are indebted for comments by D.J. Over and an anonymous reviewer.

References

Aboussalam, Z.S., and Becker, R.T., 2007, New Upper Givetian to basal Frasnian conodont faunas from the Tafilalt (Anti-Atlas, southern Morocco): Geological Quarterly, v. 51, p. 345–374.

Aboussalam, Z.S., and Becker, R.T., 2011, The global Taghanic biocrisis (Givetian) in the eastern Anti-Atlas, Morocco: Palaeogeography, Palaeoclimatology, Palaeoecology, v. 304, p. 136–164.

Anderson, W.I., 1966, Upper Devonian conodonts and the Devonian-Mississippian boundary of north-central Iowa: Journal of Paleontology, v. 40, p. 395–415.

Aristov, V.A., 1988, Devonskie konodonty tsentral'nogo Devonskogo Polya (Russkaya Platforma): Akademiya Nauk SSSR, Geologicheskiy Institut, Trudy, v. 432, 119 p. [In Russian].

Austin, R.L., Orchard, M.J., and Stewart, I.J., 1985, Conodonts of the Devonian System from Great Britain (with contributions from Barnes, R.P., Castle, C., Drummond, M., Kirchgasser, W.T., Sadler, P.M., and Selwood, E.B.), *in* Higgins, A.C., and Austin, R.L., eds., A Stratigraphical Index of Conodonts, Chichester, British Micropalaeontological Society Series, p. 93–166.

Baird, G.C., Brett, C.E., and Kirchgasser, W.T., 1989, Genesis of black shale-roofed discontinuities in the Genesee Formation, western New York, *in* McMillan, N.J., Embry, A.F., and Glass, D.J., eds., Devonian of the World, Calgary, Canadian Society of Petroleum Geologists Memoir, v. 14(2), p. 357–375. [date of imprint, 1988].

Baird, G.C., Kirchgasser, W.T., Over, D.J., and Brett, C.E., 2006, An early late Devonian bone-bed-pelagic limestone succession: the North Evans–Genundewa Limestone story. *in* Jacobi, R., ed., New York State Geological Association Field Trips (Guidebook), 78th Annual Meeting, SUNY University at Buffalo, Buffalo, New York, p. 354–395.

Baird, G.C., Over, D.J., Kirchgasser, W.T., and Brett, C.E., 2006, Middle-Upper Devonian depositional and biotic events in Western New York, *in* Jacobi, R., ed., New York State Geological Association Field Trips (Guidebook), 78th Annual Meeting, SUNY University at Buffalo, Buffalo, New York, p. 128–164.

Baliński, A., 1979, Brachiopods and conodonts from the Frasnian of the Dębnik Anticline, southern Poland: Palaeontologia Polonica, v. 39, p. 3–95.

Bardashev, I.A., 2009, New Frasnian conodonts of the genus *Palmatolepis* from the central Tajikistan Paleontological Journal, v. 43, p. 300–305. [Translated from Paleontologicheskiy Zhurnal, v. 2009 (3), p. 61–66.].

Bardashev, I.A., and Bardasheva, N.P., 2012, Platform conodonts from the Givetian-Frasnian boundary (Middle-Upper Devonian): Academy of Science, Republic of Tajikistan, Institute of Geology, Seismic Building and Seismology, Donish Publishing House, Dushanbe, 91 p. [Translation of the Russian original version by V. P. Glavcheva].

Bassler, R.S., 1925, Classification and stratigraphic use of the conodonts: Geological Society of America Bulletin, v. 36, p. 218–220.

Becker, R.T., and House, M.R., 1997, Sea-level changes in the Upper Devonian of the Canning Basin, Western Australia: Courier Forschungsinstitut Senckenberg, v. 199, p. 129–146.

Becker, R.T., and House, M.R., 2000, Devonian ammonoid zones and their correlation with established series and stage boundaries, *in* Bultynck, P., ed., Subcommission on Devonian Stratigraphy: fossil groups important for boundary definition: Courier Forschungsinstitut Senckenberg, v. 220. p. 113–151.

Becker, R.T., Gradstein, F.M., and Hammer, O., 2012, The Devonian Period, *in* Gradstein, F.M., Ogg, J.G., Schmitz, M.D., and Ogg, G.M., eds., The Geologic Time Scale 2012, Amsterdam, Elsevier, p. 559–601.

Bischoff, G., 1956, Oberdevonische Conodonten (toIδ) aus dem Rheinischen Schiefergebirge: Notizblatt des Hessischen Landesamtes für Bodenforschung zu Wiesbaden, v. 84, p. 115–137.
Bischoff, G., and Ziegler, W., 1957, Die Conodontenchronologie des Mitteldevons und des tiefsten Oberdevons: Abhandlungen des Hessischen Landesamtes für Bodenforschung, v. 22, 136 p.
Branson, E.B., and Mehl, M.G., 1933, A study of Hinde's types of conodonts preserved in the British Museum: University of Missouri Studies, v. 8, p. 133–156. 165–167.
Branson, E.B., and Mehl, M.G., 1934, Conodonts from the Grassy Creek Shale of Missouri: University of Missouri Studies, v. 8, p. 171–259. [date of imprint, 1933].
Brett, C.E., Algeo, T.J., and Mclaughlin, P.I., 2003, Use of event beds and sedimentary cycles in high-resolution stratigraphic correlation of lithologically repetitive successions: the Upper Ordovician Kope Formation of northern Kentucky and southern Ohio, *in* Harries, P.J., ed., High-Resolution Stratigraphic Paleontology, The Netherlands, Kluwer Academic Publishers, p. 315–350.
Bryant, W.L., 1921, The Genesee conodonts: Buffalo Society of Natural Sciences Bulletin, v. 13, 59 p.
Bultynck, P., 1982, Conodont succession and general faunal distribution across the Givetian-Frasnian boundary beds in the type area (with contributions by Jacobs, L.), *in* Bigey, F., et al. Papers on the Frasnian-Givetian boundary, Brussels, Geological Survey of Belgium and Subcommission on Devonian Stratigraphy, p. 34–59.
Bultynck, P., 1986, Accuracy and reliability of conodont zones: the *Polygnathus asymmetricus* "zone" and the Givetian-Frasnian boundary: Bulletin de l'Institut royal des Sciences naturelles de Belgique, Sciences de la Terre, v. 56, p. 269–280.
Bultynck, P., and Jacobs, L., 1981, Conodontes et sédimentologie des couches de passage du Givetien au Frasnien dans le Nord du Tafilalt et dans le Ma'der (Maroc présaharien): Bulletin de l'Institut royal des Sciences naturelles de Belgique, Sciences de la Terre, v. 53, p. 1–24.
Bultynck, P., Helsen, S., and Hayduckiewich, J., 1998, Conodont succession and biofacies in upper Frasnian formations (Devonian) from the southern and central parts of the Dinant Synclinorium (Belgium)—(Timing of facies shifting and correlation with late Frasnian events): Bulletin de l'Institut royal des Sciences naturelles de Belgique, Sciences de la Terre, v. 68, p. 25–75.
Clark, D.L., et al., 1981, Conodonta, *in* Robison, R.A., ed., Treatise on Invertebrate Paleontology, Part W, Miscellanea, Supplement 2, Lawerence, Geological Society of America and The University of Kansas, 202 p.
Cszonka, J., Bush, A.M., and Beard, A., 2013, Testing the correlation of the Frasnian/Famennian boundary (Late Devonian) in shallow water paleoenvironments in New York: Geological Society of America, Abstracts with Programs, v. 45(1), p. 53.
Day, J., 1990, The Upper Devonian (Frasnian) conodont sequence in the Lime Creek Formation of north-central Iowa: Journal of Paleontology, v. 64, p. 614–628.
De Witt, W., Jr., and Colton, G.W., 1978, Physical stratigraphy of the Genesee Formation (Devonian) in western and central New York: U. S. Geological Survey Professional Paper, v. 1032-A, 22 p.
Druce, E.C., 1976, Conodont biostratigraphy of the Upper Devonian Reef Complexes of the Canning Basin, Western Australia: Australia Bureau of Mineral Resources, Geology and Geophysics Bulletin, v. 158, 303 p.
Dzik, J., 2002, Emergence and collapse of the Frasnian conodont and ammonoid communities in the Holy Cross Mountains, Poland: Acta Palaeontologica Polonica, v. 47, p. 565–650.
Edwards, L.E., 1989, Supplemented graphic correlation: a powerful tool for paleontologists and nonpaleontologists: Palaios, v. 4, p. 127–143.
Ettensohn, F.R., 1985, Controls on development of Catskill Delta complex basin facies, *in* Woodrow, D.L., and Sevon, W.D., eds., The Catskill Delta: Geological Society of America Special Paper 201, p. 65–77.
Fuchs, A., 1987, Conodont biostratigraphy of the Elbingerode Reef Complex, Harz Mountains: Acta Geologica Polonica, v. 37, p. 33–50.
García-López, S., 1981, Nueva especie de *Ancyrodella* (Conodonta) del Devónico Superior de la Cordillera Cantábrica (no. de España): Estudios Geológicos, v. 37, p. 263–267.
García-López, S., 1986, Basis for the establishment of a new phylogeny of the genus *Ancyrodella*: Revista Española de Micriopaleontología, v. 18, p. 443–456.
García-López, S., 1987, Los conodontos y su aplicación al estudio de las divisions cronostratigraficas mayors del Devónico Asturleones (España), Madrid, Publicaciones Especiales del Boletín Geológico y Minero, Instituto Geológico y Minero de España, 112 p.
Girard, C., Klapper, G., and Feist, R., 2006, Subdivision of the terminal Frasnian *linguiformis* conodont zone, revision of the correlative interval of Montagne Noire Zone 13, and discussion of stratigraphically significant associated trilobites, *in* Over, D.J., Morrow, J.R., and Wignall, P.B., eds., Understanding Late Devonian and Permian-Triassic Biotic and Climatic Events: Towards an Integrated Approach: Developments in Palaeontology and Stratigraphy, v. 20, p. 181–198.
Glenister, B.F., and Klapper, G., 1966, Upper Devonian conodonts from the Canning Basin, Western Australia: Journal of Paleontology, v. 40, p. 777–842.
Gouwy, S., and Bultynck, P., 2000, Graphic correlation of Frasnian sections (Upper Devonian) in the Ardennes, Belgium: Bulletin de l'Institut royal des Sciences naturelles de Belgique, Sciences de la Terre, v. 70, p. 25–52.
Gouwy, S., Haydukiewicz, J., and Bultynck, P., 2007, Conodont-based graphic correlation of upper Givetian–Frasnian sections of the eastern Anti-Atlas (Morocco): Geological Quarterly, v. 51, p. 375–392.
Han, Y., 1987, Study on Upper Devonian Frasnian/Famennian boundary in Maanshan, Zhongping, Xiangzhou, Guangxi: Bulletin of the Chinese Academy of Geological Sciences, v. 17, p. 171–194. [In Chinese, with an English summary].
Hass, W.H., 1959, Conodonts from the Chappel Limestone of Texas: U. S. Geological Survey Professional Paper 294–J, p. 365–399.
Hinde, G.J., 1879, On conodonts from the Chazy and Cincinnati Group of the Cambro-Silurian, and from the Hamilton and Genesse-Shale divisions of the Devonian, in Canada and the United States: Quarterly Journal of the Geological Society of London, v. 35, p. 351–369.
House, M.R., 1962, Observations on the ammonoid succession of the North American Devonian: Journal of Paleontology, v. 36, p. 247–284.
House, M.R., and Kirchgasser, W.T., 1993, Devonian goniatite biostratigraphy and timing of facies movements in the Frasnian of eastern North America, *in* Hailwood, E.A., and Kidd, R.B., eds., High Resolution Stratigraphy: Geological Society of London Special Publication 70, p. 267–292.
House, M.R., and Kirchgasser, W.T., 2008, Late Devonian goniaitites (Cephalopoda, Ammonoidea) from New York State: Bulletins of American Paleontology, v. 374, 285 p.
Huddle, J.W., 1968, Redescription of Upper Devonian conodont genera and species proposed by Ulrich and Bassler in 1926: U. S. Geological Survey Professional Paper, v. 578, I–IV + 55 p.
Huddle, J.W., 1970, Revised descriptions of some Late Devonian polygnathid conodonts: Journal of Paleontology, v. 44, p. 1029–1040.
Huddle, J.W., 1981, Conodonts from the Genesee Formation in western New York (assisted by Repetski, J.E.): U. S. Geological Survey Professional Paper, 1032-B, I-VI + B1-B66.
Ji, Q., 1986, Conodonta, *in* Hou, H., Ji, Q., Xian, S., and Wang, J. Middle-Upper Devonian boundary in Maanshan of Xiangzhou, Guangxi: Beijing, Geological Publishing House, p. 18–50. 113–115, 123–130. [In Chinese with an English summary.]
Johnson, J.G., and Klapper, G., 1992, North American midcontinent T-R cycles, *in* Chaplin, J.R., and Barrick, J.E., eds., Special Papers in Paleontology and Stratigraphy: A Tribute to Thomas W. Amsden: Oklahoma Geological Survey Bulletin, v. 145, p. 127–135.
Johnson, J.G., Klapper, G., and Sandberg, C.A., 1985, Devonian eustatic fluctuations in Euramerica: Geological Society of America Bulletin, v. 96, p. 567–587.
Khalymbadzha, V.G., and Chernysheva, N.G., 1970, Konodonty rod *Ancyrodella* iz Devonskikh otlozheniy Volgo-Kamskogo kraya i ikh stratigraficheskoe znachenie, *in* Biostratigrafiya I Paleontologiya Paleozoyskikh otlozheniy vostoka Russkoy Platformy I zapadnogo priural'ya: Izdatel'stvo Kazanskogo Universiteta Vypusk, v. 1, p. 81–103. [in Russian]
Kirchgasser, W.T., 1965, The Parrish Limestone (Upper Devonian) of west central New York [M.S. thesis]: Ithaca, New York, Cornell University, 177 p.
Kirchgasser, W.T., 1967, Paleontology and stratigraphy of the concretions and limestones of the Upper Devonian Cashaqua Shale Member, Sonyea Formation, New York [Ph.D. dissertation]: Ithaca, New York, Cornell University, 82 p.
Kirchgasser, W.T., 1970, Conodonts from near the Middle/Upper Devonian boundary in north Cornwall: Palaeontology, v. 13, p. 335–354.
Kirchgasser, W.T., 1994, Early morphotypes of *Ancyrodella rotundiloba* at the Middle-Upper Devonian boundary, Genesee Formation, west-central New York, *in* Landing, E., ed.,, Studies in stratigraphy and paleontology in honor of Donald W. Fisher: New York State Museum Bulletin 481, p. 117–134.
Kirchgasser, W.T., and Klapper, G., 1992, Graphic correlation using litho- and biostratigraphic markers in the uppermost Middle and Upper Devonian (Frasnian) of New York State: Northeastern Section, Geological Society of America, Abstracts with Programs, v. 24(3), p. 32.
Kirchgasser, W.T., Over, D.J., and Woodrow, D.L., 1994, Frasnian (Upper Devonian) strata of the Genesee River Valley, western New York State, *in* Brett, C.E., and Scatterday, J., eds., New York State Geological Association Field Trip Guidebook, (66th Annual Meeting), Rochester, New York University of Rochester, p. 325–358.
Klapper, G., 1966, Upper Devonian and Lower Mississippian conodont zones in Montana, Wyoming, and South Dakota: The University of Kansas Paleontological Contributions Paper 3, 43 p.
Klapper, G., 1971, Sequence within the conodont genus *Polygnathus* in the New York lower Middle Devonian: Geologica et Palaeontologica, v. 5, p. 59–79.

Klapper, G., 1973, *Polygnathus brevis*, *P. dubius*, *P. pennatus*, *P. webbi*, *in* Ziegler, W., ed., Catalogue of Conodonts, v. 1, Stuttgart, E. Schweizerbart'sche Verlagsbuchhandlung, p. 341–342. 353–354, 373–374, 393–394.

Klapper, G., 1975, *Icriodus symmetricus*, *in* Ziegler, W., ed., Catalogue of Conodonts, v. 2, Stuttgart, E. Schweizerbart'sche Verlagsbuchhandlung, p. 151–153.

Klapper, G., 1980, Conodont systematics, *in* Johnson, J.G., Klapper, G., and Trojan, W.R., Brachiopod and conodont successions in the Devonian of the northern Antelope Range, Central Nevada: Geologica et Palaeontologica, v. 14, p. 99–104. 112–115.

Klapper, G., 1985, Sequence in conodont genus *Ancyrodella* in Lower *asymmetricus* Zone (earliest Frasnian, Upper Devonian) of the Montagne Noire, France: Palaeontographica Abteilung A, v. 188, p. 19–34.

Klapper, G., 1989, The Montagne Noire Frasnian (Upper Devonian) conodont succession, *in* McMillan, N.J., Embry, A.F., and Glass, D.J., eds., Devonian of the World, Calgary, Canadian Society of Petroleum Geologists Memoir, v. 14(3), p. 449–468. [date of imprint, 1988].

Klapper, G., 1990, Frasnian species of the Late Devonian conodont genus *Ancyrognathus*: Journal of Paleontology, v. 64, p. 998–1025.

Klapper, G., 1997, Graphic correlation of Frasnian (Upper Devonian) sequences in Montagne Noire, France, and western Canada, *in* Klapper, G, Murphy, M.A., and Talent, J.A., eds., Paleozoic sequence stratigraphy, biostratigraphy, and biogeography: studies in honor of J. Granville ("Jess") Johnson: Geological Society of America Special Paper 321, p. 113–129.

Klapper, G., 2000, Species of Spathognathodontidae and Polygnathidae (Conodonta) in the recognition of Upper Devonian stage boundaries, *in* Bultynck, P., ed., Subcommission on Devonian Stratigraphy: Fossil Groups Important for Boundary Definition: Courier Forschungsinstitut Senckenberg, v. 220, p. 153–159.

Klapper, G., 2007a, Frasnian (Upper Devonian) conodont succession at Horse Spring and correlative sections, Canning Basin, Western Australia: Journal of Paleontology, v. 81, p. 513–537.

Klapper, G., 2007b, Conodont taxonomy and the recognition of the Frasnian/Famennian (Upper Devonian) stage boundary: Stratigraphy, v. 4, p. 67–76.

Klapper, G., 2009, Upper Devonian conodonts in the Canning Basin, appendix 1, *in* Playford, P.E., Hocking, R.M., and Cockbain, A.E. Devonian Reef Complexes of the Canning Basin, Western Australia, Geological Survey of Western Australia Bulletin, v. 145, p. 405–413.

Klapper, G., and Becker, R.T., 1999, Comparison of Frasnian (Upper Devonian) conodont zonations, *in* Serpagli, E., and Corradini, C., eds., Studies on conodonts: Proceedings of the Seventh European Conodont Symposium, Bologna-Modena, June 23-25, 1998: Bollettino della Società Paleontologica Italiana, v. 37, p. 339–348.

Klapper, G., and Foster, C.T., Jr., 1986, Quantification of outlines in Frasnian (Upper Devonian) platform conodonts: Canadian Journal of Earth Sciences, v. 23, p. 1214–1222.

Klapper, G., and Foster, C. T., Jr., 1993, Shape analysis of Frasnian species of the Late Devonian conodont genus *Palmatolepis*: The Paleontological Society Memoir, v. 32, 35 p.

Klapper, G., and Kirchgasser, W.T., 1992, Zonal and graphic correlation of the New York and Australian Upper Devonian (Frasnian) conodont and ammonoid sequences: North-Central Section, Geological Society of America, Abstracts with Programs, v. 24 (4), p. 26.

Klapper, G., and Lane, H.R., 1985, Upper Devonian (Frasnian) conodonts of the *Polygnathus* biofacies, N. W. T., Canada: Journal of Paleontology, v. 59, p. 904–951.

Klapper, G., and Lane, H.R., 1989, Frasnian (Upper Devonian) conodont sequence at Luscar Mountain and Mount Haultain, Alberta Rocky Mountains, *in* McMillan, N.J., Embry, A.F., and Glass, D.J., eds., Devonian of the World, Calgary, Canadian Society of Petroleum Geologists Memoir, v. 14(3), p. 469–478. [date of imprint, 1988].

Klapper, G., and Philip, G.M., 1972, Familial classification of reconstructed Devonian conodont apparatuses, *in* Lindström, M., and Ziegler, W., eds., Symposium on Conodont Taxonomy, Geologica et Palaeontologica, SB 1, p. 97–113.

Klapper, G., Kirchgasser, W.T., and Baesemann, J.F., 1995, Graphic correlation of a Frasnian (Upper Devonian) Composite Standard, *in* Mann, K.O., and Lane, H.R., eds., Graphic Correlation: SEPM Society for Sedimentary Geology Special Publication, v. 53, p. 177–184.

Klapper, G., Kuz'min, A.V., and Ovnatanova, N.S., 1996, Upper Devonian conodonts from the Timan-Pechora region, Russia, and correlation with a Frasnian Composite Standard: Journal of Paleontology, v. 70, p. 131–152.

Klapper, G., Philip, G.M., and Jackson, J.H., 1970, Revision of the *Polygnathus varcus* Group (Conodonta, Middle Devonian): Neues Jahrbuch für Geologie und Paläontologie Monatshefte, Jarhgang, v. 1970(11), p. 650–667.

Klapper, G., Sandberg, C.A., Collinson, C., Huddle, J.W., Orr, R.W., Rickard, L.V., Schumacher, D., Seddon, G., and Uyeno, T.T., 1971, North American Devonian conodont biostratigraphy, *in* Sweet, W.C., and Bergström, S.M., eds., Symposium on Conodont Biostratigraphy: Geological Society of America Memoir, v. 127, p. 285–316.

Klapper, G., Uyeno, T.T., Armstrong, D.K., and Telford, P.G., 2004, Conodonts of the Williams Island and Long Rapids formations (Upper Devonian, Frasnian-Famennian) of the Onakawana B drillhole, Moose River Basin, northern Ontario, with a revision of Lower Famennian species: Journal of Paleontology, v. 78, p. 371–387. [Correction in 78, p. 1221.].

Kralick, J.A., 1994, The conodont genus *Ancyrodella* in the middle Genesee Formation (Lower Upper Devonian, Frasnian), western New York: Journal of Paleontology, v. 68, p. 1384–1395.

Kuz'min, A.V., 1998, New species of Early Frasnian *Palmatolepis* (Conodonta) from southern Timan: Paleontological Journal, v. 32(2), p. 174–182. [Translated from Paleontologicheskiy Zhurnal, v. 1998(2), p. 70–76.].

Liao, J.-C., and Valenzuela-Ríos, J.I., 2008, Givetian and early Frasnian conodonts from the Compte section (Middle-Upper Devonian, Spanish central Pyrenees): Geological Quarterly, v. 52, p. 1–18.

Matthews, S.C., and Riddolls, B.W., 1984, Appendix 1, Devonian conodont faunas, *in* Selwood, E.B., et al., Geology of the country around Newton Abbot: Memoir British Geological Survey, Sheet 339, p. 34–37, 173–175.

McLean, R.A., and Klapper, G., 1998, Biostratigraphy of Frasnian (Upper Devonian) strata in western Canada, based on conodonts and rugose corals: Bulletin of Canadian Petroleum Geology, v. 46, p. 515–563.

Metzger, R.A., 1989, Upper Devonian (Frasnian–Famennian) conodont biostratigraphy in the subsurface of north-central Iowa and southeastern Nebraska: Journal of Paleontology, v. 63, p. 503–524.

Miller, A.K., and Youngquist, W., 1947, Conodonts from the type section of the Sweetland Creek Shale in Iowa: Journal of Paleontology, v. 21, p. 501–517.

Miller, C.G., 2007, Growth in early species of the conodont *Ancyrodella* and implications for correlation of the Middle-Upper Devonian boundary: Geological Quarterly, v. 51, p. 443–452.

Morrow, J., 2000, Shelf-to-basin lithofacies and conodont paleoecology across Frasnian-Famennian (F-F, mid-Late Devonian) boundary, central Great Basin (western U.S.A.): Courier Forschungsinstitut Senckenberg, v. 219, 57 p.

Mouravieff, A.N., 1982, Conodont stratigraphic scheme of the Frasnian of the Ardennes, *in* Bigey, F., et al., Papers on the Frasnian-Givetian boundary: Brussels, Geological Survey of Belgium and Subcommission on Devonian Stratigraphy, p. 101–118.

Müller, K.J., 1956a, Triassic conodonts from Nevada: Journal of Paleontology, v. 30, p. 818–830.

Müller, K.J., 1956b, Zur Kenntnis der Conodonten–Fauna des europäischen Devons, 1, Die Gattung *Palmatolepis*: Abhandlungen der Senckenbergischen Naturforschenden Gesellschaft, v. 494, 69 p.

Müller, K.J., 1956c, Taxonomy, nomenclature, orientation, and stratigraphic evaluation of conodonts: Journal of Paleontology, v. 30, p. 1324–1340.

Müller, K.J., and Müller, E.M., 1957, Early Upper Devonian (Independence) conodonts from Iowa, part I: Journal of Paleontology, v. 31, p. 1069–1108.

Narkiewicz, K., and Bultynck, P., 2011, Biostratygrafia konodontowa dewonu górnego lubelszczyzny: Prace Pańśtwowego Instytutu Geologicznego, v. 196, p. 193–254. [in Polish]

Navas-Parejo, P., et al., 2009, The Frasnian Upper Kellwasser event and a lower Famennian stratigraphic gap in Calabria (southern Italy): Palaeobiodiversity and Palaeoenvironments, v. 89, p. 111–118.

Orchard, M.J., 1978, The conodont biostratigraphy of the Devonian Plymouth Limestone, south Devon: Palaeontology, v. 21, p. 107–115.

Over, D.J., 1997, Conodont biostratigraphy of the Java Formation (Upper Devonian) and the Frasnian-Famennian boundary in western New York State, *in* Klapper, G, Murphy, M.A., and Talent, J.A., eds., Paleozoic sequence stratigraphy, biostratigraphy, and biogeography: studies in honor of J. Granville ("Jess") Johnson: Geological Society of America Special Paper 321, p. 161–177.

Over, D.J., 2006, Frasnian-Famennian boundary at the type Sweetland Creek Shale locality, *in* Day, J., Luczaj, J., and Anderson, R., eds., New Perspectives and Advances in the Understanding of Lower and Middle Paleozoic Epeiric Carbonate Depositional Systems of the Iowa and Illinois Basins: Iowa Geological Survey Guidebook Series, v. 26, p. 74–79.

Over, D.J., 2007, Conodont biostratigraphy of the Chattanooga Shale, Middle and Upper Devonian, southern Appalachian Basin, eastern United States: Journal of Paleontology, v. 81, p. 1194–1217.

Over, D.J., and Rhodes, M.K., 2000, Conodonts from the Upper Olentangy Shale (Upper Devonian, central Ohio) and stratigraphy across the Frasnian-Famennian boundary: Journal of Paleontology, v. 74, p. 101–112.

Over, D.J., Hopkins, T.H., Brill, A., and Spaziani, A.L., 2003, Age of the Middlesex Shale (Upper Devonian, Frasnian) in New York State, *in* Königshof, P., and Schindler, E., eds., Mid-Palaeozoic Bio- and Geodynamics: The North Gondwana-Laurussia interaction: Courier Forschungsinstitut Senckenberg, v. 242, p. 217–223.

Over, D.J., Baird, G.C., and Kirchgasser, W.T., 2013, Middle - Upper Devonian strata along the Lake Erie shore, western New York, *in* Deakin, A.K., and Lash, G.G., eds., New York State Geological Association Field Trip Guidebook, SUNY Fredonia, Fredonia, New York, p. 182–219.

Ovnatanova, N.S., 1976, Novye pozdnedevonskie konodonty Russkoy Platformy: Paleontologicheskiy Zhurnal, v. 1976, p. 106–115. [in Russian]
Ovnatanova, N.S., and Kononova, L.I., 2001, Conodonts and Upper Devonian (Frasnian) biostratigraphy of central regions of Russian Platform: Courier Forschungsinstitut Senckenberg, v. 233, 115 p.
Ovnatanova, N.S., and Kononova, L.I., 2008, Frasnian conodonts from the eastern Russian Platform: Paleontological Journal, v. 42, p. 997–1166.
Ovnatanova, N.S., and Kuz'min, A.V., 1991, Konodonty tipovykh razrezov Domanikovoy svity na yuzhnom Timane: Izvestiya Akademii Nauk SSSR, Seriya Geologicheskaya, v. 1991(3), p. 37–50. [in Russian]
Ovnatanova, N.S., Kuz'min, A.V., and Menner, V.V., 1999, The succession of Frasnian conodont assemblages in the type sections of the southern Timan-Pechora Province (Russia), *in* Serpagli, E., and Corradini, C., eds., Studies on Conodonts: Bollettino della Società Paleontologica Italiana, v. 37, p. 349–360.
Pepper, J.F., De Witt, W., Jr., and Colton, G.W., 1956, Stratigraphy of the West Falls Formation of Late Devonian age in western and central New York: U. S. Geological Survey Oil and Gas Investigations Chart OC-55.
Perri, M.C., and Spalletta, C., 1981, *Ancyrodella pramosica* n. sp. from the Lower Frasnian of the Carnic Alps: Bollettino della Società Paleontologica Italiana, v. 20, p. 93–98.
Pham, K.N., 1979, Conodonts from limestone pieces of the Late Paleozoic conglomerates in north-west Bulgaria: Geologica Balcanica, v. 9(4), p. 77–92.
Pisarzowska, A., Sobstel, M., and Racki, G., 2006, Conodont-based event stratigraphy of the Early–Middle Frasnian transition on the south Polish carbonate shelf: Acta Palaeontologica Polonica, v. 51, p. 609–646.
Rhodes, F.H.T., 1966, *Polygnathellus*, *in* Rhodes, F.H.T., Häntzchel, W., Müller, K.J., Fisher, D.W., and Teichert, C., Treatise on Invertebrate Paleontology, Part W, Conodonts, Conoidal Shells, Worms, Trace Fossils: Comments and Additions: Lawrence, The University of Kansas Paleontological Contributions Paper 9, p. 4.
Roundy, P.V., 1926, The Micro-fauna, *in* Roundy, P.V., Girty, G.H., and Goldman, M.I., Mississippian Formations of San Saba County, Texas: U.S. Geological Survey Professional Paper, v. 146, p. 5–23.
Sandberg, C.A., Ziegler, W., and Bultynck, P., 1989, New standard conodont zones and early *Ancyrodella* phylogeny across Middle-Upper Devonian boundary, *in* Walliser, O.H., and Ziegler, W., eds., Contributions to Devonian Palaeontology and Stratigraphy: Part I, Chinese - German Collaboration, Part II: Various Devonian Topics: Courier Forschungsinstitut Senckenberg, v. 110, p. 195–230.
Sandberg, C.A., Hasenmueller, N.R., and Rexroad, C.B., 1994, Conodont biochronology, biostratigraphy, and biofacies of Upper Devonian part of New Albany Shale, Indiana, *in* Königshof, P., and Werner, R., eds., Willi Ziegler Festschrift I: Courier Forschungsinstitut Senckenberg, v. 168, p. 227–253.
Sandberg, C.A., Morrow, J., and Ziegler, W., 2002, Late Devonian sea-level changes, catastrophic events, and mass extinctions, *in* Koeberl, C., and MacLeod, K.G., eds., Catastrophic Events and Mass Extinctions: Impacts and Beyond: Geological Society of America Special Paper, v. 356, p. 473–487.
Savage, N.M., 1992, Late Devonian (Frasnian and Famennian) conodonts from the Wadleigh Limestone, southeastern Alaska: Journal of Paleontology, v. 66, p. 277–292.
Savage, N.M., 2013, Late Devonian Conodonts from Northwestern Thailand: Eugene, Oregon, Bourland Printing/Trinity Press, 48 p.
Seddon, G., 1970a, Frasnian conodonts from the Sadler Ridge-Bugle Gap area, Canning Basin, Western Australia: Journal of the Geological Society of Australia, v. 16, p. 723–753.
Seddon, G., 1970b, Pre-Chappel conodonts of the Llano Region, Texas: Bureau of Economic Geology Report of Investigations, v. 68, 130 p.
Shaw, A.B., 1964, Time in Stratigraphy, New York, McGraw-Hill, xi + 365 p.
Stauffer, C.R., 1938, Conodonts of the Olentangy Shale: Journal of Paleontology, v. 12, p. 411–443.
Szulczewski, M., 1971, Upper Devonian conodonts, stratigraphy and facial development in the Holy Cross Mts: Acta Geologica Polonica, v. 21, p. 1–129.
Ulrich, E.O., and Bassler, R.S., 1926, A classification of the toothlike fossils, conodonts, with descriptions of American Devonian and Mississippian species: U. S. National Museum Proceedings, v. 68(12), 61 p.
Uyeno, T.T., 1967, Conodont zonation, Waterways Formation (Upper Devonian), northeastern and central Alberta: Geological Survey of Canada, Paper 67-30, 21 p.
Uyeno, T.T., 1982, Systematic conodont paleontology, *in* Norris, A.W., Uyeno, T.T., and McCabe, H.R. Devonian Rocks of the Lake Winnipegosis – Lake Manitoba outcrop belt, Manitoba: Geological Survey of Canada Memoir, v. 392, p. 73–95.
Uyeno, T.T., 1992, Conodonts, *in* Norris, A.W., Uyeno, T.T., Sartenaer, P., and Telford, P.G., Brachiopod and conodont faunas from the uppermost Williams Island Formation and lower Long Rapids Formation (Middle and Upper Devonian), Moose River Basin, northern Ontario: Geological Survey of Canada Bulletin, v. 434. p. 71–79, 122–133.
Uyeno, T.T., and Wendte, J.C., 2005, Conodont biostratigraphy and physical stratigraphy in two wells of the Beaverhill Lake Group, upper Middle to lower Upper Devonian, central Alberta, Canada: Bulletins of American Paleontology, v. 369, p. 151–171.
Ver Straeten, C.A., Brett, C.E., and Sageman, B.B., 2011, Mudrock sequence stratigraphy: a multi-proxy (sedimentological, paleobiological and geochemical) approach, Devonian Appalachian Basin: Palaeogeography, Palaeoclimatology, Palaeoecology, v. 304, p. 54–73.
Wittekindt, H., 1966, Zur Conodontenchronologie des Mitteldevons: Fortschritte in der Geologie von Rheinland und Westfalen, v. 9, 621–646. [date of imprint, 1965].
Woodrow, D.L., and Sevon, W.D., eds., 1985, The Catskill Delta: Geological Society of America Special Paper 201, 246 p.
Youngquist, W.L., 1945, Upper Devonian conodonts from the Independence Shale (?) of Iowa: Journal of Paleontology, v. 19, p. 355–367.
Youngquist, W.L., 1947, A new Upper Devonian conodont fauna from Iowa: Journal of Paleontology, v. 21, p. 95–112.
Youngquist, W.L., and Miller, A.K., 1948, Additional conodonts from the Sweetland Creek Shale of Iowa: Journal of Paleontology, v. 22, p. 440–450.
Zambito, J.J. IV, Baird, G.C., Brett, C.E., and Bartholomew, A.J., 2007, Re-examination of the type Ithaca Formation: correlation with sections in western New York, *in* McRoberts, C.A., ed., New York State Geological Association Field Trip Guidebook, (79th Annual Meeting): Cortland, New York, SUNY Cortland, p. 83–105.
Zambito, J.J. IV, Baird, G.C., Brett, C.E., and Bartholomew, A.J., 2009, Depositional sequences and paleontology of the Middle-Upper Devonian Transition (Genesee Group) at Ithaca, New York: a revised lithostratigraphy for the northern Appalachian Basin, *in* Over, D.J., ed., Studies in Devonian Stratigraphy: Proceedings of the 2007 International Meeting of the Subcommission on Devonian Stratigraphy and IGCP 499: Palaeontographica Americana, v. 63. p. 49–69.
Ziegler, W., 1958, Conodontenfeinstratigraphische Untersuchungen an der Grenze Mitteldevon/Oberdevon und in der Adorfstufe: Notizblatt des Hessischen Landesamtes für Bodenforschung zu Wiesbaden, v. 87, p. 7–77.
Ziegler, W., 1962, Taxionomie und Phylogenie Oberdevonischer Conodonten und ihre stratigraphische Bedeutung: Abhandlungen des Hessischen Landesamtes für Bodenforschung, v. 38, 166 p.
Ziegler, W., 1971, Conodont stratigraphy of the European Devonian, *in* Sweet, W.C., and Bergström, S.M., eds., Symposium on Conodont Biostratigraphy: Geological Society of America Memoir, v. 127, p. 227–284.
Ziegler, W., and Klapper, G., 1964, *Polygnathus asymmetrica ovalis* n. subsp, *in* Ziegler, W., Klapper, G., and Lindström, M., The validity of the name *Polygnathus* (Conodonta, Devonian and Lower Carboniferous): Journal of Paleontology, v. 38, p. 421–423.
Ziegler, W., and Klapper, G., 1982, The *disparilis* conodont zone, the proposed level for the Middle - Upper Devonian boundary: Courier Forschungsinstitut Senckenberg, v. 55, p. 463–491.
Ziegler, W., and Sandberg, C.A., 1990, The Late Devonian standard conodont zonation: Courier Forschungsinstitut Senckenberg, v. 121, p. 115 p.
Ziegler, W., Ovnatanova, N., and Kononova, L., 2000, Devonian polygnathids from the Frasnian of the Rheinisches Schiegergebirge, Germany, and the Russian Platform: Senckenbergiana lethaea, v. 80, p. 593–645.

Accepted 11 July 2015

Appendix 1. Localities

New York localities and sampled beds listed in approximate stratigraphic order. Sample numbers in the Genesee Group with SD notation (Silurian-Devonian) refer to United States Geological Survey (U. S. G. S.) samples in deWitt and Colton (1978) and Huddle (1981). U. S. G. S. SD samples in the Sonyea and West Falls groups were collected in 1974 by John Huddle (JH) of the U. S. G. S. and U. S. National Museum and William Kirchgasser (WK). Among other collectors were James Kralick (JK) and Gilbert Klapper (GK); the names of less frequently cited collectors are written out; these follow the sample numbers at end of each locality description. Locality, bed and sample numbers from New York follow Kirchgasser (1965, 1967), Klapper et al. (1995) and House and Kirchgasser (1993, 2008); asterisk (*) indicates horizon is identified in illustrated section. Latitude and Longitude values from Google Earth. Iowa and Australian localities listed separately after those of New York.

Most of the samples were collected before the metric system became the preferred scale for measurement of distance and bed and section thickness in New York stratigraphy. Later collecting used the metric system directly. The English-scale measurements have been converted to the metric scale with the necessary rounding and are not given in the locality descriptions.

NEW YORK

UG: Genundewa Point, Canandaigua Lake, Yates County, NY, Middlesex 7.5' Quad., NE ¼ NAPLES 15' Quad. Genundewa Limestone (Genesee Group), **Upper Genundewa (UG), Bed 23b/6.** Type locality of Genundewa Limestone along east side of Canandaigua Lake (opposite Seneca Point on west side of lake), north of Genundewa Point [42°44'15.60"N, 77°19'31.11"W], 900, East Lake Road, 1.6 km north of Vine Valley. Genundewa Limestone at this locality is a 2.43 m interval of styliolinid lenses alternating with gray shales that overlie a 10 cm-thick black shale (House and Kirchgasser, 2008, p. 29); sample bed 6715 SD is the bed immediately above the 10 cm black shale in the section of deWitt and Colton (1978, pl. 4*). Conodont Sample 6718-SD of Huddle (1981) [= Bed 23b/5 of House and Kirchgasser (2008)] is a baritic, styliolinid ledge with the goniatite *Tornoceras* common, which lies between 1.14 and 1.45 m above the 10 cm black shale. Conodont Sample 3958-SD of Huddle (1981) [= Bed 23b/6 of House and Kirchgasser (2008)], is from a prominent ledge of styliolinid limestone with poor barite-replaced goniatites, 1.96 to 2.13 m above the base of the Genundewa; the top of the bed dips below lake level about 43 m north of the point. The top of Bed 23b/6 underlies a 30 cm interval of thin styliolinid limestones that is taken as the top bed of the Genundewa Limestone. Locality Nap-4 of deWitt and Colton (1978, 6718-SD and 3958-SD, pl. 4*). Goniatite Division: *Timanites* (Frasnian I-C); NY Regional Zone: *Manticoceras contractum* (17a). Frasnian Conodont Zone 3.
Sample: Bed 23b/5: 6718-SD: W. H. Hass, 2 of 9.18.57 (Huddle, 1981, p. B51, table 1, sheet 5). **Sample: Bed 23b/6: 3958-SD**: W. H. Hass, 2 of 9.12.56 (Huddle, 1981, p. B51, table 1, sheet 5).

HB: Fall Brook, Geneseo, Livingston County, NY, Geneseo 7.5' Quad., SE ¼ CALEDONIA 15' Quad. Lower West River Shale (Genesee Group), **Huddle Bed (HB)**, Bed 19a/2 of House and Kirchgasser (2008 p. 30, 31; fig. 9*). Five cm-thick styliolinid bed, 2.3 m above the top of the Genundewa Limestone (caprock of high falls) in Fall Brook Creek, upstream (east) of NY Rte. 63 overpass at 42°46'28.23"N 77°49'38.63"W, about 2.4 km south of Geneseo. Horizon about 28 m above base of Geneseo Shale (Genesee Group). Sample 8122-SD of deWitt and Colton (1978, plate 2*); Huddle (1981, p. B-52). Lower West River Shale (LWR) of Kirchgasser et al. (1994, p. 354, figs. 3*, 10*). Huddle Bed of Baird et al. (2006, p. 380-381, fig. 10*), named in honor of John Huddle. Bed H of Zambito et al. (2007, p. 96, fig. 4*), in microcycle 2 of the 23 West River Shale microcycles, and Zambito et al. (2009, p. 64, fig. 6*). Goniatite Division: *Timanites* (Frasnian I-C); NY Regional Zone: *Manticoceras contractum* (17a). Frasnian Conodont Zone 3.
Samples: Bed 19a/2: 8122-SD: W. H. Hass 2 of 9.21.57 = **4062**: WK 2 of 8.30.90.

BP: South Middlesex, Middlesex, Yates County, NY, Middlesex 7.5' Quad., NE ¼ NAPLES 15' Quad. Middle West River Shale, **Bluff Point Bed (BP)**, informal name herein, Bed Nap-8/1 of House and Kirchgasser (2008, p. 32). Loose, 8 cm-thick fossil-log styliolinid concretion, with pyrite, barite, plant debris and rich fauna of conodonts, gastropods, lingulids and goniatites. Probably from line of concretions 3 m below the 5 cm-thick, convolute-bedded Bluff Point Siltstone that crops out about 6 m above where exposures begin in the creek that crosses NY Rte. 245 at 42° 41'39.50"N 77°16'45.52"W, 1.3 km south of village of Middlesex. Horizon lies between two 8 cm-thick black shales that define the first sedimentary microcycle (microcycle 13) below the microcycle with the Bluff Point Siltstone (microcycle 14). Bed Nap-8/1 is about 21 m below base Middlesex Shale in microcycle 13 of the 23 West River Shale microcycles. Locality Nap-8 of deWitt and Colton (1978). Goniatite Division *Timanites* (Frasnian I-C); NY Regional Zone: *Koenenites beckeri* (17b). Frasnian Conodont Zone 4.
Samples: Bed Nap-8/1: 3884: WK 5 of 7.31.77, 5 of 5.28.79 = **4058**: WK 1 of 8.27.90.

WB: Snyder's Gully, Woodville, Ontario County, NY, Middlesex 7.5' Quad., NE ¼ NAPLES 15' Quad. Upper West River Shale, **Williamsburgh Bed (WB)**, **Bed 46c/1** of House and Kirchgasser (2008, p. 30, 31, fig. 9*). Fossil-log styliolinid concretionary bed (22 cm-thick), with goniatites and abundant lingulid brachiopods, in dark gray shales of the upper West River Shale. The base of the bed is 4.97 m below base Middlesex Shale, in Snyder's or Snyder Gully, southwest end of Canandaigua Lake, which is crossed by NY Rte. 21 at 42°39'54.81"N 77°21'53.52"W, 0.5 km south of Woodville. Top of bed is .90 m below a 10 cm-thick black shale. Probable equivalent of Williamsburgh Bed of Over et al. (2003) and Bed 18a/4b of House and Kirchgasser (2008, p. 31, FL: fig. 9*) at Beards Creek (see following locality). Microcycle 18 of the 23 West River Shale microcycles. Goniatite Division *Timanites* (Frasnian I-C); NY Regional Zone: *Koenenites beckeri* (17b). Frasnian Conodont Zone 4.
Sample: Bed 46c/1: 4056: WK 2 of 8.26.90.

BC: Beards Creek, **Leicester**, Livingston County, NY, Leicester 7.5' Quad., SW ¼ CALEDONIA 15' Quad. Upper West River Shale, **Beards Creek Horizon** (**BC**), **Bed 18a/5** of House and Kirchgasser (2008, p. 30, 31, fig. 9*). Prominent septarian concretion bed, 2.4 m below base Middlesex Shale in upper Beards Creek, above Dunkley Road bridge that crosses the creek at 42° 46'27.91"N 77°54'51.85"W, about 1.6 km northwest of Leicester. Microcycle 19-20 of 23 West River Shale microcycles. Goniatite Division: *Timanites* (Frasnian I-C); NY Regional Zone: *Koenenites beckeri* (17b). Frasnian Conodont Zone 4.
Samples: Bed 18a/5: M. R. House and WK, horizon 10 of 7.30.65 = **3948**: WK 4 of 4.21.75.

CP: Chidsey Point, **Keuka Lake**, **Branchport**, Yates County, NY, Pulteney 7.5' Quad., SW ¼ PENN YAN 15' Quad. Upper West River Shale, **Chidsey Point Bed (CP)**, informal unit named herein, **Bed Py-7/2** of House and Kirchgasser (2008, p. 32-33). Pyritic and baritic fossil-log, styliolinid, concretion bed with goniatites, 3.4 m below base Middlesex Shale in creek crossing NY Rte. 54A at 42°34'27.66"N 77°09'04.25"W, above Chidsey Point, West Branch Keuka Lake, 2.7 km south of Branchport. Graphic correlation indicates horizon is not a correlative of Williamsburgh Bed (WB) at Beards Creek, Bed 18a/4b of House and Kirchgasser (2008, p. 30, 31, fig. 9*), but instead graphs to a position above the Beards Creek Horizon (BC) (Fig. 3). [The productive Sample 6754-SD of Huddle (1981, table 1, sheet 6) and of deWitt and Colton (1978, pl. 6*) is the 5 cm-thick, pyritic, styliolinid band, 6.7 m below base Middlesex Shale]. Goniatite Division *Timanites* (Frasnian I-C); NY Regional Zone: *Koenenites beckeri* (17b). Frasnian Conodont Zone 4.
Sample: Bed Py-7/2: 4046: WK 1 of 6.1.90.

30/1: Eighteenmile Creek, **North Evans**, Erie County, NY, Eden 7.5'Quad., NW ¼ EDEN 15' Quad. Base Cashaqua Shale (Sonyea Group), **Bed 30/1** of House and Kirchgasser (2008, p. 35, fig. 10*). Concretion-bed at base Cashaqua Shale, immediately above top Middlesex Shale, in south bank of creek about 183 m upstream (east side) of the railroad bridge at 42°41"15.21"N 78°56'50.93"W, below North Evans. Horizon is 13 m below base Rhinestreet Shale (West Falls Group). Goniatite Division: *Probeloceras* (Frasnian I-E); NY Regional Zone: *Probeloceras lutheri* (19). Frasnian Conodont Zone 5.
Samples: Bed 30/1: WK 9.24.64 = **12057-SD**: JH and WK 5 of 8.9.74.

WS: Whetstone Brook, Honeoye, Ontario County, NY, Honeoye 7.5'Quad., SE ¼ HONEOYE 15' Quad. Base Cashaqua Shale, **Whetstone Brook Bed (WS)**, informal name herein, **Bed 42/1** of House and Kirchgasser (2008, Fig. 10*). Silty, calcareous, concretion-bed, 8-15 cm-thick, with abundant styliolinids and annulated dacryoconarids ("tentaculites") near base Cashaqua Shale, 0.30 m above topmost siltstones of the Rock Stream Siltstone, which cap the first falls in Whetstone Brook, upstream of U. S. Rte. 20A crossing at 42°47'20.06"N 77°33'23.27"W, 3.2 km west of Honeoye. Bed is about 40 m below base Rhinestreet Shale (West Falls Group). Goniatite Division: *Probeloceras* (Frasnian I-E); NY Regional Zone: *Probeloceras lutheri* (19). Frasnian Conodont Zone 5.
Samples: Bed 42/1: WK 8.20.63 = **4000**: WK 3 of 5.25.87.

44/3: **Randall Gully, Bristol Center**, Ontario County, NY, Bristol Center 7.5' Quad., SW ¼ CANANDAIGUA 15' Quad. Cashaqua Shale, **Bed 44/3** of House and Kirchgasser, 2008 (p. 41, fig. 10*). Concretion-bed (38 mm-thick) in floor of creek, with baritized goniatites, about 6.4 m above base Cashaqua Shale (top Rock Stream Siltstone (elevation ~1120 ft), in Randall Gully, below Dugway Road; 2.4 m above a pair of thin siltstones at the top of a 4-m interval of silty shale. Bed 44/3 is about 28 m below base Rhinestreet Shale (West Falls Group). NY Rte. 64 crosses Randall Gully at 42°46'33.61"N 77°24'13.69"W, 4 km south of Bristol Center. Goniatite Division: *Probeloceras* (Frasnian I-E); NY Regional Zone: *Probeloceras lutheri* (19). Frasnian Conodont Zone 5.
Sample: Bed 44/3: WK 8.15,19.63.

42/5: **Whetstone Brook, Honeoye**, Ontario County, NY, Honeoye 7.5'Quad., SE ¼ HONEOYE 15' Quad. Cashaqua Shale, **Bed 42/5** of House and Kirchgasser (2008, p. 40, fig. 10*). Concretion bed with baritized goniatites in floor of Whetstone Brook, upstream of U S Rte. 20A crossing at 42°47'20.06"N 77°33'23.27"W, 3.2 km west of Honeoye. Bed 42/5 is about 6.7 m above first marker black shale in section and 30 m below base Rhinestreet Shale (West Falls Group). Goniatite Division: *Probeloceras* (Frasnian I-E); NY Regional Zone: *Probeloceras lutheri* (19). Frasnian Conodont Zone 5.
Sample: Bed 42/5: WK 8.20, 21.63.

43/3: Briggs Gully, Honeoye Lake, Ontario County, NY, Springwater and Bristol Springs 7.5'Quads., NE 1/4 WAYLAND and NW ¼ NAPLES 15' Quads. Cashaqua Shale, **Bed 43/3** of House and Kirchgasser (2008, p. 40, fig. 10*). Horizon of small concretions with baritized goniatites in third stream north of Briggs Gully, crossed by East Lake Road (southeast side of Honeoye Lake) at 42°43'21.50"N 77°30'06.41"W. Horizon is 7.9 m above first marker black shale in section, 2.4 m above a thin, prominent siltstone, and 20 m below base Rhinestreet Shale (West Falls Group). Goniatite Division: *Probeloceras* (Frasnian I-E); NY Regional Zone: *Probeloceras lutheri* (19). Frasnian Conodont Zone 5.
Sample: Bed 43/3: WK 8.19.63.

PL: Conklin Gully, Naples, Ontario County and Yates County, NY, Middlesex 7.5' Quad., NE ¼ NAPLES 15' Quad.: **Parrish Limestone** (**PL**), type locality, **Bed 47/2** of House and Kirchgasser (2008, p. 42, fig. 10*). Distinctive, red-green, nodular limestone (10.2 cm-thick) (*Knollenkalk*) with goniatites, 2.1 m above first falls and Rock Stream Siltstone-Cashaqua Shale contact, in Conklin (formerly Parrish) Gully southeast of intersection of Rumpus (Parish) Hill Road and NY Rte. 245 overpass at 42°38'07.44"N 77°22'02.58"W, 6.7 km northeast of Naples. Goniatite Division: *Probeloceras* (Frasnian I-E); NY Regional Zone: *Probeloceras lutheri* (19). Frasnian Conodont Zone 5.
Samples: Bed 47/2: WK 1962-1963 = **4066**: WK and JK 1 of 5.30.90.

44/4: Randall Gully, Bristol Center, Ontario County, NY, Bristol Center 7.5' Quad., SW ¼ CANANDAIGUA 15' Quad. Cashaqua Shale, **Bed 44/4** of House and Kirchgasser (2008, p. 41, fig. 10*). Argillaceous limestone lens (5-10 cm-thick) with goniatites, 2.3 m above a thin but prominent siltstone cropping out about 2 m above where a side stream enters Randall Gully from the north at about 1170 ft. elevation, in section below Dugway Road. NY Rte. 64 crosses Randall Gully at 42° 46'33.61"N 77°24'13.69"W, 4 km south of Bristol Center. Bed 44/4 is about 14.6 m below base Rhinestreet Shale (West Falls Group). Goniatite Division: *Probeloceras* (Frasnian I-E); NY

Regional Zone: *Probeloceras lutheri* (19). Frasnian Conodont Zone 5.
Sample: Bed 44/4: WK 8.15,19.63.
SH: North McMillan Creek, Conesus Lake, Livingston County, NY, Conesus 7.5' Quad., NE ¼ WAYLAND 15' Quad. Upper Cashaqua Shale, **Shurtleff Septarian Horizon** (**SH**), **Bed 41a/5** of House and Kirchgasser (2008, p. 40). Septarian concretion horizon with baritized (pink and white) goniatites and other mollusk groups, in north bank of North McMillan Creek that is crossed by East Lake Road (southeast end of Conesus Lake) at 42°43'23.32"N 77°42'08.39"W. Horizon is 1.37 m below base Rhinestreet Shale (West Falls Group) (~880 ft elev.). Goniatite Division: *Prochorites* (Frasnian I-F); N. Y. Regional Zone *Prochorites alveolatus* (20). Frasnian Conodont Zone 6.
Samples: Bed 41a/5: WK 8.27.63 = **4043**: WK 2 of 5.25.87; JH and WK 1 of 8.7.74.

BR: Acme Shale Co. pit, Weyer (formerly Shaleton), Erie County. Eden 7.5'Quad., NW ¼ EDEN15' Quad. Rhinestreet Shale (West Falls Group). **Base Rhinestreet Shale** (**BR**), **Bed 30b/1.** Interval (0.0-0.15 m-thick) of black shale at top of abandoned shale pit at Weyer. East wall at about 42°43'29.53"N 78°54'58.77"W. Locality of Ulrich and Bassler (1926, p. 3) cited in Huddle (1968, p. 1-2). Goniatite Division: *Prochorites* (Frasnian I- F); NY Regional Zone *Prochorites alveolatus* (20). Frasnian Conodont Zone 6.
Sample: Bed 30b/1: 4247: WK 9.3.64

BR: Pike Creek, Jerusalem Corners, Erie County, NY, Angola 7.5' Quad., NE ¼ SILVER CREEK 15' Quad. **Base Rhinestreet Shale (BR)**, **Bed 30a/12.** Fissile black shale, 46 cm above base Rhinestreet Shale, above a low falls in Pike Creek, upstream (north) of Lake Shore Road, 2.1 km northeast of Jerusalem Corners. Pike Creek is crossed by NY Rte. 5 at 42°41'29.72"N 79°00'05.81"W. Continuation of Cashaqua Shale Locality 30a of House and Kirchgasser (2008, p. 38). Goniatite Division: *Prochorites* (Frasnian I-F); NY Regional Zone *Prochorites alveolatus* (20). Frasnian Conodont Zone 6.
Sample: Bed 30a/12: 4246: WK 9.3.64.

BR: Cayuga Creek, Cowlesville, Wyoming County, NY, Cowlesville 7.5' Quad., SW ¼ ATTICA 15' Quad. **Base Rhinestreet Shale** (**BR**), **Bed 33/22.** Fissile black shale, 0.0 to 15 cm above base Rhinestreet Shale at Cowlesville, upstream of Urf Road bridge crossing of Cayuga Creek at 42°50'27.67"N 78°28'12.33"W. Continuation of Cashaqua Shale Locality 33 of House and Kirchgasser (2008, p. 38, Fig. 10*), without bed number; Bed 33/22 of Kirchgasser (1967, p. 133) . Goniatite Division: *Prochorites* (Frasnian I-F); NY Regional Zone *Prochorites alveolatus* (20). Frasnian Conodont Zone 6.
Sample: Bed 33/22: WK 9.10,15.64.

CT: Cazenovia Creek, Tributary, Spring Brook, Erie County, NY, Orchard Park 7.5' Quad., SW ¼ DEPEW 15' Quad. Rhinestreet Shale, **Cazenovia Creek Tributary Bed,** informal unit named herein, **Bed 32/23**. Septarian concretions and surrounding black shale immediately above the falls below the road culvert, at about 42°48'20.56"N 78°40'41.56"W, in ravine of northwesterly flowing tributary to Cazenovia Creek, below (downstream) of the North Davis-Conley Road intersection, 1.3 km south of Spring Brook. Bed 32/23 is 6.25 m above base Rhinestreet Shale. Continuation of Locality 32 of House and Kirchgasser (2008, p. 28, fig. 10). Goniatite Division: *Mesobeloceras* (Frasnian I-G1); NY Regional Zone *Naplesites iynx* (21a). Frasnian Conodont Zone 7.
Sample: Bed 32/23: WK 9.13.63.

BK: Buck Run, Mount Morris, Livingston County, NY, Mt. Morris 7.5' Quad., NW ¼ NUNDA 15' Quad. Rhinestreet Shale, **Buck Run Creek Bed**, informal unit named herein, Bed 65/1 of House and Kirchgasser (2008). Dark, styliolinid concretion horizon with goniatites and plant fragments, 13 m above base Rhinestreet Shale (~755 ft. elev.) in upper part of Buck Run, downstream of Swanson Road bridge crossing creek at 42°41'25.51"N 77°53'09.12"W, 16 km southeast of Mount Morris. Bed 65/1 [Fossil Log (FL)] of House and Kirchgasser (2008, p.49, figs. 11*, 23) = Bed 39/25 in continuation of Cashaqua Shale Locality 39 of House and Kirchgasser (2008, p. 39-40, fig. 10). Goniatite Division: *Mesobeloceras* (Frasnian I-G1); NY Regional Zone *Naplesites iynx* (21a). Frasnian Conodont Zone 7.
Samples: Bed 65/1 (= 39/25): MR House and WK 7.31.66, 8.26.66; JH and WK 3 of 8.7.74 = 9415-SD = **4064:** WK 1 of 8.31.90.

SC: Seascape, Lake Erie shore, Erie County, NY, Angola 7.5' Quad., NE ¼ SILVER CREEK 15' Quad. Rhinestreet Shale, **Seascape Conodont Bed** (**SC**), informal unit named herein. Conodont-fish-bone lag at top of 5 cm-thick black shale and base of 5 cm-thick cross-bedded siltstone, 1 m above a K-bentonite ash bed [Rhinestreet Ash Bed (RA), informal unit named herein (possible Belpre Ash Bed): see discussion in Baird et al. (2006) and Over et al. (2013)]. **Seascape Conodont Bed** is about 9 m above base of Rhinestreet Shale, in the bluff below the Seascape Estate of the Sisters of St. Mary, Lake Erie shore at 42°41'51.00"N 79°01'21.75"W, 1.6 km northwest of Jerusalem Corners. Locality 30c/1 following House and Kirchgasser (2008). Locality of Baird et al. (2006, p. 139-140, 157-158, fig. 7*, Stop 3) and Over et al. (2013, fig. 7AB* and p. 190, 213-215). Horizon at base of prominent intra-Rhinestreet gray-green shale unit, informal field designation herein: **"False Cashaqua"** (**FC**), a reference to its similarity to the gray-green shales of pre-Rhinestreet Cashaqua Shale (Sonyea Group). Goniatite Division: *Mesobeloceras* (Frasnian I-G1); NY Regional Zone *Naplesites iynx* (21a). Frasnian Conodont Zone 7.
Sample: 4094: WK and G. Baird 2 of 8.21.92 = **4119:** WK and P. Levin 2 of 8.25.93.

NB: Sturgeon Point, Lake Erie shore, Erie County, NY, Angola 7.5' Quad., NE ¼ SILVER CREEK 15' Quad. Rhinestreet Shale, ***Naplesites* Bed** (**NB**). Concretions from the black shale horizon with the goniatite *Naplesites* cropping out along Lake Erie shore, east of Sturgeon Point Marina and car park at 42°41'27.09"N 79°02'49.03"W; continuous shale cliff section near outflow pipes of Derby waterworks. The ***Naplesites Bed***, at or near the base of the black shale band that caps the **False**

Cashaqua (FC) interval of gray-green shale (~2.5 m-thick), is about 11.5 m above base Rhinestreet Shale. Locality 30d/1 following House and Kirchgasser (2008). Locality of Baird et al. (2006, p. 139-140, 157-158, fig. 7* (Stop 4) and Over et al. (2013, fig. 7AB*, p. 190, 195-196, 215-217). Goniatite Division: *Mesobeloceras* (Frasnian I-G1); NY Regional Zone *Naplesites iynx* (21a). Frasnian Conodont Zone 7.
Sample: 4285: WK 10.7.06.

RL: Bed 60/3: Relyea Creek, South Warsaw, Wyoming County, NY, Warsaw 7.5' Quad., NW ¼ PORTAGE 15' Quad., Rhinestreet Shale, **Relyea Creek Horizon (RL)**. Bed 60/3 of House and Kirchgasser (2008, p. 48, fig. 13*), 5.5 m below the Rhinestreet Shale - Angola Shale contact. Concretion bed with goniatites, above a 23 cm-thick black shale and about 0.84 m above a thin siltstone capping a small falls upstream of the farm-track crossing Relyea Creek (or Gibson's Glen), where section commences about 460 m west of NY Rte. 19 at about 1100 ft. elevation. NY Rte. 19 crosses Relyea Creek at 42° 42'45.73"N 78° 07'48.74"W. Goniatite Division: *Neomanticoceras* (Frasnian I-J); NY Regional Zone *Sphaeromanticoceras rhynchostomum* (22b). Frasnian Conodont Zone 11.
Sample: Bed 60/3: 12050-SD: JH and WK 2 of 8.8.74 = **4080:** WK and JK 1 of 8.12.91 and WK and GK on 10.12.91.

RL: Bed 61/1: Stony Creek, Warsaw, Wyoming County, NY, Warsaw 7.5' Quad., NW ¼ PORTAGE 15' Quad. Rhinestreet Shale, **Relyea Creek Horizon (RL),** Bed 61/1 of House and Kirchgasser (2008, p. 48-49, fig. 13*). Concretion bed with goniatites, in a 0.6 m interval of gray shale between 10 and 15 mm-thick black shales, that is 7.5 m below the 1 m-thick black shale that marks Rhinestreet Shale-Angola Shale contact, in the waterfall section in Stony Creek, below the railroad crossing, 2 km southwest of Warsaw. The 1 m-thick marker black shale at the base of the Angola Shale is about 11 m below the base of the siltstone on which the railroad bridge is built and 7.3 m below the base of the 0.3 m-thick siltstone that caps the main falls at 42°43'57.87"N 78° 09'10.18"W. Goniatite Division: *Neomanticoceras* (Frasnian I-J); NY Regional Zone *Sphaeromanticoceras rhynchostomum* (22b). Frasnian Conodont Zone 11.
Sample: Bed 61/1: 12049-SD: JH and WK 1 of 8.8.74

PB: Bed 73/6: **Big Sister Creek**, Angola, Erie County, NY, Angola 7.5' Quad., NE ¼ SILVER CREEK 15' Quad. Angola Shale (West Falls Group), **Point Breeze Goniatite Bed (PB)**, Bed 73/6 of House and Kirchgasser (2008, p. 54 fig. 15*), in 6th microcycle, 12 m above base Angola Shale. Concretion bed with goniatites beneath a thin black shale and 0.6 m below prominent 0.15 m-thick siltstone in the bluff section on the east bank of Big Sister Creek, 183 m upstream from the railroad bridge crossing of the creek at 42°38'31.11"N 79°01'23.47"W. Goniatite Division: *Neomanticoceras* (Frasnian I-J); NY Regional Zone *Sphaeromanticoceras rhynchostomum* (22b). Frasnian Conodont Zone 11.
Sample: Bed 73/6: 12039-SD: JH and WK 2 of 8.2.74.

PB: Bed 74/6b: **Hampton Brook**, Hamburg, Erie County, NY, EDEN 15' Quad. Angola Shale, **Point Breeze Goniatite Bed (PB)**, Bed 74/6b of House and Kirchgasser (2008, p. 54, fig. 15*), in 6th microcycle 13 m above base Angola Shale. Concretion bed with goniatites in Hampton Brook, downstream of the East Eden or Hamburg Road bridge crossing at 42°41'28.49"N 78° 50'01.19"W, 2.5 km south of Hamburg. The first falls downstream of the bridge are over a siltstone above a 0.60 m-thick black shale which caps the 9th microcycle. Goniatite Division: *Neomanticoceras* (Frasnian I-J); NY Regional Zone *Sphaeromanticoceras rhynchostomum* (22b). Frasnian Conodont Zone 11.
Sample: Bed 74/6b: 12043-SD: JH and WK 1 of 8.5.74.

PB: Bed 75/6: **Cazenovia Creek**, Griffins Mills, Erie County, NY, COLDEN 15' Quad. Angola Shale. **Point Breeze Goniatite Bed (PB)**. Bed 75/6 of House and Kirchgasser (2008, p. 55, fig. 15*), in 6th microcycle, 13 m above base Angola Shale. Concretion bed with goniatites in Cazenovia Creek at Griffins Mills is beneath a 30 cm-thick black shale at base of microcycle 7 downstream from a 30 cm-thick black shale at base of microcycle 8 within which is the prominent siltstone that forms a low falls below Jewetville/Mill Road bridge at 42°32'27.62"N 78°40'12.36"W. Goniatite Division: *Neomanticoceras* (Frasnian I-J); NY Regional Zone *Sphaeromanticoceras rhynchostomum* (22b). Frasnian Conodont Zone 11.
Sample: Bed 75/6: 12044-SD: JH and WK 2 of 8.5.74.

SF: Bed 79/8a: Stony Brook, Varysburg, Wyoming County, NY, ATTICA 15' Quad. Angola Shale. **Stony Brook Farm-track Beds (SF)**, informal units named herein. Bed 79/8a of Locality 79 of House and Kirchgasser (2008, p. 55, fig. 15*: bed shown but not labeled), is in microcycle 8, 14.5 m above base Angola Shale. Nodular limestone with goniatites in Stony Brook, east of Varysburg. **Bed 79/8a** is above the 0.46 m-thick black shale at base of microcycle 8 and is capped by the thin black shale at base of microcycle 9. The pair of black shales (20 and 25.4 cm-thick) capping microcycle 9 at about 1180 ft. elevation are the first prominent black shales downstream of farm-track crossing creek at about 42°46'02.33"N 78°16'40.23"W, north of US Rte. 20A. Goniatite Division *Neomanticoceras* (Frasnian I-J); NY Regional Zone: *Sphaeromanticoceras rhynchostomum* (22b). Frasnian Conodont Zone 12.
Sample: Bed 79/8a: 12051-SD: JH and WK 3 of 8.8.74.

SF: Bed 79/10: Stony Brook, Varysburg, Wyoming County, NY, ATTICA 15' Quad. Angola Shale, **Stony Brook Farm-track Beds (SF)**, informal units named herein. Bed 79/10 of House and Kirchgasser (2008, p. 55, fig. 15*), 23.5 m above base Angola Shale. Nodular limestone with goniatites, in Stony Brook east of Varysburg, is below a 25 cm-thick black shale at base of the second microcycle upstream of farm-track crossing of the creek at 42°46'02.33"N 78°16'40.23"W, north of US Rte. 20A. Goniatite Division: *Neomanticoceras* (Frasnian I-J); NY Regional Zone: *Sphaeromanticoceras rhynchostomum* (22b). Frasnian Conodont Zone 12.
Sample: Bed 79/10: 12052-SD: JH and WK 4 of 8.8.74.

Bed 77/3: Glade Creek, Strykersville, Wyoming County, NY, ARCADE 15' Quad. Angola Shale. Concretion bed 77/3 with goniatites, 0.48 m above base of 30 cm-thick black shale marking base of "Trinity" black shales (TR) of upper Angola Shale

(House and Kirchgasser, 2008, p.55, fig. 15*) in Glade Creek, 1.1 km north of Strykersville. Section upstream of Dutch Hollow road crossing of creek at 42°42'27.14"N 78°27'04.69"W (and upstream of NY Rte. 78) and below a falls over a 0.8 m-thick sandstone at about 1,075 ft. elevation (taken as base Nunda Sandstone); horizon is downstream of bridge foundations. Goniatite Division: *Neomanticoceras* (Frasnian I-J); NY Regional Zone: *Sphaeromanticoceras rhynchostomum* (22b). Frasnian Conodont Zone 12.
Sample: Bed 77/3: 12047-SD: JH and WK 3 of 8.6.74.

SG: Bed 80/14: **Stony Brook (Gassman Road), Varysburg**, Wyoming County, NY, ATTICA 15' Quad. Angola Shale. **SG** is the **Gassman Road Red *Knollenkalk* Bed**, informal unit named herein. Nodular red and green limestone (10 cm-thick) with goniatites, about 1.8 m above old bridge foundation where Gassman Road crossed Stony Brook at 42°46'02.33"N 78°16'40.23"W, 3 km east of Varysburg. **Bed 80/14,** at about 1375 ft elevation on north bank of creek, is high in Angola Shale, above measured section in House and Kirchgasser (2008, p.55, fig. 15) and is estimated to be about 73 m above base Angola Shale. It may be the middle or upper of three nodule bands in the Nunda Sandstone interval illustrated in Pepper et al. (1956, fig. 2). Goniatite Division: *Neomanticoceras* (Frasnian I-J); NY Regional Zone: *Sphaeromanticoceras rhynchostomum* (22b). Frasnian Conodont Zone 12.
Sample: Bed 80/14: 12053-SD: JH and WK 5 of 8.8.74 = **4079b** JK and WK 1 of 8.13.91 = **4079c**: WK and GK 5 of 10.12.91.

CB: Bed 92/2: **Beaver Meadow Creek**, Java, Wyoming County, NY, ARCADE 15' Quad. Hanover Shale (West Falls or Java Group), ***cataphractum* Bed,** informal unit named herein, Bed 92/2 of House and Kirchgasser (2008, p. 59, fig. 16*), 7.7 m above the base of the 7.6 m-thick black Pipe Creek Shale. Horizon of small, irregularly shaped limestone nodules with the goniatite *Delphiceras cataphractum* in floor of creek near base Hanover Shale where road track crosses (fords) Beaver Meadow Creek at Java. **CB** is about 140 m upstream of the NY Rte. 78 bridge that crosses creek at 42°40'19.64"N 78°26'08.86"W, and Angel Falls over the Nunda Sandstone. Goniatite Division: *Archoceras* (Frasnian I-K); NY Regional Zone: *Delphiceras cataphractum* (23). Frasnian Conodont Zone 12.
Sample: Bed 92/2: 12046-SD: JH and WK 1 of 8.6.74 = **4097:** WK and J. Over 2 of 8.22.92.

Bed 89a/4: Walnut Creek, Silver Creek, Chautauqua County, NY, SILVER CREEK 15' Quad. Hanover Shale. Concretion horizon with goniatites in lower Hanover Shale on east bank of Walnut Creek, upstream of NY Rte. 20 bridge crossing at 42°32'17.84"N 79°10'08.88"W, south of Silver Creek. Bed 89a/4 of House and Kirchgasser (2008, p. 58, fig. 16*) is at stream level about 37 m upstream of the bridge, underlies a 10 cm-thick black shale, and is 3 m above base black Pipe Creek Shale (0.61m thick), the top of which is exposed under the bridge. Goniatite Division: *Crickites* (Frasnian I-L); NY Regional Zone: *Crickites lindneri* (24a). Frasnian Conodont Zone 12 – Subzone 13a.
Sample: Bed 89a/4: 12042-SD: JH and WK 3 of 8.4.74.

BM: Bed 92/5: Beaver Meadow Creek, Java, Wyoming County, NY, ARCADE 15' Quad. Hanover Shale, **Red *Knollenkalk* Bed**, informal unit named herein. **Bed 92/5** is about 8.4 m below base Dunkirk Shale (Canadaway Group; Over (1997, fig. 7); House and Kirchgasser (2008, p. 59, fig. 16: bed not shown). Nodular, red and green limestone bed (4 cm-thick) in the upper Hanover Shale of Beaver Meadow Creek, above a 50 cm-thick siltstone capping a low falls about 37 m downstream of the first high falls in the creek. NY Rte. 78 crosses Beaver Meadow Creek at 42°40'19.64"N 78°26'08.86"W in the village of Java. Goniatite Division: *Crickites* (Frasnian I-L); NY Regional Zone: *Sphaeromanticoceras rickardi* (24b). Frasnian Conodont Subzone 13b.
Sample: 4098: WK and J. Over 3 of 8/22/92.

91/7a: Glade Creek, upper part, Strykersville, Wyoming County, NY, ARCADE 15' Quad. Hanover Shale. Nodular, red and green limestone (6.4 cm-thick) in upper Hanover Shale in upper Glade Creek northwest of Strykersville. Bed 91/7a is first carbonate unit above Bed 91/7 of House and Kirchgasser (2008, p. 59, fig. 16*), and is about 7.6 m below base Dunkirk Shale. Bed 91/7, the lower of two beds labeled 7x, is a bed of siltstone that yielded a single goniatite (*Sphaeromanticoceras rickardi*), 7.9 m below base Dunkirk Shale. The base of Dunkirk Shale crops out at creek level just above where a farm-track crosses upper Glade Creek at about 42°42'53.82"N 78°25'12.70"W, below Bartz (Sheldon) Road, 3 km north of Strykersville. Goniatite Division: *Crickites* (Frasnian I-L); NY Regional Zone: *Sphaeromanticoceras rickardi* (24b). Frasnian Conodont Subzone 13b.
Sample: Bed 91/7a: 12048-SD: JH and WK 6 of 8.6.74 = **12056-SD**: JH and WK 3 of 8.9.74; GK and WK 2 of 7.20.89.

IL: Bed 90/2: Irish Gulf, North Boston, Erie County, NY, EDEN and SPRINGVILLE 15' Quads. Hanover Shale, **IL *linguiformis* Limestone Bed**, informal unit named herein. Thin limestone (2.0-2.5 cm-thick) with crinoids and small gastropods, the conodont *Palmatolepis linguiformis* and the highest Frasnian goniatites in New York (House and Kirchgasser, 2008), capping a low falls in upper part of Irish Gulf, 2.6 km southeast of North Boston, 4.7 m below base Dunkirk Shale, Canadaway Group (Over, 1997, fig. 8*, marked by concretion symbol; House and Kirchgasser, 2008, p. 58-59, fig. 16*), indicated by concretion band below the Frasnian-Famennian boundary. NY Rte. 219 crosses lower Irish Gulf at 42°40'10.57"N 78°45'13.33"W. Goniatite Division: *Crickites* (Frasnian I-L); NY Regional Zone: *Sphaeromanticoceras rickardi* (24b). Frasnian Conodont Subzone 13b.
Sample: Bed 90/2: 4101: WK and J. Over 3 of 8.23.92.

UG: Bed 91/a: Glade Creek, Strykersville, Wyoming County, NY, ARCADE 15' Quad. Hanover Shale, **Upper Glade Creek Beds**, informal units named herein. Prominent calcareous siltstone (7-15 cm-thick) in upper Hanover Shale, at top of a low falls below where a farm-track crosses upper Glade Creek at 42°42'53.82"N 78°25'12.70"W, below Bartz (Sheldon) Road, 3 km north of Strykersville. **Bed 91/a** (House and Kirchgasser, 2008, fig. 16* - horizon marked "lip of falls"), is 3.4 m below base Dunkirk Shale. Goniatite Division: *Crickites* (Frasnian I-L); NY

Regional Zone: *Sphaeromanticoceras rickardi* (24b). Frasnian Conodont Subzone 13b.
Sample: Bed 91/a: 12055-SD: JH and WK 2 of 8.9.74; GK and WK 4 of 7.20.89.

UG: Bed 91/b: Glade Creek, Strykersville, Wyoming County, NY, ARCADE 15' Quad. Hanover Shale, **Upper Glade Creek Beds**, informal units named herein. Nodular limestone (15 cm-thick) in upper Hanover Shale, immediately below where a farm track crosses upper Glade Creek at 42°42'53.82"N 78°25'12.70"W, below Bartz (Sheldon) Road, 3 km north of Strykersville. Bed 91/b (House and Kirchgasser, 2008, fig. 16* - horizon above black Rider Bed marked 7x) is 1.1 m below base Dunkirk Shale. Goniatite Division: *Crickites* (Frasnian I-L); NY Regional Zone: *Sphaeromanticoceras rickardi* (24b). Frasnian Conodont Subzone 13c.
Sample: Bed 91/b: 12054-SD: JH and WK 1 of 8.9.74; GK and WK 5 of 7.20.89.

WESTERN AUSTRALIA

Timanites Hill, Canning Basin, Western Australia. Gogo Formation. Thin platy limestones with goniatite cephalopod *Timanites* cropping out at top of low anticlinal knoll, informal Timantites Hill, Bugle Gap. WAPET D section of Glenister and Klapper (1966, p. 836, fig. 1, table 9), AMG Zone 52, $_{1}$88200E $_{79}$32400N. Locality 370, Becker and House (1997, fig. 2, locality map). Goniatite Division: *Timanites* (I-C); Australian Regional Zone: *Timanites angustus*. Frasnian Conodont Zone 4.
Sample: Beds 370A and 370B: GK and R. S. Nicoll, 8.13.88.

IOWA

Sweetland Creek, Muscatine County, Iowa. Illinois City Quad., type section [N ½ SW ¼ sec. 27, T77N, R 1W). East bank of Sweetland Creek at 41°26'26.63"N 90°57'17.19W; position of section shown in Over (2006, p. 75)]. Section north of Iowa Rte. 22 bridge, about 6.5 km east of junction with US Rte. 61, in Muscatine. The sample of Miller and Youngquist (1947) from which two of their types are reillustrated on Figs. 9.13, 9.16 herein, is probably from within the interval of 1.85-2.30 m above base of type section. This is based on the restricted occurrences of their species, especially *Ancyrognathus calvini* (Miller and Youngquist, 1947; see Johnson and Klapper, 1992, fig. 2, and Klapper, 1990, p. 1006, 1010). Frasnian Conodont Subzone 13a.

Appendix 2

For those species illustrated in Figures 7–11 and/or listed in Table 2, but not formally described in the Systematic Paleontology section, an abbreviated synonymy is given here.

Ancyrodella africana García-López, 1981, p. 264, pl. 1, figs. 1–14 [figs. 1–3 = holotype]; Klapper, 1985, p. 28, pl. 8, figs. 11–22, pl. 9, figs. 1–16, text–figs. 3 S, T, AA, BB; Over et al., 2003, pl. 1, fig. 4. Figures 7.3, 7.4 herein.

Ancyrodella alata Glenister and Klapper, 1966, p. 799, pl. 85, figs. 1–8 [figs. 7, 8 = holotype; not pl. 86, figs. 1, 2 = *A. recta* Kralick, 1994, figs. 3, 4 = *A. pramosica* Perri and Spalletta, 1981]; Klapper, 1985, p. 27, pl. 6, figs. 1, 2 [only; not figs. 3–12 = *A. recta*], pl. 7, figs. 1–11, pl. 8, fig. 8, text–figs. 3 Q, R [only, not figs. 3 K, L, O, P = *A. recta. Ancyrodella alata* s.s. = essentially the late form of Klapper, 1985]; Over et al., 2003, pl. 1, figs. 16, 17. Figures 7.1, 7.2, 7.6, 7.7, 7.11, 7.12 herein.

Ancyrodella curvata (Branson and Mehl, 1934) early form of Klapper, 1989, p. 457, pl. 3, figs. 18, 19; Gouwy and Bultynck, 2000, p. 40, pl. 2, figs. 5, 6; Gouwy et al., 2007, p. 389, figs. 15 P–S.

Ancyrodella curvata (Branson and Mehl, 1934) late form of Klapper, 1989, p. 457, pl. 3, fig. 20; Bultynck et al., 1998, p. 55, pl. 5, figs, 8–10, pl. 6, figs. 1–3 [These authors distinguish a late form = pl. 6, figs. 1, 2, the rest of the illustrated specimens as a latest form]; Gouwy and Bultynck, 2000, p. 40, pl. 2, figs. 1–4 [fig. 4 = latest form]; Gouwy et al., 2007, p. 389, fig. 15 T.

Ancyrodella recta Kralick, 1994, p. 1387, figs. 3.5, 3.6, 3.11, 3.12, 4.11, 4.12, 6.1, 6.2, 6.5, 6.6, 6.9, 6.10 [figs. 6.1, 6.2 = holotype]; Klapper, 2000, p. 154, pl. 1, figs. 2–4, 8 [figs. 2, 3 = reillustration of holotype]; Miller, 2007, p. 447, figs. 4 A–4Y, 5A, 5D–5Y. Figures 7.15, 7.16 herein.

Ancyrodella rugosa Branson and Mehl, 1934, p. 239, pl. 19, figs. 15, 17 [= holotype]; Klapper, 1985, p. 30, pl. 11, figs. 1, 2, 5–14, text–figs. 3 U, V; Kralick, 1994, p. 1393, figs. 3.7, 3.8, 3.13, 3.14, 4.9, 4.10; Over et al., 2003, pl. 1, figs. 18, 19. Figures 7.13, 7.14, 7.17, 7.18 herein.

Ancyrodella triangulata Kralick, 1994, p. 1390, figs. 3.3, 3.4, 3.9, 3.10, 4.1–4.4, 6.3, 6.4, 6.7, 6.8, 6.11, 6.12 [figs. 3.3, 3.4, 6.11, 6.12 = holotype].

Ancyrognathus aff. *A. altus* Müller and Müller, 1957, p. 1095, pl. 141, fig. 5; Klapper, 1990, p. 1001, figs. 2.7–2.9.

Ancyrognathus amana Müller and Müller, 1957, p. 1095, pl. 138, fig. 5 [= holotype]; Klapper, 1990, p. 1001, figs. 2.1–2.6; Bultynck et al., 1998, p. 55, pl. 7, figs. 9–11.

Ancyrognathus ancyrognathoideus (Ziegler, 1958), p. 69, pl. 9, figs. 8, 16, 17, 20 [figs. 8, 17, = holotype; not figs. 11, 19 = *A. primus* Ji, 1986, not fig. 18 = ?]; Klapper, 1990, p. 1003, figs. 2.10, 2.11, 3.8, 3.9. Figure 10.12 herein.

Ancyrognathus asymmetricus (Ulrich and Bassler, 1926), p. 50, pl. 7, fig. 18 [= holotype]; Huddle, 1968, p. 7, pl. 13, figs. 11, 12 [reillustration of holotype]; Klapper, 1990, p. 1003, figs. 4.1–4.16, 5.9–5.16, 6.4, 6.7, 6.10, 7.10–7.13; Savage, 2013, p. 9, figs. 7.17–7.21.

Ancyrognathus iowaensis Youngquist, 1947, p. 97, pl. 25, fig. 22 [= holotype]; Müller and Müller, 1957, p. 1096, pl. 137, fig. 5; Klapper, 1990, p. 1014, figs. 3.11–3.16 [fig. 3.13 = reillustration of holotype]. Figure 10.14 herein.

Ancyrognathus n. sp. L? [questionably related to *A.* n. sp. L of Klapper, 1989, p. 458, pl. 4, fig. 14; Klapper, 1990, p. 1021, figs. 2.15–2.20].

Ancyrognathus primus Ji, 1986, p. 28, 113, pl. 6, figs. 9–14 [figs. 13, 14 = holotype], text–fig. 4; Klapper, 1990, p. 1015, figs. 2.12–2.14. Figures 10.6, 10.11 herein.

Ancyrognathus triangularis Youngquist, 1945, p. 356, pl. 54, fig. 7 [lectotype selected by Müller and Müller, 1957, p. 1097; see comment by Klapper, 1990, p. 1019]; Klapper, 1990, p. 1017, figs. 7.1–7.6, 7.9, 11.3–11.21 [fig. 11.8 = reillustration of lectotype]. Figure 10.13 herein.

Ancyrognathus? deformis (Anderson, 1966), p. 411, pl. 50, figs. 1, 2, 4, 5 [figs. 1, 5 = holotype]; Metzger, 1989, p. 516, figs. 14.17, 14.18, 14.23, 14.24; Day, 1990, p. 623, figs. 11.9, 11.10,11.15, 11.17; Klapper, 1990, p. 1010, 1014. Figure 10.10 herein.

Elsonella prima Youngquist, 1945, p. 358, pl. 56, fig. 5 [= lectotype selected by Müller, 1956a, p. 825]; Klapper, 1966, p. 24, pl. 5, fig. 9 [reillustration of lectotype].

Icriodus symmetricus Branson and Mehl, 1934, p. 226, pl. 13, figs. 1–3 [fig. 3 = lectotype selected by Klapper, 1975, p. 151]; Klapper, 1975, p. 151, *Icriodus* – pl. 3, figs. 7, 8 [fig. 8 = reillustration of lectotype in three views];Uyeno, 1992, p. 71, pl.16, figs. 7–16; Over, 2007, p. 1202, figs. 10.18–10.20.

Mehlina gradata Youngquist, 1945, p. 363, pl. 56, fig. 3 [lectotype selected by Müller and Müller, 1957, p. 1083]; Müller and Müller, 1957, p. 1083, pl. 135, figs. 10, 11 [these authors assigned *M. gradata* to the genus *Ctenognathus,* a junior homonym, see Clark et al., 1981, p. W165]; Uyeno, 1982, p. 77, pl. 37, figs. 28–43 [full multielement reconstruction]; Klapper and Lane, 1985, p. 921, fig. 12.1.

Mesotaxis asymmetrica (Bischoff and Ziegler, 1957), p. 88, pl. 16, figs. 18, 20–22 [fig. 20 = holotype], pl. 21, fig. 3 [proposed as *Polygnathus dubia asymmetrica*]; Klapper and Philip, 1972, p. 100, pl. 1, figs. 20–27, pl. 2, figs. 14–17 [multielement reconstruction, identified as *Mesotaxis asymmetrica* asymmetrica]; Ziegler and Klapper, 1982, p. 469, pl. 1, figs. 7, 8 [fig. 8 = reillustration of holotype; identified as *Polygnathus asymmetricus asymmetricus*]; Ziegler and Sandberg, 1990, p. 44, pl. 1, figs. 5–7 [figs. 5, 6 = reillustration of holotype]; Dzik, 2002, p. 592, figs. 30 L–T [full multielement reconstruction]; Over et al., 2003, pl. 1, figs. 14, 15. Figures 8.18, 8.19 [Figures 8.16, 8.17 = *M. asymmetrica* transitional with *Palmatolepis transitans* Müller, 1956b] = Pa elements, Figures 10.5, 10.9 = Pb elements herein.

Mesotaxis johnsoni Klapper et al., 1996, p. 140, figs. 6.13–6.16 [figs. 6.14, 6.15 = holotype]; Ovnatanova and Kononova, 2001, p. 76, pl. 11, figs. 6, 7. Figure10.8 herein.

Mesotaxis ovalis (Ziegler and Klapper, 1964), p. 423 [Ziegler, 1958, p. 57, pl. 1, figs. 1, 2 = holotype; proposed as *Polygnathus asymmetrica ovalis* in the 1964 paper]; Klapper, 1989, p. 458, pl. 3, figs. 15, 16; Ziegler and Sandberg, 1990, p. 43 [identified as *Klapperina ovalis*]; Over et al., 2003, pl. 1, figs. 6–9; Bardashev and Bardasheva, 2012, p. 53, pl. 5, figs.17, 18, 21, 22, 25, 26 [identified as *Zieglerina ovalis* of which genus it was chosen as the type species; *Z. monikae* Bardashev and Bardasheva is based only on minor differences in the platform outline]. Figure 8.14, 8.15 herein.

Ozarkodina bidentatiformis (Pham, 1979), p. 89, pl. 6, figs. 8, 9 [fig. 8 = holotype; proposed as *Spathognathodus bidentatiformis*]; Klapper, 1989, p. 458, pl. 3, figs. 1, 2; Klapper et al., 1996, p. 137, fig. 6.6. Figure 10.1 herein.

Ozarkodina nonaginta Klapper, et al., 1996, p. 137, figs. 6.3–6.5 [fig. 6.4 = holotype]; Pisarzowska et al., 2006, p. 625, fig. 13 J; Figure 10.2 herein.

Palmatolepis bogartensis (Stauffer, 1938), p. 436, pl. 48, fig. 30 [= holotype; proposed as *Nothognathella bogartensis*]; Klapper and Foster, 1993, p. 17, figs. 13.4–13.16, 19.1–19.5 [fig. 19.2 = reillustration of holotype of *N. bogartensis*], 20.1–20.11 [full multielement reconstruction]; Klapper, 2007a, p. 517, figs. 1.1, 1.2; Klapper, 2007b, p. 70, pl. 1, figs. 1–13; Narkiewicz and Bultynck, 2011, pl. 10, figs. 1–6, 8–11.

Palmatolepis boogaardi Klapper and Foster, 1993, p. 18, figs. 13.3, 14.1–14.10, 17.1, 17.2, 19.13–19.15 [fig. 14.5 = holotype]; Klapper et al., 1996, p. 143, figs. 8.9, 8.11, 8.12.

Palmatolepis foliacea Youngquist, 1945, p. 364, pl. 56, figs. 11, 12 [fig. 12 = lectotype selected by Müller and Müller, 1957, p. 1102]; Müller and Müller, 1957, p. 1102, pl. 140, figs. 6, 7, 9 [not fig. 8 = *P.* cf. *P. foliacea*];Ziegler and Sandberg, 1990, p. 49, pl. 5, figs. 1, 3, 4, 6 [only; fig. 6 = reillustration of lectotype]; Klapper and Foster, 1993, p. 8, figs. 6.1–6.9, 7.17–7.20; Ovnatanova et al., 1999, p. 356, pl. 2, figs. 19, 20. Figures 12.3, 12.5 herein.

Palmatolepis hassi Müller and Müller s.s., 1957, p. 1102, pl. 139, fig. 2, pl. 140, figs. 2–4 [fig. 4 = holotype]; Ziegler and Sandberg, 1990, p. 55, pl. 2, fig. 2 [only; fig. 2 = reillustration of holotype]; Klapper and Foster, 1993, p. 22, figs. 15.1–15.9, 18.12, 19.16–19.18 [fig. 15.4 = reillustration of holotype]; Over, 1997, p. 169, figs. 6.4, 6.5; Bultynck et al., 1998, p. 58, pl. 2, fig. 6, pl. 3, figs. 2–7; Klapper, 2007a, p. 521, figs. 3.1–3.6. Figure 12.4 herein.

Palmatolepis hassi Müller and Müller s.l., Bultynck et al., 1998, p. 58, pl. 2, figs. 1–5. Figure 12.6 herein.

Palmatolepis juntianensis Han, 1987, p. 186, pl. 1, figs. 15, 16 [fig. 15 = holotype]; Ziegler and Sandberg, 1990, p. 52, pl. 14, figs. 6, 7; Klapper et al., 2004, p. 378, figs. 6.1–6.3; Klapper, 2007a, p. 535, figs. 5.1, 5.2.

Palmatolepis linguiformis Müller, 1956b, p. 24, pl. 7, figs. 1–7 [fig. 4 = holotype]; Ziegler and Sandberg, 1990, p. 59, pl. 14, figs. 8–10; Sandberg et al., 1994, p. 252, pl. 2, figs. 1–4; Klapper et al., 2004, p. 386, fig. 6.11; Klapper, 2007a, p. 535, fig. 2.6. Figure 12.1 herein.

Palmatolepis punctata (Hinde, 1879), p. 367, pl. 17, fig. 14 [= holotype]; Klapper and Foster, 1993, p. 15, figs. 5.4–5.9, 8.11, 8.12, 10.18–10.21; Over et al., 2003, pl. 1, figs. 1, 2; Pisarzowska et al., 2006, p. 626, fig. 14 K; Klapper, 2007a, p. 527, figs, 8.8–8.12. Figures 8.6–8.13 = Pa elements, Figures 10.4, 10.7? = Pb elements herein.

Palmatolepis semichatovae Ovnatanova, 1976, p. 110, pl. 9, figs. 3, 4 [fig. 3 = holotype; proposed as *Palmatolepis gigas semichatovae*]; Klapper and Lane, 1985, p. 928, figs. 15.8–15.10; Aristov, 1988, p. 75, pl. 7, figs. 20, 21 [as *P. gigas* semichatovae]; Ziegler and Sandberg, 1990, p. 58, pl. 11, figs. 1, 2, pl. 13, figs. 3–11; Klapper, 2007a, p. 535, fig. 2.9. Figure 12.2 herein.

Palmatolepis spinata Ovnatanova and Kuz'min, 1991, p. 47, pl. 3, figs. 4–7 [fig. 6 = holotype]; Klapper et al., 1996, p. 148, fig. 9.13; Klapper, 2007a, p. 535, figs. 8.5, 8.6. Figures 8.1, 8.2 = Pa elements, Figure 10.3 = Pb element herein.

Palmatolepis transitans Müller, 1956b, p. 18–19, pl. 1, fig. 1 [only; = holotype]; Ziegler and Sandberg, 1990, p. 45, pl. 1, fig. 9; Klapper et al., 1996, p. 149, fig. 9.14; Kuz'min, 1998, p. 76, pl. 7, fig. 1, pl. 8, figs. 6, 7; Over et al., 2003, pl. 1, figs. 11–13; Klapper et al., 2004, p. 387, fig. 6.7; Klapper, 2007a, p. 535, fig. 8.7; Ovnatanova and Kononova, 2008, p. 1107; pl. 1, figs. 1–5, 8 [fig. 8 = reillustration of holotype; figs. 6, 7 = ?]. Figures 8.3–8.5 herein. *Palmatolepis keyserlingi* Kuz'min, 1998, p. 74, pl. 8, figs. 2–5 is a probable junior synonym.

Palmatolepis winchelli (Stauffer, 1938), p. 423, pl. 48, fig. 33 [= holotype; proposed as *Bryantodus winchelli*]; Klapper and Foster, 1993, p. 24, figs. 13.1, 13.2, 18.1–18.8, 18.10, 18.11 [fig. 18.5 = lectotype of *Palmatolepis subrecta* Miller and Youngquist, 1947], 19.6–19.12 [fig. 19.12 = reillustration of holotype of *Bryantodus winchelli*], 20.12–20.24 [full multielement reconstruction]; Klapper, 2007a, p. 529, figs. 1.9–1.11; Klapper, 2007b, p. 72, pl. 1, figs. 14–16. Figure 12.7 herein.

Polygnathus aequalis Klapper and Lane, 1985, p. 930, figs. 16.7–16.14 [fig. 16.13 = holotype]; Ziegler et al., 2000, p. 634, pl. 7, figs. 13, 14.

Polygnathus brevis Miller and Youngquist, 1947, p. 514, pl. 74, fig. 9 [= holotype]; Klapper, 1973, p. 341, *Polygnathus* – pl. 1, fig. 2 [= reillustration of holotype]; Klapper and Lane, 1985, p. 944, figs. 17.1, 17.6; Savage, 1992, p. 286, figs. 5.26–5.28 [only]; Klapper, 2007a, p. 536, fig. 7.11; Ovnatanova and Kononova, 2008, p. 1117, pl. 23, figs. 8–11.

Polygnathus collieri Huddle, 1981, p. B27, pl. 9, figs. 20–25, pl. 10, fig. 22, pl. 11, figs. 1–4, pl. 12, figs. 1–3 [= holotype], pl. 13, fig. 11; BULTYNCK, 1986, p. 276, pl. 1, fig. 6; Aboussalam and Becker, 2007, p. 368, figs. 6 J, K.

Polygnathus decorosus Stauffer, 1938, p. 438, pl. 53, figs. 5, 6, 10, 15, 16 [only; fig. 6 = lectotype selected by Huddle, 1970, p. 1034]; Klapper et al., 1970, p. 652–654, pl. 3, figs. 1–6 [figs. 4-6 = reillustration of lectotype]; Huddle, 1970, p. 1033; Klapper and Lane, 1985, p. 935, fig. 18.7; Uyeno, 1992, p. 77, pl. 14. figs. 9–17; Over, 1997, p. 174, fig. 10.11; Dzik, 2002, p. 590, figs. 21 A–M [as *Avignathus decorosus,* multielement reconstruction]; Over, 2007, p. 1202, figs. 12.8, 12.13, 12.14.

Polygnathus dubius Hinde, 1879, p. 362, pl. 16, fig. 17 [only; lectotype selected by Roundy, 1926, p. 13]; Huddle, 1970, p. 1037, pl. 138, figs. 1–17, 22, 23 [figs. 5, 6 = netotype of *P. dubius* proposed by Huddle, 1970, p. 1033, at the same time it was designated as the lectotype of *P. foliatus* Bryant, 1921, reillustrated from Bryant's pl. 10, fig. 16; figs. 22, 23 =lectotype of *P. dubius,* now lost]; Klapper, 1973, p. 353, *Polygnathus* – pl. 1, figs. P, O_1, N, $A_{1–3}$, 1 [fig. 1 = reillustration of Bryant, 1921, pl. 10, fig. 16]; Uyeno, 1992, p. 78, pl. 13, figs. 24–30; Over, 2007, p. 1202, figs. 12.9–12.12.

Polygnathus dengleri Bischoff and Ziegler, 1957, p. 87, pl. 15, figs. 14, 15, 17–24 [fig. 18 = holotype], pl. 16, figs. 1–3 [not fig. 4 = *P. dengleri* narrow form, see below]; Klapper, 1980, p. 102, pl. 4, figs. 24–28 [not fig. 30 = *P. dengleri* narrow form]; Huddle, 1981, p. B29, pl. 6, figs. 15–23; Uyeno, 1992, p. 77, pl. 13, figs. 16–18; Kirchgasser, 1994, p. 127, pl. 3, fig. H; Aboussalam and Becker, 2007, p. 356, figs. 6C–6F.

Polygnathus dengleri Bischoff and Ziegler narrow form of Klapper, 1989, p. 458, pl. 3, fig. 9.

Polygnathus pennatus Hinde, 1879, p. 366, pl. 17, fig. 8 [= holotype]; Branson and Mehl, 1933, p. 144, pl. 11, fig. 3 [= reillustration of holotype]; Huddle, 1970, p. 1038, pl. 137, figs. 1–19; Klapper, 1973, p. 373, *Polygnathus* – pl. 1, fig. 7; Uyeno, 1992, p. 78, pl. 13, figs. 19–23; Kirchgasser, 1994, p. 127, pl. 3, figs. A, B, F, G; Over, 2007, p. 1202, figs. 12.15, 12.16.

Polygnathus samueli Klapper and Lane, 1985, p. 943, figs. 17.13–17.18 [figs. 17.16, 17.17 = holotype]; Aristov, 1988, p. 84, pl. 3, fig. 9 [identified as *P. brevis*; fig. 10 = ?]; Savage, 1992, p. 287, fig. 2.13; Over, 1997, p. 174, fig. 6.1; Morrow, 2000, p. 56, pl. 5, fig. 3; Klapper, 2007a, p. 536, figs. 7.12, 7.13.

Polygnathus unicornis Müller and Müller, 1957, p.1089, pl. 135, figs. 5–7 [fig. 5 = holotype], pl. 141, fig. 10; Klapper and Lane, 1985, p. 944, figs. 19.1–19.10; Savage, 1992, p. 287, figs. 3.7–3.9.

Polygnathus webbi Stauffer, 1938, p. 439, pl. 53, figs. 25, 26, 28, 29 [figs. 28, 29 = lectotype selected by Wittekindt, 1966, p. 641]; Klapper, 1971, p. 66, pl. 1, figs. 25–28 [fig. 26 = reillustration of lectotype; fig. 27 = reillustration of holotype of *P. normalis* Miller and Youngquist, 1947]; Klapper, 1973, p. 393, *Polygnathus* – pl. 2, fig. 7 [= reillustration of Klapper, 1971, pl. 1, fig. 28, not fig. 25 as stated]; Bultynck, 1982, pl. 3, figs. 24, 26, 35; Klapper and Lane, 1985, p. 944, fig. 16.18.